3-24-2016

Multi-Trajectory Automatic Ground Collision Avoidance System with Flight Tests (Project Have ESCAPE)

John V. Trombetta

MULTI-TRAJECTORY AUTOMATIC GROUND COLLISION AVOIDANCE SYSTEM WITH FLIGHT TESTS (PROJECT HAVE ESCAPE)

THESIS

John V. Trombetta, Major, USAF

AFIT-ENY-MS-16-M-244

DEPARTMENT OF THE AIR FORCE
AIR UNIVERSITY

AIR FORCE INSTITUTE OF TECHNOLOGY

Wright-Patterson Air Force Base, Ohio

AFIT-ENY-MS-16-M-244

MULTI-TRAJECTORY AUTOMATIC GROUND COLLISION AVOIDANCE SYSTEM WITH FLIGHT TESTS (PROJECT HAVE ESCAPE)

THESIS

Presented to the Faculty

Department of Aeronautical and Astronautical Engineering

Graduate School of Engineering and Management

Air Force Institute of Technology

Air University

Air Education and Training Command

in Partial Fulfillment of the Requirements for the

Degree of Master of Science in Aeronautical Engineering

John V. Trombetta, B.S.A.E., M.B.A., M.S.F.T.E.

Major, USAF

March 2016

AFIT-ENY-MS-16-M-244

MULTI-TRAJECTORY AUTOMATIC GROUND COLLISION AVOIDANCE SYSTEM WITH FLIGHT TESTS (PROJECT HAVE ESCAPE)

John V. Trombetta, B.S.A.E., M.B.A., M.S.F.T.E.
Major, USAF

Committee Membership:

Richard G. Cobb, PhD
Chair

Donald L. Kunz, PhD
Member

Col Angela W. Suplisson, PhD
Member

Lt Col Jose R. Gutierrez, PhD
Member

Abstract

Multi-trajectory automatic collision avoidance techniques for heavy-type aircraft are explored to increase aviation safety procedures and decrease losses due to controlled flight into terrain. Additionally, this research includes flight test results from the United States Test Pilot School's Test Management Project (TMP) titled Have Emergency Safe Calculated Autonomous Preplanned Exit (ESCAPE). Currently, the heavy aircraft community lacks an automatic collision avoidance system that has proven to save lives in fighter-type aircraft. The tested algorithm includes both a 3-path and a 5-path avoidance technique that is compared to an optimal solution which minimizes aircraft control to avoid terrain. The research utilizes Level 1 Digital Terrain Elevation Data (DTED) to analyze the terrain and a 3-Degrees of Freedom (DOF) Equations of Motion (EOM) model to predict potential terrain avoidance paths for the aircraft based on current location. The algorithm then waits until all paths collide and automatically activates the path with the longest time until collision with an appropriate time safety margin. The research also characterizes terrain based on changing slope and presents a new classification of aircraft based on performance capabilities. The result was used for algorithm parameter specification of path execution times and pre-planned maneuver creation so that the system can be modified for a wide variety of aircraft. Finally, the algorithm was flight tested against DTED in a simulated environment using the Calspan Learjet to determine actual 3 and 5-path performance, parameter specification, and comparison to the optimal solution. The important recommendations include a need for flexible entry parameters based on current aircraft state, continued evaluation of the terrain during avoidance maneuver execution, and more precise control of the aircraft flight path angle. Finally, due to comparison with the optimal solution, it is concluded that an acceptable terrain avoidance algorithm is possible using only a 3-path solution given that all three paths include a climbing maneuver.

To my wife, this research effort would not have been possible without your ceaseless motivation and support. Your unwavering strength through this journey has been incredible, and our family certainly could not have done it without you. I am forever grateful. And to my parents, who never forgot to call and to constantly encourage me to do my best.

Acknowledgments

I would first like to thank my research advisor, Dr. Richard Cobb, for not only the invaluable academic and research guidance but for always making himself available for the endless questions that I brought his way. Thank you for always giving me the tools to solve a problem myself while keeping me pointed in the right direction.

I would also like to thank Colonel Angela Suplisson (PhD) for her tireless help and constant motivation during the nearly 3 years we worked on this project. Your vision and drive are contagious. Thank you for the many hours of mentoring and always reminding me of the bigger picture. I would be remiss if I did not mention your research. Your ground breaking optimal solutions for collision avoidance were the foundation upon which this research rests.

Finally, I would like to thank my TMP group from Test Pilot School (TPS) class 15A. The flight test of this research would absolutely not have been possible without the months of hard work we put into this project. I would personally like to thank: Capt Russell "Splash" Neice, Capt Sebastien "TTT" Allard (RCAF), Capt Yoichiro Kita (JASDF), and Capt Justin "Chill" Wilson. You guys made my life easy, and thank you for making a long, hard year fun and memorable.

John V. Trombetta

Table of Contents

Page

Page

Page

List of Figures

Figure Page

List of Tables

Table Page

List of Symbols

Symbol	Definition
a	acceleration
D	drag
F	force
G	geoid height
g	gravity
H	height above ellipsoid
L	lift
M	mean sea level height
m	mass
N_z	vertical acceleration (g)
r	radius
T	thrust
t	time
V	velocity
v_{Wx}	x-direction wind velocity
v_{Wy}	y-direction wind velocity
v_{Wz}	z-direction wind velocity
x	x-axis position
$\dot{x}$	x-axis velocity
y	y-axis position
$\dot{y}$	y-axis velocity
z	z-axis position
$\dot{z}$	z-axis velocity

Symbol	Definition
α	angle of attack
γ	flight path angle
ϕ	bank angle
χ	heading angle

List of Acronyms

Acronym	Definition
AFRL	Air Force Research Laboratory
AFI	Air Force Instruction
AFIT	Air Force Institute of Technology
AGL	Above Ground Level
CDR	Conflict Detection and Resolution
CDTM	Compressed Digital Terrain Map
CFIT	Controlled Flight into Terrain
CFR	Code of Federal Regulations
CRM	Crew Resource Management
CTRF	Conventional Terrestrial Reference Frame
DAP	Data Analysis Plan
DAS	Data Acquisition System
DEM	Digital Elevation Model
DoD	Department of Defense
DOF	Degrees of Freedom
DTED	Digital Terrain Elevation Data
ESCAPE	Emergency Safe Calculated Autonomous Preplanned Exit
EGM-96	1996 Earth Geopotential Model
ENU	East-North-Up
EOM	Equations of Motion
FAA	Federal Aviation Administration
FLTS	Flight Test Squadron
fpm	Feet Per Minute

Acronym	Definition
GCAS	Ground Collision Avoidance System
GEDACS	Global Elevation Data Adaptive Compression System
GPS	Global Positioning System
GPWS	Ground Proximity Warning System
HAE	Height Above Ellipsoid
INS	Inertial Navigation System
KIAS	Knots Indicated Airspeed
MAJCOM	Major Command
MFD	Multi-Functional Display
MOP	Measure of Performance
MSL	Mean Sea Level
NASA	National Aeronautics and Space Administration
NED	National Elevation Database
NGA	National Geospatial-Intelligence Agency
nm	Nautical Mile
ORT	Oblique Recovery Trajectory
ODE	Ordinary Differential Equation
RMS	Root Mean Square
RMSE	Root Mean Square Error
SIR-C	Shuttle Imaging Radar-C
SRTM	Shuttle Radar Topography Mission
TAWS	Terrain Awareness Warning System
TCAS	Traffic Collision Avoidance System
TMP	Test Management Project
TPA	Trajectory Prediction Algorithm

Acronym	Definition
TPS	Test Pilot School
UAV	Unmanned Aerial Vehicle
USGS	United States Geological Survey
VRT	Vertical Recovery Trajectory
VSS	Variable Stability System
WGS-84	World Geodetic System 1984

MULTI-TRAJECTORY AUTOMATIC GROUND COLLISION AVOIDANCE SYSTEM WITH FLIGHT TESTS (PROJECT HAVE ESCAPE)

I. Introduction

The constant pursuit of aviation safety has been a hallmark of manned flight since the inception of the airplane. Throughout this time, controlled flight into the ground has been a constant threat to pilots and passengers with no true solution except increased training. Recently, developments in computing speed, the characterization of the world's terrain, and more advance aircraft have opened the door for automatic tools to prevent aircraft from impacting the ground. Unfortunately, the need for heavy aircraft automatic terrain avoidance has been downplayed due to financial constraints, emphasis on fighter aircraft, and mission requirements. Recent academic interest, increased aircraft expense, the success of the fighter systems, and constantly fluctuating mission sets have opened the door for the introduction of these systems for heavy aircraft. Ideally, optimally derived solutions would be calculated for terrain avoidance. To date, these solutions, though available, are too slow for real-time integration. This research aims to bridge this technological gap and provide the safety advancements these heavy aircraft and their crew need now by using constantly calculated pre-planned maneuver algorithms to avoid terrain. To do this, simulator and flight test data will be required to analyze these algorithms to determine their robustness against varying terrain features. To this end, the present Air Force Institute of Technology (AFIT) research will be coupled with a United States Air Force Test Pilot School (TPS) Test Management Project (TMP) to provide the necessary flight test data to make real-world conclusions. The project is named: Have Emergency Safe Calculated Autonomous Preplanned Exit (ESCAPE).

1.1 Motivation

In response to the continual, unacceptable loss of aircraft and aircrew, the Secretary of Defense issued a mandate in 2003 to reduce fatal aircraft mishaps by 50 percent across the Department of Defense (DoD) [30]. In response, a Defense Safety Oversight Council was established, and among other recommendations, concluded that to reduce the Controlled Flight into Terrain (CFIT) mishap rate any further, a technical solution was required and that we have achieved all we are going to with training alone [30]. To this end, aggressive measures were taken to provide an Automatic Ground Collision Avoidance System (GCAS) solution. Though these initial efforts were pointed squarely at fighter-type aircraft, the CFIT accidents of record included aircraft of all types.

As of 2014, the F-16 Auto GCAS has been being operationally fielded in combat Air Force units. Having already been credited for numerous aircraft and pilot saves [35], the door is wide open for further work in automated algorithms for other airframes. Unfortunately, direct application of the F-16's system to heavy aircraft is unreasonable due to performance disparities. Therefore, another solution is required.

Additionally, there exists a need to classify aircraft and terrain in a manner that groups them both on performance and mission, if applicable. This grouping will allow for Auto GCAS solutions to be flexible across aircraft type within the heavy category for a given terrain thus reducing the need for a different algorithm for every airframe.

1.2 Problem Statement

As will be shown in Chapter 2, the current level of research, and in some cases development, of automatic collision avoidance software for aircraft has focused on either fighter-type airframes or air-to-air avoidance. The only legitimate optimal air-to-ground research for heavy aircraft was developed by Suplisson at AFIT [35], but it will take time until computing speed catches up with the real-time requirements of optimization algorithms. For this reason, there is a major gap in heavy aircraft terrain avoidance

research. Fortunately, the optimal code can still be used as a truth source to compare with algorithm performance. Currently, there is no automatic separation algorithm for manned, heavy aircraft, only manual systems that require pilot input. Such systems, though reliable, can become obfuscated during low altitude, high workload situations warranting a more advanced solution. Additionally, there is no specific characterization of terrain that would facilitate a logical approach to nuisance free aircraft avoidance models. National Aeronautics and Space Administration (NASA) relies heavily on the terrain detection algorithm utilized by the F-16 Auto GCAS. There may be benefits to simply using raw information instead of compression and rastorizing techniques that introduce error, and this research will develop techniques using this raw data. The final, major hurdle, is the lack of any flight test data aimed specifically at Auto GCAS for heavy aircraft. Without this flight research, no development will proceed and no major gains will be made toward the complete elimination of CFIT in US Air Force aircraft. The successful implementation and flight test of the Have ESCAPE algorithm will provide a baseline for future Auto GCAS research and help prevent unnecessary loss of life and assets.

To be effective, this research must answer specific questions that relate directly to the functional requirements of an Auto GCAS algorithm. Additionally, these questions must focus on the problems presented through real-time integration with actual flight test. With this in mind, the present research will aim to answer the following questions:

- Can raw Digital Terrain Elevation Data (DTED) be used as a collision evaluation tool for an Auto GCAS algorithm?
- Is the bubble propagation method adequate for terrain collision prevention?
- How long should the ESCAPE paths be propagated forward, and is it a function of the type of terrain encountered?
- How many ESCAPE paths should be propagated?

- For heavy-type aircraft, are the ESCAPE paths performance dependent?
- Is the 3-Degrees of Freedom (DOF) Equations of Motion (EOM) model and subsequent control adequate for this Auto GCAS algorithm?
- Can the algorithm be adequately implemented in real-time?
- Should the algorithm evaluate terrain at all times?
- Is the optimal path a 'better' solution than preplanned trajectories?

1.3 Research Methodology, Scope, and Contribution

Ground collision algorithms typically require flexibility in the maneuver dimension due to the unpredictable nature of terrain and the performance capabilities of different aircraft. The F-16 can benefit from a single maneuver due to its thrust to weight capability. Heavy aircraft, on the other hand, must have options based on the type of terrain and their location relative to it. For this reason, the algorithm must be robust enough to provide for a combination of different maneuvers based on when and where a collision is predicted to occur.

This research will be broken into two major phases. First, the theory behind heavy aircraft terrain avoidance will be reviewed and analyzed to determine the appropriate algorithms for an actual ground avoidance model. This will entail creating various maneuvers to avoid the terrain while balancing path prediction accuracy with computational efficiency within the capabilities of current aircraft navigation systems. Sensitivity analyses on the equations of motion defining these paths will be performed as there is no current research adequately evaluating the accuracy of the aircraft EOM to the applied integration method. Additionally, aircraft classifications based on performance specifications will be built to group airframes so that adequate algorithm parameters can be designed for a particular aircraft's capabilities. Finally, terrain classifications will be developed to

allow for Trajectory Prediction Algorithm (TPA) flexibility and robustness against varying terrain, from flat to mountainous. (for the purposes of this research, TPA is synonymous with escape path.) This analysis will provide for adaptive protection based on aircraft location and will serve as a tool for future research.

The second facet will include the flight test of project Have ESCAPE using the Calspan Variable Stability System (VSS) Learjet. Due to the limited nature of aircraft availability, and to fit within TPS's limited TMP execution window, the flight test data will focus on a worst case (most challenging) scenario for nominal heavy aircraft capabilities. To this end, the research will be flown against mountainous terrain using both a 3-path and 5-path TPA solution. The specifics of this flight test will be discussed within the Methodology section of Chapter 3.

It is expected that it will be possible to categorize both the terrain and heavy aircraft into groupings that will allow for acceptable algorithm performance throughout all terrain categories. Much like F-16 Auto GCAS, it is furthermore expected that the Have ESCAPE algorithms will require iterative modifications in both path propagation and aircraft control before operational use. This research aims to build the foundation for future heavy aircraft Auto GCAS flight tests by providing a complete solution that can be quickly tailored to nearly any heavy aircraft. Additionally, this research and flight test data will establish procedures, guidelines, and recommendations for further algorithm development.

1.4 Research Organization

1.4.1 Theoretical Analysis.

As previously explained in Section 1.3, this research will be broken into two major phases: theoretical analysis and flight test. The theoretical analysis must be completed before actual aircraft integration or flight tests and includes:

- Derivation of a 3-DOF model with aircraft control

- Construction of the Have ESCAPE TPAs
- DTED analysis
- Aircraft performance categorization
- Terrain characterization model
- TPA propagation times
- Integration method sensitivity analysis

Once the theoretical work is complete, the research will enter the flight test phase and will be conducted using the Air Force's disciplined test management principles, safety guidelines, and flight test techniques established at TPS. Within this construct, the flight test will be organized to achieve an overall test objective utilizing specific objectives based on research goals. If required, each specific test objective will be analyzed using one or more Measure of Performance (MOP). A MOP is an organizational tool to define what actually needs to be evaluated to meet the given specific test objective.

1.4.2 Flight Test Objectives for Have ESCAPE.

The overall test objective is to compare 3 and 5 path limited option Automatic Ground Collision Avoidance System algorithms for climb limited aircraft against optimally derived ground avoidance algorithms. All stated objectives will be evaluated with results presented in Chapter 4. The MOPs for each objective is listed below. The definition of each MOP is defined in Chapter 4.

1.4.2.1 Specific Test Objective 1: Evaluate the 3 TPA Solution.

- MOP 1: Algorithm Path Selection
- MOP 2: Aircraft Response
- MOP 3: Ground Miss Distance

1.4.2.2 Specific Test Objective 2: Evaluate the 5 TPA Solution.

- MOP 1: Algorithm Path Selection
- MOP 2: Aircraft Response
- MOP 3: Ground Miss Distance

1.4.2.3 Specific Test Objective 3: Determine Algorithm Parameters.

- MOP 1: Bubble Size for Level 1 DTED
- MOP 2: Overall Processing Time

1.4.2.4 Specific Test Objective 4: Compare the 3 and 5 TPA solution with the Optimal Solution.

- MOP 1: Proper Path Selection
- MOP 2: Terrain Miss Distance and Activation Time Differences between the optimal and chosen path.

In summary of the research contained herein, the Literature Review of Chapter 2 will provide a baseline for where the current research resides with respect to Auto GCAS. The Methodology outlined in Chapter 3, as well as the Results and Analysis in Chapter 4, are specifically tailored to provide the data and evaluation required to adequately address these stated objectives using the tools and algorithms designed through the theoretical analysis outlined in Section 1.4.1. Finally, Chapter 5 summarizes the results of this research and flight test efforts and offers recommendations for future Have ESCAPE work to ultimately provide a safe, reliable, accurate solution to the problem outlined in Section 1.2. The Appendices within this research include supplementary data to the methodology and results. Appendix A contains the Test Matrix, Appendix B contains the Data Analysis Plan (DAP), Appendix C contains the Form 5314 for post-flight comments, and Appendix D contains all additional plots not presented in the body of the research.

II. Literature Review

2.1 Overview

Collision avoidance systems exist for a variety of real-world applications to include integration with aircraft and automobiles [35]. In fact, these products are becoming more prevalent due to increased computing capacity and generalized trust in systems engineering. Previous research from Kuchar and Yang developed a "framework to categorize Conflict Detection and Resolution (CDR) methods and models for collision avoidance" [21, 22]. They state that "the goal for the CDR system is to *predict* that a conflict is going to occur in the future, *communicate* the detected conflict to a human operator and, in some cases, assist in the *resolution* of the conflict situation" [22, 35]. The following literature review will outline the previous work in automatic collision avoidance as well as describe background information on the tools used within the presented methodology. For this reason, it will be necessary to describe existing technologies, most of which are informative in nature only and do not present automatic solutions to collision events as these algorithms are still in their infancy. Additionally, the required use of DTED and the characterization of terrain necessitates the evaluation of existing terrain morphology research. The existing structure of aircraft classifications will also be discussed briefly in an effort to categorize tactical military aircraft based on performance parameters and operational mission requirements. Finally, since this research has the unique opportunity to gather real-world flight test data, existing research on the Calspan Learjet, to include past flight tests, will be reviewed to present a baseline for the research and provide realistic expectations for the collected data.

2.2 Conflict Detection and Resolution Modeling Methods

Historically, aircraft collision avoidance techniques have focused mainly on air-to-air scenarios. Though different in its intent, air-to-ground collision avoidance models follow the same basic framework. Kuchar and Yang's previously mentioned methodology categorized the CDR techniques into five distinct sections 1) state propagation, 2) state dimensions, 3) conflict detection threshold, 4) conflict resolution method, 5) maneuvering dimensions, and 6) management of multiple aircraft conflicts [22, 35]. Only the first five sections are relevant to this discussion, so the sixth will be ignored. This information was developed through the study of 68 different algorithms [22], and it forms a solid framework summarizing the current application of the solution method for terrain avoidance models.

2.2.1 State Propagation.

Kuchar and Yang speak to three basic methods of state propagation, again under the context of air-to-air conflict resolution as discussed below [22]. The first, and most basic, is the nominal method. In this context, "the current states are projected into the future along a single trajectory, without direct consideration of uncertainties" [22]. Essentially, the nominal method uses aircraft state information to predict only where the aircraft is going. This method is straightforward to apply, but could lack robustness in highly dynamic scenarios or, from a ground collision perspective, in mountainous terrain.

The next propagation technique discussed is the probabilistic method. A typical probabilistic approach will "develop a complete set of possible future trajectories, each weighted by a probability of occurring." This model is more robust than the nominal method, but it presents some difficulty in application. Both the modeling of the trajectories and the computational expense of these models may make this method too slow for immediate application.

The final method is the worst-case projection. "Here it is assumed that an aircraft will perform any of a range of maneuvers. If any one of these maneuvers could cause a conflict,

then a conflict is predicted" [22]. This method allows for worst-case scenario look-ahead trajectories to be calculated so that avoidance algorithms can be applied. This approach can help to determine if a conflict is possible. As applied to air-to-ground avoidance, the method poses a potential solution to state propagation. As used in the research herein, the worst-case methodology can be interpreted as maximum aircraft performance. In this way, multiple aircraft paths can be propagated and analyzed, and since these paths are predetermined, their calculations and control history can be quickly applied. This then allows for the determination of a collision with terrain and an executable maneuver to avoid it.

2.2.2 State Dimensions.

State dimensions represent "whether the state information used in the model involves the horizontal plane, vertical plane, or both" [22]. In general, the majority of air-to-air models cover the horizontal plane or both the horizontal and vertical plane. The necessary planes are merely a function of the avoidance algorithm required to predict and avoid collisions. For air-to-air scenarios, models including only the horizontal plane can be realistically accurate for avoidance techniques. The ubiquitous Traffic Collision Avoidance System (TCAS) is an example of a horizontal plane system whereas the Ground Proximity Warning System (GPWS) uses vertical only [22, 35]. Due to the rugged nature of some terrain, neither the horizontal plane nor vertical plane alone could adequately model the likelihood of an aircraft impacting terrain. For example, a canyon scenario has both horizontally and vertically located features that could cause a collision. For this reason, a 3-dimensional model should be used for automatic terrain collision avoidance systems as will be applied in the research herein [35].

2.2.3 Conflict Detection Threshold.

Conflict detection thresholds are metrics created from the aircraft state information that are necessary to make decisions [21]. "Some examples of conflict detection thresholds

are current range to the point of closest approach (to terrain or to other aircraft) as well as time to point of closest approach, miss distance if no escape trajectory is implemented, maneuvering cost, or probability of conflict" [21, 35]. The key to CDR methods is that they be useful, accurate, and timely. For automatic terrain avoidance systems, the conflict (terrain) threshold needs to relate to some terrain database or real-time measuring equipment. Current candidates include, but are not limited to, Shuttle Radar Topography Mission (SRTM) DTED, terrain following radar, and radar altimeters. Importantly, the terrain information used must be immediately available for not only the current aircraft location, but for all future positions as well. For these reasons, a Digital Elevation Model (DEM) is the most readily available and realistically applicable terrain model for automatic ground collision avoidance algorithms.

2.2.4 Conflict Resolution Method.

The ultimate goal of any conflict resolution algorithm is to avoid a collision, whether that be an air-to-air or air-to-ground collision. The five methods prescribed by Kuchar and Yang are prescribed, optimized, force field, manual, and no method [22]. Only the optimized and prescribed solutions will be described in this research. For more information on the other methods, reference Kuchar and Yang's "A Review of Conflict Detection and Resolution Modeling Methods" [22] or Suplisson's work titled "Optimal Escape Trajectories for Automatic Ground Collision Avoidance Systems" [35].

The optimal control maneuver minimizes a predetermined cost functional to optimize some aspect of the aircraft's performance [35]. Typical methods include maximizing miss distance or generating minimum control inputs to avoid a collision. Admittedly, optimal control is the future of aircraft collision avoidance algorithms from both an air-to-air and air-to-ground perspective. One example is work by Smith on developing a basic framework and working algorithm for specific optimal air-to-air avoidance situations [31]. Unfortunately, these algorithms, though powerful, require extensive computing time and

thus have limited applicability to current aircraft integration for dynamic real-time use. The benefits in the optimal control research stem from their current ability to provide 'truth' data to other algorithms that bridge the technological gap until optimal solutions can be employed in real-time.

Excluding optimal control, another method of conflict resolution is the formulation of pre-planned maneuvers to avoid terrain. "Prescribed resolution maneuvers are fixed during system design based on a set of predefined procedures" [22]. As discussed in Chapter 1, an example of this is the Air Force's F-16 Auto GCAS. It is considered a prescribed solution because it has one predetermined maneuver that it uses for every avoidance situation and it automatically activates taking control from the pilot [1]. With automatic activation, the prescribed maneuvers benefit from the simplicity of design and ease of execution of a preplanned maneuver. Unfortunately, these maneuvers can be less effective because they are not altered based on the dynamic situation [22]. Another method is manual activation. With manual activation, "prescribed maneuvers may have the benefit that operators can be trained to perform them reflexively" [22]. They are performed open-loop, and thus, may require extensive activation buffers to protect against extreme terrain. The major benefit is that they can be integrated quickly and with little computational expense. As introduced in Chapter 1, the proposed research will use a group of predetermined maneuvers to both propagate against the terrain and automatically avoid it if necessary.

2.2.5 Maneuver Dimensions.

The final category of the CDR framework that will be discussed is the manner in which the maneuver is executed. Much like the state dimensions in Section 2.2.2, each maneuver can include lateral components, vertical components, speed changes, or a combination of each to avoid a collision [22]. The nature of air-to-air collision avoidance allows for different control applications to effectively avoid a collision. For example, GPWS uses a

vertical only maneuver dimension [22], while the F-16 Auto GCAS uses both a roll and climb maneuver [1].

The CDR framework developed by Kuchar and Yang was described in some detail because it outlines the basic structure of any aircraft collision avoidance system. As has been explained, there exists a gap in the current literature for the application of this framework for heavy aircraft automatic ground collision avoidance. The current literature provides little insight into the nature of ground collision avoidance, focusing more on air-to-air scenarios. The use of DEMs and aircraft performance capabilities will require additional conflict detection and resolution methods not currently addressed by Kuchar and Yang's framework.

2.3 Terrain Databases

Before a thorough examination of current aircraft ground collision avoidance systems can be described, it is paramount to understand the underlying tools used to model and predict terrain. This research will focus on tools that use terrain databases as opposed to real-time terrain following systems such as radar altimeters or look-ahead terrain following radars. These systems have practical applications, but they are limited in their ability to anticipate terrain at a significant distance ahead of the aircraft and are very limited in their ability to assess terrain laterally. For these reasons, preexisting databases provide the most practical method when comparing to aircraft path propagation. There are three main DEMs that are currently used for terrain analysis [35]. A DEM is "any digital representation of the continuous variation of relief over space" [4]. The main DEM used for the purposes of this research will be the SRTM DTED. The other two DEMs are legacy DTED and the National Elevation Database (NED) [35]. It is important to note that SRTM DTED and legacy DTED are often both simply called DTED although there are inherent differences. For the purposes of this research, the term DTED alone will always refer to SRTM DTED.

2.3.1 SRTM DTED.

Since SRTM DTED is the terrain database used in this research, it will be discussed in detail first. The SRTM DTED was obtained by the shuttle Endeavour on a mission launched from Kennedy Space Center on February 11, 2000 [16]. The shuttle orbited the earth 159 times over 10 days using a special synthetic aperture radar developed specifically for terrain data gathering called the Shuttle Imaging Radar-C (SIR-C) which evolved into the tools used for the mission named C-RADAR and X-RADAR [16]. The data itself was validated against a Global Positioning System (GPS) truth source. The result was 9 m vertical accuracy with the greatest error occurring over steep terrain [16]. One of the major drawbacks of SRTM DTED is that it represents radar returns from whatever object first reflected the energy. As would be expected, areas of dense vegetation or urban centers would return data that is not the bare terrain below [16]. In general, this may result in inaccuracies over these regions, but they are inaccuracies that would cause acceptable, conservative errors. For example, if an aircraft were flying over densely forested terrain, the SRTM DTED would likely have reported the top of the trees as the terrain floor. The provided algorithm would then maintain the aircraft a safe distance from the most relevant threat [35]. In general, it is not recommended to expect this in every situation, but SRTM DTED is, in this way, conservative in nature and thus a good candidate for automatic ground collision avoidance software. Most recently, SRTM-2 data has been released for public use [16]. This DTED has the most detailed resolution obtained by the SRTM and represents a solid foundation for terrain analyses. The data itself is represented as latitude and longitude with a relevant height. For this research, a DTED return will be referred to as a 'post' that is infinitely thin and spaced at a predetermined distance. Table 2.1 shows the post spacing for the different levels of legacy DTED and SRTM DTED. The data was processed by the NASA Jet Propulsion Laboratory in connection with the National Geospatial-Intelligence Agency (NGA) before public release [25].

2.3.2 Legacy DTED.

In short, legacy DTED is a mosaic of different data sources taken over decades with each source having varying degrees of accuracy [35]. Due to the different sources of data, there exists sometimes extreme discontinuities in the information with most of the inaccuracy being in altitude. Unfortunately, incorrect altitude data can cause serious problems for a ground collision avoidance algorithm making the use of legacy DTED unwise. NASA evaluated the use of legacy DTED for its small Unmanned Aerial Vehicle (UAV) Auto GCAS report and found that "although legacy DTED was a useful source in its time it has many issues with discontinuities across latitude-longitude boundaries and localized artifacts that can result in vertical errors of hundreds of feet (in some cases over a thousand feet of vertical error)" [34]. For this very important reason, legacy DTED will not be used for this research since more accurate, practical data is available. Again, Table 2.1 displays the specifications of legacy DTED and SRTM DTED.

Table 2.1: Digital Terrain Elevation Data Types [25, 35]

DTED Level	Post Spacing (arc-seconds)	Post Spacing (Ground Distance)	Cells/Degree
DTED-0	30 arc-sec	900 m	120
DTED-1/SRTM-1	3 arc-sec	90 m	1,200
DTED-2/SRTM-2	1 arc-sec	30 m	3,600
DTED-3	$\frac{1}{3}$ arc-sec	10 m	10,800

2.3.3 National Elevation Dataset.

The final DEM that will be discussed is the NED. The NED is only available for the United States, but it is released to the public and has a higher resolution than SRTM 2 [35, 38]. From a practical standpoint, it is a useful alternative to DTED. Militarily,

it is not consistent with the expeditionary mindset of the United States Air Force. For all practical purposes, Air Force aircraft must be capable of operating all over the globe, and their systems must be usable in all those same locations. For this reason, despite its outstanding accuracy and availability, the NED is not a realistic option for military use. Interestingly, the NASA DROID Small UAV program uses a combination of NED and DTED based on where the UAV is flying [34]. This is a potential solution to the geographically limited NED, but since the current SRTM DTED provides enough detail for the proposed application, it is unnecessary to include the NED in the proposed algorithm herein.

2.4 Existing Ground Avoidance Systems

2.4.1 Fighter Type Aircraft.

A detailed discussion on automatic ground collision avoidance systems can be found in Suplisson [35]. The following fighter review will focus on the systems that are applicable in nature to the presented research with the understanding that other fighter systems, both automatic and manual, exist but they are not specifically relevant to this research.

2.4.1.1 F-16 Auto GCAS.

Any automatic ground collision avoidance discussion typically begins with aircraft that have high historic loss rates as a result of CFIT. Due to mission requirements, pilot task saturation, and aircraft flight profiles, it is fighter aircraft that stand to gain the most from automatic algorithms. For this reason, most literature and technical development about the subject has been related to fighters. Within the United States Air Force, the F-16 Auto GCAS algorithm is fully developed and fielded on Block 40 and 50 F-16s. There was a need for the development of the system as CFIT had become the #1 cause of fatality for fighter aircraft and the Secretary of Defense mandated to reduce mishaps by 50% [35]. The actual algorithm itself differs due to the dynamic capabilities of fighter aircraft. The F-16's Auto GCAS is unique because it "does not assume the pilot is in the loop nor that the pilot

can respond" [35]. The system takes advantage of the fighter's performance and therefore executes one escape maneuver which is a roll to wings level and a 5-g pull to safety [36]. The F-16 Auto GCAS, as of 2014, is being operationally fielded in combat Air Force units. Having already been credited for aircraft and pilot saves [35], there is a need for further work in automated algorithms for other airframes, though direct application of the F-16's system to heavy aircraft is unreasonable due to performance disparities.

2.4.1.2 Navy Terrain Awareness Warning System.

The only other fighter system applicable to the research is the US Navy Terrain Awareness Warning System (TAWS). The TAWS system is interesting because it propagates two predicted trajectories, the Vertical Recovery Trajectory (VRT) and the Oblique Recovery Trajectory (ORT) [26]. The propagation and detection method used in TAWS is similar to the proposed algorithm so it will be discussed in detail with an emphasis on escape path techniques, collision detection, and system-aircraft-pilot interface. In general, the benefit of TAWS over previous Navy systems such as GPWS is that it provides a look-ahead capability [26, 35]. "TAWS uses SRTM Level 1 DTED for the high-speed fighter and attack aircraft to provide the forward-looking capability not possible with radar altimeter alone" [35]. The VRT path propagated by the TAWS system provides a wings-level roll and 5-g pull, similar to the F-16 Auto GCAS [35]. The ORT is still a 5-g pull but it maintains the current level of bank [3]. The actual propagation of the ORT path is interesting because the number of iterations is a function of the aggressiveness of the maneuver. For example, at higher bank angles and roll rates the ORT is shorter and, thus, less propagated iterations are required [35]. This is an important consideration because it prevents overlapping iterations from occurring and it helps to minimize computational requirements. Computational speed is a major factor in the present research and the TAWS path length adaptation helps minimize these propagation times. "TAWS also provides the pilot directive visual cues for how to perform a manual recovery to avoid the terrain"

[35]. This added benefit will not be included as part of this research, but the infrastructure provided by this research will make such a tool possible in the future.

The F-16 Auto GCAS and Navy TAWS have been successful programs, and both have been credited with aircraft saves [35], but they still lack the robustness required to protect heavy type aircraft. Both systems take advantage of their respective airframe's enhanced performance capabilities. Due to these abilities, no additional functionality based on type of terrain is included or necessary. Terrain type, as discussed in Section 3.8.3, is another issue that will need to be addressed for heavy aircraft. In addition, extra considerations for avoidance maneuvers will be necessary to successfully detect and deconflict terrain for larger, less maneuverable aircraft.

2.4.2 Heavy Type Aircraft.

As previously stated, there are many preexisting systems in the aircraft that alert the pilot to the location of the terrain. The following section will focus on the systems dedicated to avoidance alone and/or that have forward looking capabilities for heavy aircraft.

2.4.2.1 Air Force Terrain Awareness and Warning System.

Similar in name to the Navy's system, the Air Force uses TAWS in some of its heavy aircraft such as the C-17 [7]. The C-17 version of the system is used in multiple capacities, from normal high-altitude flight, to low-level missions, to approach and landing [7]. The system needs some crew interaction based on different modes of operation to include Normal Mode, Tactical Mode, and Runway Mode [7]. TAWS will work in default upon power-on, but its more robust tactical and runway modes need to be hand selected. Additionally, TAWS can provide adjustable altitude settings for operation in the low-level environment [7]. The system itself is advisory in nature only and has no automatic control authority, though it does present its results on a color Multi-Functional Display (MFD). Figure 2.1 shows the MFD output.

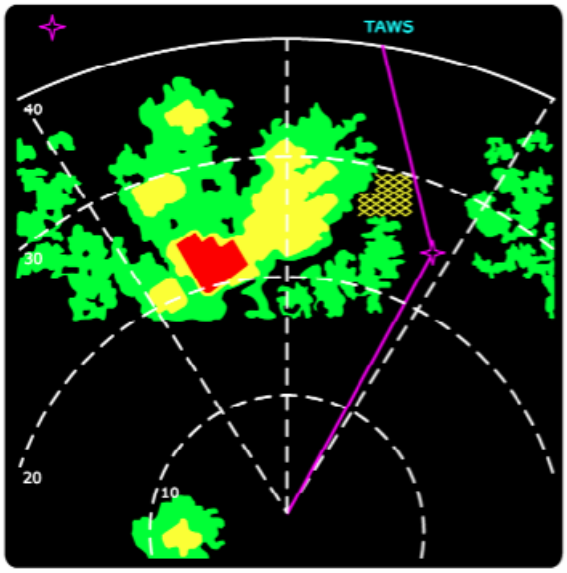

Figure 2.1: C-17 TAWS MFD Color Output [7]

The color display shows the location of the most prevalent threats and color codes them based on the height of the object and the altitude of the aircraft. The system also includes an aural warning of "TERRAIN, TERRAIN" "when the clearance over the terrain/obstacle is predicted to be less than a minimum clearance height. The prediction is based on a straight ahead climb calculated from aircraft capabilities, configuration, and standard crew reaction times" [7]. Since this is a manual only system, the single propagated path is sufficient because the system assumes an aware pilot and functions only in an advisory role. TAWS is the most robust of the heavy aircraft terrain avoidance systems, yet it will not prevent controlled flight into terrain and it does not anticipate aircraft maneuvers outside of a straight ahead climb. Interestingly, in an effort to avoid nuisance warnings, the system can be manually set to 0 ft, which would prevent any indications to be sent to the pilot at all [7]. The biggest functional benefit is the pilot's display which can give advance notice for impending terrain. In general, this system is excellent for advising the pilot of terrain, but

its lack of automatic control and its inability to provide warnings for lateral objects limits its functionality in preventing CFIT.

2.4.2.2 C-17 Ground Proximity Warning System.

The GPWS system for heavy aircraft is addressed next since it does provide input on terrain avoidance, but the system has no forward look-ahead, and thus is not extremely relevant to the discussion outside of its mere existence. The system is designed by Honeywell and can be found on all US jet transport aircraft [35]. "The GPWS inputs include the aircraft configuration (flap and gear positions), radar altimeter, barometric altitude, vertical velocity, glide slope deviation, and pilot inputs" [7]. As with TAWS, the crew has input into the level and amount of reporting from GPWS, though warnings in the flight publications mandate that the system remain active [7]. Additionally, GPWS has six alerting modes based on different flight profiles and terrain collision scenarios [7, 35]. Functionally, the system only looks straight down from the aircraft's current location and makes a calculation based on distance and closure to present an indication to the pilot [7]. One of the major uses of GPWS is to advise the crew of aircraft configuration issues based on the current flight profile (i.e. landing gear extension due to a flight path matching a landing approach). The algorithm is not predictive in nature, nor does it use any specific DEM to determine the location of the terrain below. In general, GPWS is a good tool to make the pilot aware of current, potentially dangerous flight situations, but it is not meant as a tool to evaluate terrain or propagate information forward, and it does not make any automatic corrections. As a note, "US Federal Aviation Administration (FAA) Circular AC23-18 [published] in 1974...mandated that all large turbine and turbojet commercial aircraft install GPWS" [14, 35].

The presented tools for heavy aircraft, TAWS/GPWS, are valuable aids for increasing pilot situational awareness. Each tool is adequately integrated into the avionics of the aircraft and they both benefit from weight and configuration information [7]. Unfortunately,

the tools will not prevent CFIT if the pilot does not take action to manually recover the aircraft. The major takeaways from both systems is that sound integration with the existing avionics can allow for added flexibility in the programming of the software. Without it, conservative estimates on aircraft performance must be made to cover all flight envelopes. In general, this could degrade flight performance, increase computational expense, and cause unnecessary nuisance warnings. For these reasons, a long term goal should be to integrate proposed automatic collision avoidance systems into each aircraft's specific flight computer to take advantage of the real-time configuration information.

2.4.3 Remotely Piloted Vehicles.

The last system discussed and the most relevant Auto GCAS algorithm was recently tested by NASA on a small remotely piloted vehicle, a.k.a. UAV, and it is the conceptual starting point for this research. The paper titled, "Small UAV Automatic Ground Collision Avoidance System Design Considerations and Flight Test Results," outlines the methodology and flight tests of their algorithm [34]. The system will be discussed in detail in the next three sections as many of the findings and recommendations are germane to this research. The program based much of its initial design requirements on the F-16 Auto GCAS so there are considerable similarities between the two, yet NASA's team modified the algorithm to take into consideration the performance differences of the small UAV. The following discussion focuses on the terrain model, conflict detection, and conflict resolution algorithm.

2.4.3.1 Terrain Model.

Interestingly, NASA's system uses an Android phone embedded with the required DEM information and the Auto GCAS algorithm coded in Java [34]. The point of using this device was to prove that the data and logic can be encased in a small lightweight system with limited storage capacity, a major concern for relatively small and under-powered UAVs. "It was determined that the best widely accessible DEM source for Auto

GCAS applications was the National Elevation Database produced by the United States Geological Survey (USGS)" [34]. Since this database contains only data for the continental US, SRTM DTED was used for areas not inherently covered by the NED. In an effort to make DEM information more accessible and applicable to differing mission sets, NASA developed numerical techniques to generate Compressed Digital Terrain Maps (CDTMs) that compressed the world's data from 400 G Bytes to 170 M Bytes with minimal loss in accuracy [34]. The two numerical methods were named "Tip-Tilt" and "semi-regular tree networks" [34]. The Tip-Tilt method was a means of making the model of the terrain more accurate to the actual slope of the terrain without using as many data points. Figure 2.2 displays an example output of the terrain algorithm.

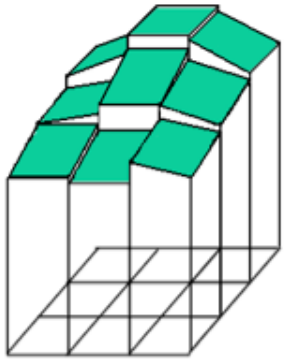

Figure 2.2: Tip-Tilt Algorithm Output [34]

The Tip-Tilt method "used linear regression to fit the sloped tile to the terrain data underneath it" [34]. This method admittedly reduces accuracy, but the tiles were built to minimize a targeted error tolerance, so that the data would be sufficient for Auto GCAS while modeling the terrain more closely with less data [34]. The semi-regular tree networks created in CDTM are simply a way to model large areas of similar terrain with far fewer

data points [34]. For example, in the Great Plains, one large "tile" could accurately cover a large portion of ground without requiring the numerous underlying data points. The combination of these terrain modeling techniques are part of a tool called the Global Elevation Data Adaptive Compression System (GEDACS) [34]. The combined effects can be seen in Figure 2.3. These techniques formed the terrain model used in NASA's small UAV program.

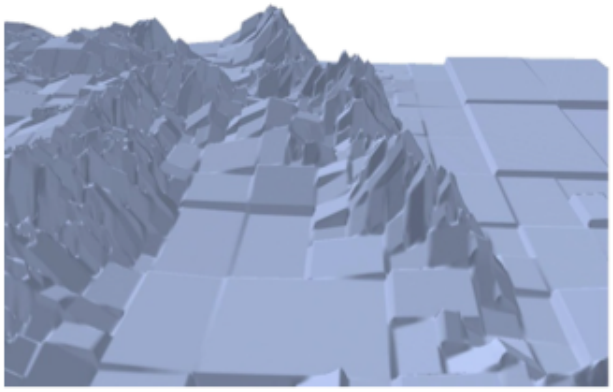

Figure 2.3: Global Elevation Data Adaptive Compression System Example [34]

2.4.3.2 Small UAV Conflict Detection.

As previously mentioned, performance limitations in heavy aircraft and UAV platforms necessitates the need for conflict detection methods that differ significantly from fighter platforms. NASA's small UAV employs a terrain detection process that utilizes the three avoidance paths, plus uncertainty, that the aircraft would potentially use to avoid terrain [34]. The detection method analyzes the terrain below each of the three paths using the GEDACS model discussed in Section 2.4.3.1. Much like the F-16 Auto GCAS, NASA's

algorithm takes into account an allowance for track and navigation uncertainty [34]. Figure 2.4 shows the terrain 'scan' method using NASA's algorithm.

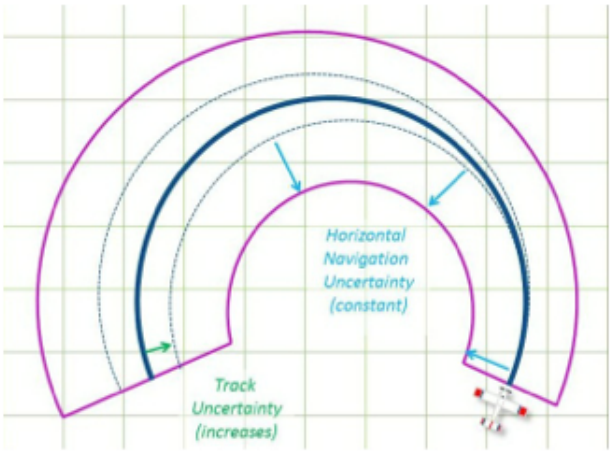

Figure 2.4: NASA Small UAV Turning Terrain Scan Pattern with Uncertainty [34]

As can be seen, the detection path (the total scanned terrain for a given maneuver), outlined in magenta, grows as position uncertainty increases for the model. It is important to note that for a small UAV, much of the track inaccuracy will be a function of wind, which has a large effect on small, light, slow aircraft [34]. NASA recommends that wind should be included in the path prediction model if the wind magnitude will be greater than 15%-30% of the aircraft speed [34]. The specific detection path algorithm used by NASA evaluates each DTED bin that the aircraft path uncertainty space overlays. For example, the gridded squares in Figure 2.4 each represent a rasterized bin space around each DTED (or NED) post which would be found at the center of each rectangle. If the path touches one of those rectangles, then the system evaluates its corresponding bin elevation. The final product will, as a result, effectively scan more data points than if the inclusion of the post alone

was used. The model then predicts if a collision is to occur based on bin height and aircraft altitude buffers [34].

2.4.3.3 Small UAV Conflict Resolution.

The three paths used in NASA's algorithm are built on performance assumptions for a typical UAV type platform and include a forward path, a left path, and a right path. The conflict resolution is based on a "last man standing" approach. The system evaluates each propagated path and determines if a collision with terrain is anticipated for each of the three as described in the previous section. If all intersect terrain, than the last one to predict a collision is implemented [34]. The forward path is propagated as a wings level climb, capturing 1000 Feet Per Minute (fpm) climb and 60 Knots Indicated Airspeed (KIAS), [34]. The turning paths were planned to be symmetric with 40° of bank capturing 800 fpm climb and 60 KIAS [34]. The actual paths intersecting with terrain can be seen in Figure 2.5.

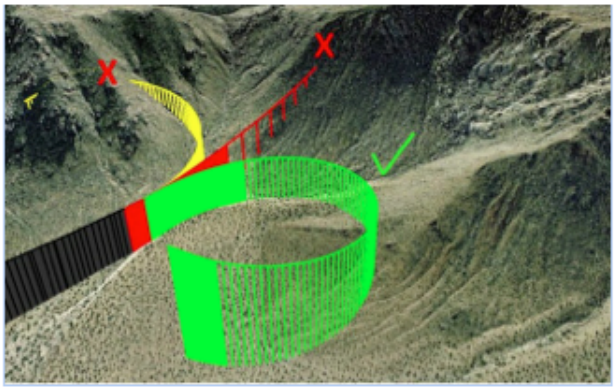

Figure 2.5: NASA Small UAV Avoidance Maneuvers and Conflict Resolution [34]

The resolution approach used by NASA assumes that the pilot is purposely flying near terrain to accomplish a mission objective, therefore, the last man standing approach allows

the mission objective to be accomplished until an aggressive maneuver is necessary to avoid terrain. This method is also useful in avoiding nuisance activations. NASA also states that "a full six degree of freedom simulation is not required to model the trajectory predictions" [34]. Since the specific path of the UAV is modeled with an uncertainty buffer, the path includes all the terrain than can actually be covered so exact precision in the propagation equations is unnecessary. This subsequently helps improve computational speed which is a driving factor for system performance. Additionally, it is recommended that the avoidance paths use a large portion of the available maneuvering capabilities of the aircraft [34]. This helps prevent nuisance activation because the aircraft is only analyzing terrain at the limits of its capabilities which is typically far greater than what would occur during normal operations.

The information obtained from NASA's small UAV program is a great knowledge base for a transition of Auto GCAS to heavy-type aircraft. NASA's analysis lays the framework for path propagation and detection for aircraft that do not have fighter performance capabilities. Additionally, it addresses multiple recommendations for future work that will be utilized by the research herein.

2.5 Equations of Motion

As stated in Section 2.4.3.3, 6-DOF is unnecessary for the actual calculation of the EOM governing the propagation of the aircraft's paths. The work by Raghunathan et al. titled, "Dynamic Optimization Strategies for Three-Dimensional Conflict Resolution of Multiple Aircraft," outlines a 3-DOF model that can accurately represent aircraft motion over a shortened interval [28]. The research was specifically designed for air-to-air deconfliction using optimal conflict resolution algorithms [28], but it has been proven to have applications beyond air-to-air. In fact, Suplisson's research uses Raghunathan's methodology in her optimal Auto GCAS algorithm [35]. "The key concept in [Raghunathan's] paper is a mathematical programming-based dynamic optimization

framework for the accommodation of detailed dynamic aircraft models for the purposes of construction of optimal conflict-free trajectories for a given aircraft set" [28]. The model itself, also referenced in Section 3.2 with subsequent simplification, is formulated as follows:

$$\dot{x} = V\cos\gamma\cos\chi + v_{Wx} \tag{2.1}$$

$$\dot{y} = V\cos\gamma\sin\chi + v_{Wy} \tag{2.2}$$

$$\dot{z} = -V\sin\gamma + v_{Wz} \tag{2.3}$$

$$\dot{V} = \frac{T\cos\alpha - D - MG\sin\gamma}{M} \tag{2.4}$$

$$\dot{\gamma} = \frac{(T\sin\alpha + L)\cos\phi - Mg\cos\gamma}{MV} \tag{2.5}$$

$$\dot{\chi} = \frac{(T\sin\alpha + L)\sin\phi}{MV\cos\gamma} \tag{2.6}$$

where the states, $\dot{x}$, $\dot{y}$, and $\dot{z}$ are velocity in the flight path direction, lateral direction, and vertical direction respectively. Additionally, V is ground speed, γ is flight-path angle, χ is heading angle [31] and g is gravity. The model assumes a point mass and is a practical representation of aircraft dynamics [28]. The proposed equations assumes a constant air density, though this could be altered in real-time with look-up tables. Additionally, the model takes into account winds, v_W, though as addressed in Section 2.4.3.2, this can be neglected for larger, faster aircraft. The simplified derivation of this 3-DOF model has been used accurately in past simulations for both air-to-air and air-ground applications [31]. Longer propagation timelines will obviously cause increased inaccuracies that can make the states of the aircraft unusable for collision detection purposes. For this reason, care must be taken in determining propagation lengths, or higher fidelity equations must be employed. This important point will be addressed in detail within this research. In general though, these equations and subsequent research have proved viable for aircraft collision avoidance applications.

2.6 Terrain Morphology

As part of the research, a proposed mapping of terrain will be performed to establish requirements on how long to propagate the EOM. Some background information on these topics is provided next. An area of concern often overlooked with respect to Auto GCAS algorithms is a characterization of the terrain below the aircraft in an effort to group terrain in larger classification structures to determine path propagation lengths. The information for the terrain classification already exists within the inherent DEM data the systems use to evaluate conflicts, but it is not currently characterized efficiently. This section will address relevant research concerning terrain morphology, classification, and existing Air Force terrain regulations.

2.6.1 Terrain Characterization and Modeling.

Typical methods to classify terrain have been through field survey, or aerial photographs [10]. In general, these methods are time-consuming, labor intensive, and somewhat inaccurate when compared to the existing level of refined data. Fortunately, "integrating satellite, aircraft and terrestrial RS systems to achieve a scale-dependent set of observations can be achieved through operational systems and current technologies" [10]. Typically, terrain analyses have been a direct function of the desired end-state application. This has caused numerous classification schemes that are difficult to interpret outside of their intended use. More robust methods using topographic derivatives such as slope, aspect, profile curvature, topoclimatic index and slope length can now be easily obtained making classification schemes more adaptive and useful. Using this information, a need has arisen to identify a classification of landforms that cover vast swaths of land yet still be applicable to other data sets [10]. The method proposed by Dragut et al. will "delineate areas of relative homogeneity within the spatial layers of topographic variables such as slope and curvature." This methodology uses profile curvature, plan curvature, slope gradient, and altitude to characterize and group terrain. It looks at the whole picture

over a large area of terrain and defines the landforms based on dominate features and slope. The benefit to this is that it applies a generalized view of the terrain instead of just focusing on one feature. This prevents one steep hill in the Great Plains from skewing the larger classification structure. Dragut's research classifies landforms in three hierarchical levels [10]. The levels consist of Upland, Midland, and Lowland with varying sub-levels. These levels were established based on a relative elevation criterion. "Relative altitudes were used...to develop a classification system applicable to different datasets" making it easily transferable [10]. The major takeaway from this research is that it is possible to categorize terrain into only three categories based on generalized landforms and slope information. The actual use of the classification will still be somewhat application specific, but the inherent framework has been established.

2.6.2 Additional Digital Elevation Model.

Section 2.3 contained the discussion on the most relevant terrain databases. Another digital elevation model titled the 3D Elevation Program, is currently being designed by the United States Geological Survey (USGS) and it has the potential to be a useful tool for terrain elevation information within the United States. In fact, one of its stated applications is "improved elevation data for cockpit navigation and flight simulators" that should "save lives each year by reducing accidents resulting from the inability to safely fly over obstacles in airspace" [32]. The end state goal for the model is to replace the NED. The 3D Elevation Program will "systematically collect enhanced elevation data in the form of high-quality light detection and ranging data" [32] over the US. This product will eventually be a useful upgrade to the NED and it will provide an additional option for aircraft integration. Unfortunately, the information will only be available for use over the conterminous United States [32] and, thus, has limited military application.

2.6.3 Air Force Terrain Classification.

For flying purposes, the Air Force classifies terrain in only two categories, mountainous or non-mountainous. Air Force Instruction (AFI) 11-202 Volume 3 outlines this delineation. "In the absence of other Major Command (MAJCOM) guidance, USAF aircrews shall consider as mountainous: those areas defined in 14 Code of Federal Regulations (CFR) §95.11 for the continental US, Alaska, Hawaii and Puerto Rico. For all other areas of operation, use a 500 ft surface elevation change over a $\frac{1}{2}$ Nautical Mile (nm) distance to define the location of mountainous terrain" [18]. This classification is legacy in nature and was designed for the overarching use of the military fleet. It is not aircraft specific nor is it designed for specific mission use. Its general use is to define a minimum altitude for flight over certain areas, typically much higher than low-level altitudes. The usefulness of this application is that it defines specific mountainous areas over the US, while still allowing some flexibility for those areas that are not defined. It also gives insight into the Air Force's categorization of mountainous terrain.

2.7 Aircraft Performance Classification

This section will cover the Air Force's current classification scheme with respect to aircraft. An understanding of the existing classifications is important because, as noted previously, aircraft performance capabilities can dramatically affect flight dynamics and anti-collision maneuvers. Classifying aircraft allows for generalized Auto GCAS algorithms to be built that should seamlessly integrate into a variety of aircraft, thus decreasing production costs.

Currently, the Air Force categorizes their aircraft based on mission/type or via performance classes. The classification based on mission is usually denoted by the letter prefixing the formal aircraft designation. For example, the 'F' in F-16 stands for fighter, whereas the 'C' in C-17 stands for cargo. There are numerous other classifications, but in general, all the designations are generic in nature and can cover a wide swath of aircraft

performance capabilities. For example, there is a large difference between the propeller driven C-130 and the heavy jet transport, the C-5. For this reason, a more detailed delineation is required.

The military also classifies aircraft for the purposes of military acquisition standardization [8]. The MIL-STD-1797 outlines this classification in detail and Table 2.2 outlines the basic descriptions of each. In general, this classification is more fitting for automatic

Table 2.2: MIL-STD-1797 Aircraft Classification [8]

Class I	Class II	Class III	Class IV
Small Light	Med Weight/Agility	Heavy Weight/Low Agility	High Agility

ground collision avoidance software since it addresses the maneuverability potential. Unfortunately, there can still be large discrepancies within the same class. For example, a B-1 Lancer bomber aircraft and a C-17 Globemaster would both fall under Class III. They both are categorized as heavy aircraft with low-to-medium agility, but they both operate at very different speeds [8]. Large variations in speed, upwards of 150 kts, drastically changes look-ahead propagation times and aircraft maneuverability. For this reason, the classification standard may not be suitable for ground collision avoidance software. There exists a need to classify aircraft in a manner that groups them both on performance and mission if applicable. Section 3.8.2 will address this issue.

2.8 Calspan Learjet Flight Test Background

One of the major objectives of this research is to conduct flight tests to evaluate the performance of the Auto GCAS algorithm in a real-world scenario. The testbed for this will be the Calspan Learjet flown from Edwards AFB. “Calspan Corporation has been the primary innovator, developer, and operator of in-flight simulators in the United States as

well as the rest of the world" [40]. The presented research will take advantage of the Calspan Learjet's VSS to safely operate the algorithm without the opportunity for critical flight safety errors occurring. The Learjet was chosen by Calspan because it met the requirements to host a VSS, and it had wings capable of high roll rates that would allow it to closely model fighter type aircraft [40]. Figure 2.6 shows the actual aircraft that will be used in flight test for this research.

Figure 2.6: Calspan Learjet Photo [40]

The VSS is a 4-DOF system with upgrades that allow pre-programmed gains to be quickly changed in flight [40]. This modification is unique and beneficial for Auto GCAS research as different aircraft gains can be quickly chosen to test a program against different airframes. "The VSS is designed to take commands from either a pilot onboard the aircraft, a sensor operator in the main cabin, a UAV operator on the ground, or an autonomous control algorithm. The system architecture is set up such that extensive validation and verification testing is not required before flight" [6]. Currently, the Calspan Learjet has been involved in 21 different flight test programs three of which include automatic activation in some capacity. Additionally, software within the Learjet is specifically designed for integration with MATLAB, the underlying source code for this project's algorithm. For

these reasons, the Calspan Learjet is the best available TPS flight platform to conduct Auto GCAS testing.

2.9 Summary

This Chapter reviewed the relevant literature pertaining to aircraft avoidance models, DEMs, terrain characterization, aircraft classification, aircraft EOM, and germane flight test assets. The presented review displays that some required information remains to be analyzed and a multi-path algorithm for manned heavy aircraft has yet to be realized. The way forward requires an evaluation of different military aircraft as well as a classification for terrain so that the proposed algorithm can have applicability across airframes with different capabilities operating in all corners of the world.

III. Methodology

3.1 Introduction

The following chapter will outline the methodology leading to the flight test of project Have ESCAPE. This will entail a derivation of the 3-DOF EOMs that will propagate aircraft paths forward in time. This will include transitioning between reference frames and altitude realizations required for actual aircraft integration. Additionally, terrain classifications and aircraft performance characterizations will be introduced and defined to specify essential algorithm parameters such as path propagation length and protective sphere size. Also, a sensitivity analysis on the integration methods will be presented to maximize computational efficiency. Finally, the flight test methodology will be presented in detail to include test resources, the test matrix, the data analysis plan, and flight conduct requirements. In the end, this chapter will outline the tools required to gather the data to meet the stated research objectives that are analyzed in Chapter 4.

3.2 Equations of Motion

The equations of motion used to propagate the potential escape trajectories forward for the proposed algorithm must strike a balance between physical accuracy, computational efficiency, and required flight dynamics. As described in Chapter 2, a 3-DOF non-linear point mass model, built based on simplifying assumptions of the standard 6-DOF model, can be used to accurately depict the performance of the escape paths over their propagated timeline. The primary objective of this model is to accurately predict the aircraft state for a maximum of 45 seconds. In general, for low maneuvering aircraft where response times are not on the order of fractions of seconds and for scenarios that are not increasingly dynamic nor requiring extremely high fidelity state information, this model will provide the appropriate amount of accuracy and speed [31]. From a controls standpoint the subsequent

3-DOF model will, when necessary, command the autopilot or VSS of the aircraft using only, bank angle (ϕ) for lateral control and load factor (N_z) for z-axis control [31].

3.2.1 Derivation of the 3-DOF Model.

As described in Chapter 2, the 3-DOF Model used by Raghunathan et al. [28] appears in Equations (2.1-2.6) [31]. The calculation of the state laws in the following formulation of the aircraft equations of motion follow directly from Newton's Second Law, $a = \frac{F}{M}$ with specific derivations as referenced from Raghunathan et al. [28] and the following discussion. Figure 3.1 displays the basic aerodynamic forces acting on a generalized aircraft and is the origination for any flight dynamics mathematical development. Eq. (3.1)

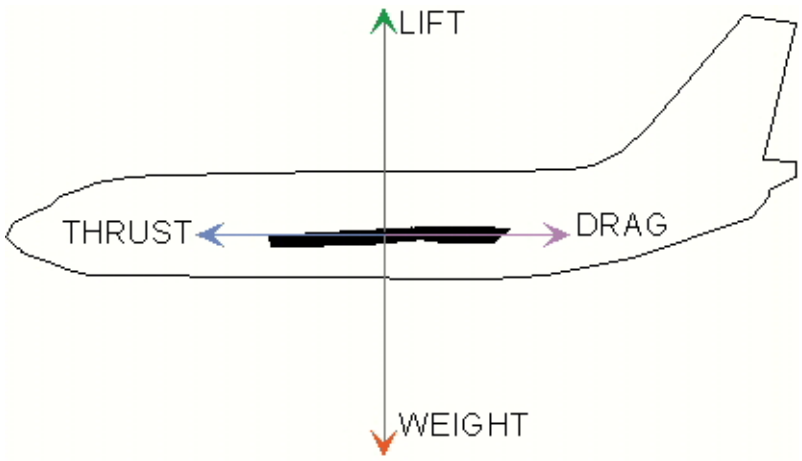

Figure 3.1: Basic Aerodynamic Forces [33]

and Eq. (3.2) are a result of the summation of the forces in the longitudinal and vertical axes.

$$mN_z = L + T\sin\alpha \tag{3.1}$$

$$T\cos\alpha - D = mg\sin\gamma \tag{3.2}$$

Within these equations, M is mass, L is lift, T is thrust, and D is drag. The angle α is the angle between the aircraft chord line and the resulting free stream if the aircraft had a non-zero angle of attack. More specifically, Eq. (3.2) shows that the force components along

the longitudinal (x-axis) would sum to zero meaning that the aircraft is not accelerating and thus the velocity is constant. This is another simplification of the point mass model, though over short intervals it does not significantly alter a solution and, in this analysis, it is assumed that the aircraft is operating at its tactical low-level airspeed. It is understood that an application of the autopilot will require a change in thrust to maintain a constant airspeed throughout the maneuver. Some aircraft, such as the C-17, have this capability inherently. For other platforms, pilot action or aircraft upgrades may be necessary and are beyond the scope of this research. An additional assumption is that the sideslip angle (β) is zero and the side force is negligible [31] which is reasonable with modern flight control systems that automatically remove sideslip and "are standard aircraft assumptions for this type of application" [31]. A more in-depth review of the EOM can be found in Raghunathan and Bicchi [2, 28]. A further simplification will be made for the purpose of this analysis by setting wind, v_{Wx}, v_{Wy}, and v_{Wz} to zero in Eq. (2.1) through Eq. (2.3). The terms can be easily added for future use if required. It is understood that winds will change the dynamics depending on their direction and magnitude, but for a generalized solution, the zero wind approximation will suffice, and a constantly updated aircraft position and fast computational speed will help mitigate these effects. As previously stated, research from NASA has concluded that winds can be considered negligible unless they are more than 15%-30% of aircraft speed [34]. Additionally, typical aerodynamic terms such as thrust, drag, mass, angle of attack, and coefficient of drag are simplified using 3-DOF approximations and the relationships in Eq. (3.1) and Eq. (3.2).

These equations allow for the aforementioned aerodynamic forces to be solved for in terms of N_z and γ. To do this, Eqns. (3.1 & 3.2) are substituted into Eqns (2.4-2.6) resulting in the five state equations, Eq.(3.3-3.7) [31]:

$$\dot{x} = V \cos\gamma \cos\chi \tag{3.3}$$

$$\dot{y} = V \cos\gamma \sin\chi \tag{3.4}$$

$$\dot{z} = V \sin\gamma \tag{3.5}$$

$$\dot{\gamma} = \frac{N_z \cos\phi - g\cos\gamma}{V} \tag{3.6}$$

$$\dot{\chi} = \frac{N_z \sin\phi}{V\cos\gamma} \tag{3.7}$$

Equations (3.3-3.7) form the developed 3-DOF model used in this research and they represent the equations of motion that will propagate the aircraft escape paths forward using the controls N_z and ϕ. It is important to note that the flight path angle and heading angle are not fixed for the purpose of this analysis and will change based on the initial aircraft state and control trajectories. Limits will need to established for each of these parameters for safety of flight concerns. In general, the state of the aircraft will be such that it ultimately recovers to a position that avoids obstacles and is within a flyable envelope for transfer of control back to the pilot. Future research could use optimization techniques within the flight dynamics to fly this maneuver minimizing a predetermined cost functional and ultimately facilitating command back to the pilot after the maneuver is complete.

3.2.2 EOM Scope.

As discussed in Section 3.2, it is necessary in all cases to constrain vertical acceleration, bank angle, and flight path angle so that the aircraft maintains a safe operating regime throughout the automated maneuver. The flight dynamics in the EOMs are independent of aircraft type and do not explicitly contain protections against unsafe flight parameters. For example, there is no predetermined limit on the flight path angle which could theoretically allow the aircraft to climb to angles that would cause an unrecoverable stall. To prevent this situation, specific limits have been set. For heavy aircraft, it was decided that 15° is a practical limit that balances the need to avoid terrain vertically without presenting a dangerous situation. It is understood that some aircraft will be able to outperform this climb angle while others may require a lower value. The same situation would be necessary for bank angle, but this control is set specifically for each escape path and paired with an appropriate N_z to prevent excessive bank angles. For example, the

lateral paths are set at 60° of bank and 2 g's. This will result in a level turn and never put the aircraft at risk. Admittedly, there exists aircraft that may require more or less stringent controls which would require specific alterations to the EOM, but in general, the presented equations and limits are conservative for most tactical aircraft. The limits are currently set at $-60^\circ \leq \phi \leq 60^\circ$ and $0g \leq N_z \leq 2g$.

3.2.3 Aircraft Control.

One of the main research objectives for this study is to control the Calspan Learjet through its VSS with preplanned escape maneuvers. For this to occur, a control history for each maneuver must be established so that bank angle (ϕ) and vertical acceleration, (N_z), can be sent to the aircraft and executed if a collision with terrain is imminent. With physical accuracy and computational speed being important analysis factors, two different control history methods were analyzed, a polynomial fit, and a time/control matrix look-up to maneuver the aircraft. In either case, the control itself had to be calculated from desired aircraft maneuver capabilities and flight path accuracy. This resulted in control vectors specific to each avoidance maneuver that will be propagated forward.

First, the decision was made to avoid a polynomial fit and instead execute a matrix look-up for the control. The choice was based on the inaccuracies of a polynomial fit within the function propagating the EOM. Specifically, a low-order polynomial fit, though computationally cheap, would cause physical inaccuracies due to its predictive nature of future control. On the other hand, the evaluation of the matrix look-up can be executed exactly at the timestep, and it can be predetermined once. This negates the need to recalculate the control vector at every propagation step. Additionally, a predetermined matrix look-up will allow for easy, autonomous integration with any aircraft flight control. It should be noted that smoothing of the control vector may be required due to actual flight dynamics.

The forward path control is a vector of N_z's fit to a specified time vector. The N_z vector was calculated based on the first time at which the propagated forward path reached both 14° and 15° flight path angles (γ). These times are important because 15° is the flight path angle limit so 14° represents the point where N_z would need to begin decreasing to a steady-state value to maintain 15°. The vector was built assuming an initial 2-g pull, essentially 1 g more than level flight. The control remains constant until 14° is reached. At this point, a linearly spaced decrease in N_z is applied to reach the N_z that holds 15°, approximately 0.96 g. The N_z required to maintain 15° was calculated using Eq. (3.6), solving for N_z where $\dot{\gamma}$ and ϕ equal zero. This simplifies to Eq. (3.8).

$$N_z = \cos\gamma \tag{3.8}$$

From here, a time step of 0.001 seconds over a 60 second window was used to build the vector. These numbers were chosen because 0.001 is a much finer step than will be executed in the actual integration and 60 seconds is well past the point of where a constant flight path angle would be reached. Once calculated, the vector was analyzed against the truth code propagated by ODE45. It was found that the presented control was within 0.3 s of the 14° and 15° benchmarks.

The lateral path's N_z and ϕ were calculated differently. For this reason, they can be chosen independent of the equations of motion. The relationship in Eq. (3.9) is used to relate bank angle and load factor.

$$N_z = \frac{1}{\cos\phi} \tag{3.9}$$

The bank angle was calculated based on an accepted roll rate for heavy-type aircraft. For this analysis, a roll rate of 15° per second was chosen. This is a reproducible roll rate for low to high speed aircraft. It must be noted that higher performance aircraft may benefit from a faster roll rate, though, 15° per second is a reasonable estimate for all considered airframes. This roll rate was multiplied by the same time vector previously mentioned and limited to 60° of bank. This vector now contains all the bank angles, at very small intervals to get the

aircraft to 60° at 15° per second. The bank vector is then inserted into Eq (3.9) to create the corresponding N_z vector. From a sensitivity standpoint, the simulated model has a max deviation over the time interval of less than 1 meter in altitude for the level maneuver, an easily acceptable error range. The effective and simplistic nature of these control algorithms allow for easy application to different aircraft or different missions based on roll or pitch restrictions that may be imposed due to high gross weights. This same control algorithm is used for each additional path or for more maneuverable aircraft with different g and flight path angle limits.

3.3 TPA Description

Now that the path control has been established, it is necessary to outline how the control will be used to design the avoidance paths. Two different algorithms will be researched. The first is a three-path avoidance algorithm while the second is a five-path avoidance algorithm. The three-path solution takes advantage of the maximum maneuver capabilities in both the vertical and lateral directions. In the vertical direction, it is comprised of a forward path that is a direct 2-g pull up to a 15° flight path limit (or as required by aircraft performance parameters). The lateral right and left paths are designed with a 2-g 60° level banked turn. These three path maneuvers are designed to protect against obstacles that can be out-climbed as well as obstacles that must be avoided with a turn. Figure 3.2 shows the maneuvers graphically with the associated numbering scheme.

The five-path avoidance algorithm uses the three maneuvers already described as well as two lateral-up maneuvers. These two additional paths are, again, mirror images of one another in the right and left directions. They are executed with a 15° roll in one second followed by a 2-g pull with a 15° flight path angle limit (or as required by aircraft performance parameters). The maneuver is meant to limit asymmetric g by accomplishing the roll then the pull. Figure 3.3 shows the maneuvers graphically with the associated numbering scheme. Ultimately, these two different algorithms will be researched to

determine which provides the most effective protection against collisions with terrain and whether more or less paths are necessary for adequate ground collision avoidance.

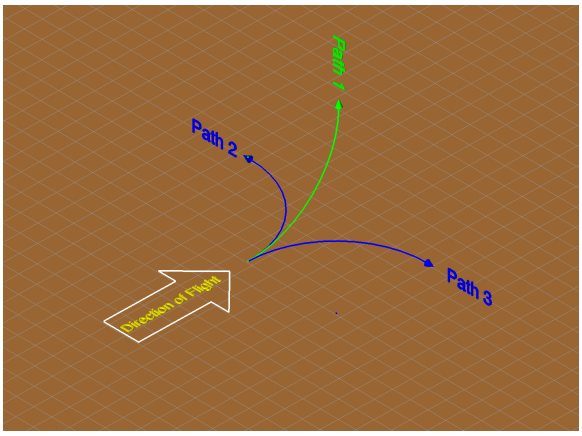

Figure 3.2: Have ESCAPE 3-TPA Path Graphic

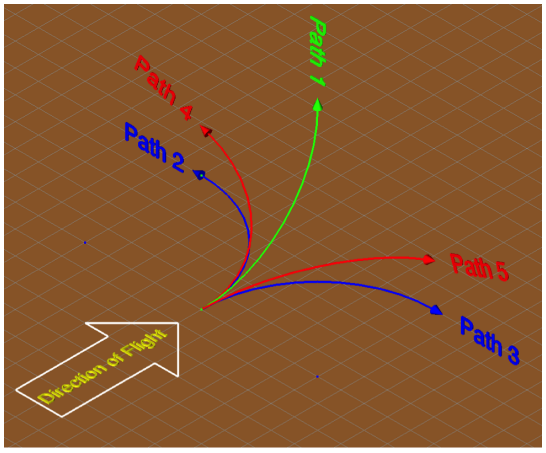

Figure 3.3: Have ESCAPE 5-TPA Path Graphic

3.4 Reference Frames

For conflict detection it is necessary to determine the relative aircraft position to the relevant DTED posts, and thus it is necessary to translate reference frames. The aircraft's native geodetic frame must be converted to a local Cartesian based East-North-Up (ENU) reference frame suitable for the EOM used to propagate the aircraft's state forward. For navigation purposes, "east, north, up coordinates are essential in determining the line of sight for terrain data given as latitude, longitude and height, such as DTED" [11].

To begin, a thorough explanation of both reference frames is required. The geodetic reference frame used by the aircraft is specifically defined by the Conventional Terrestrial Reference Frame (CTRF) system utilizing a terrestrial pole, center of mass of the Earth, and a reference meridian. The current realization of this reference frame is the World Geodetic System 1984 (WGS-84) utilizing the Greenwich Meridian. This system is used as the predominant navigation tool by the DoD and for aircraft Inertial Navigation System (INS)/GPS data. To define a location using the described geodetic reference frame, it is necessary to specify three parameters: [Latitude, Longitude, Height]. Conventionally for aircraft use, latitude and longitude are in units of degrees-decimal-degrees and height is in units of feet. Unfortunately, typical aircraft equations of motion are designed around a local origin and propagate along a Cartesian reference frame. For this, the ENU frame is appropriate.

The ENU reference frame is a local-level frame that is defined at any arbitrary point along the Earth's surface. The frame itself is tangent to the Earth at the frame's user-defined origin and can be thought of as a flat surface with positive directions defined as East and North with the Up vector defined positive pointed away from the Earth's center in the form [East, North, Up].

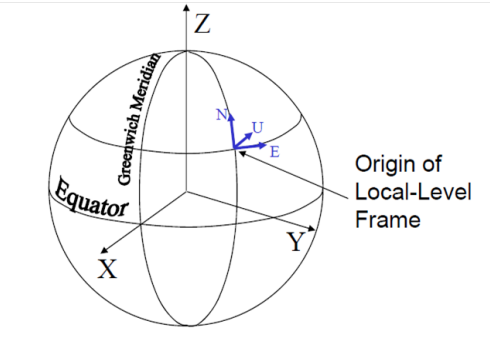

Figure 3.4: East-North-Up Reference Frame overlay [29]

Figure 3.4 displays a representation of the frame as it would be viewed on an overlay of Earth. The benefits of this frame include the ease of path propagation from a specified point in a manner that is intuitive and computationally inexpensive. Additionally, the units can be arbitrarily set within the constraints of the EOM.

To implement the rotation, it is required to obtain the current aircraft position passed from the Learjet's combined INS/GPS data. Once obtained, the current position is defined as the initial position for propagation purposes, but it still must be rotated into the ENU frame. The inherent MATLAB command, 'geoedetic2enu', accomplishes this rotation within the WGS-84 system. To do this, the function requires the initial aircraft position over the terrain, the current aircraft position and altitude, as well as an ellipsoidal reference. Obviously, for this analysis, the Earth was used as the function reference within WGS-84. This initial aircraft position now serves as the ENU local-level frame origin and all path propagation will occur based on this specified point. The differential equations governing the aircraft's motion will provide an ENU vector with distances away from this point for the required time interval. Each specific escape path for a given origin will be evaluated for a collision with terrain and, if no impact is expected, the new (updated from the INS/GPS) aircraft position will act as the new origin and the process will repeat. Essentially, the

algorithm will calculate new origins and escape paths for each aircraft position reported or within the constraints of computational speed.

3.5 Height and Altitude Realizations

Up to this point, height and altitude (elevation) have been used nearly interchangeably. Unfortunately, there are multiple different realizations of height and altitude that must be addressed for the effective use of the presented algorithm. The three main heights that will be discussed are Mean Sea Level (MSL), Height Above Ellipsoid (HAE), and Geoid Height. An accurate representation of height is imperative for proper rotations between reference frames, exact analysis of impending collision with terrain, and precise interactions with the aircraft's VSS. Figure 3.5 shows the relationship between the three different altitude representations discussed.

"WGS-84 provides an ellipsoidal model of the Earth's shape. In this model, cross-sections of the Earth parallel to the equatorial plane are circular. The equatorial cross-section of the Earth has radius 6,378.137 km, which is the mean equatorial radius of the Earth. In the WGS-84 Earth model, cross-sections of the Earth normal to the equatorial plane are ellipsoidal" [19]. Within this model, the major axis is the same as the mean equatorial radius, the semi-minor axis is 6,356.752 km, with an eccentricity, e^2, of 0.0066944. This ellipsoidal model is useful as it allows for a mathematically specific surface from which accurate calculations can be made. From this definition, HAE is defined as the altitude above (positive) or below (negative) the WGS-84 reference ellipsoid. In reality, the Earth is not a perfect ellipsoid and WGS-84 does not accurately reflect the height above the ground all over the Earth, nor does it form a practical platform for aircraft navigation.

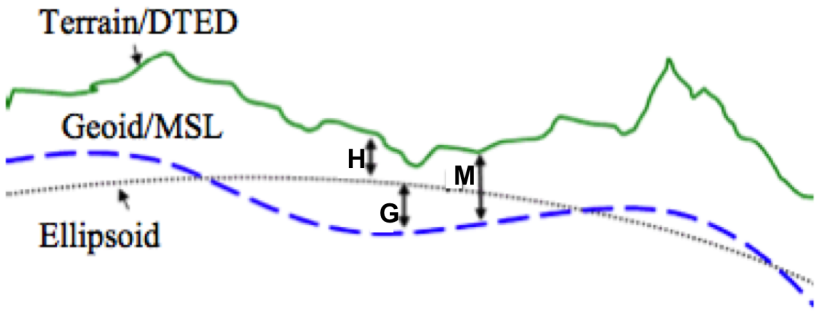

Figure 3.5: Graphical Representation of Different Altitude Realizations [12]

Nearly all aircraft navigation, both civilian and military, use MSL altitudes as the primary source of information for both altitude reporting purposes and operational application. Heights above MSL are referenced from Earth's geoid, or surface of constant gravitational potential. There are an infinite number of geoids, but the most commonly used one aligns with global mean sea level when viewed from a least squares sense [19]. This geoid is often referred to as the 1996 Earth Geopotential Model (EGM-96) and is the standard for reference with WGS-84 [12]. The geoid itself is not constant across the earth and varies with the earth's density and geographic topography at a specific location.

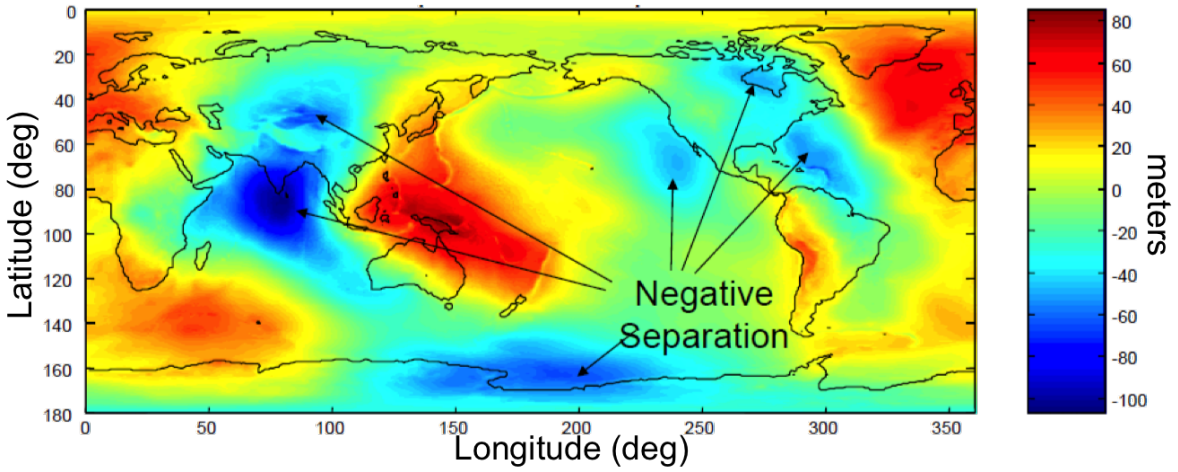

Figure 3.6: Map of Earth's Geoid Separation [29]

Figure 3.6 displays the geoid undulation across the entire Earth. As can be seen, the separation between the geoid and Earth's ellipsoidal model can vary drastically and must be applied appropriately for accurate altitude modeling. Eq. 3.10, referring back to Figure 3.5, displays the relationship between MSL altitude, HAE, and the Geoid where M is MSL altitude, H is HAE, G is geoid height [12].

$$M = H - G \tag{3.10}$$

For analysis purposes, all altitudes were converted to HAE allowing for consistency with numerous MATLAB functions used to rotate reference frames and propagate the aircraft's position forward in time. Specifically, the functions 'geodetic2enu' and 'enu2geodetic' require the use of HAE as they perform rotations to and from the ENU reference frame. Additionally, all altitudes are maintained in HAE as the aircraft paths are propagated using 'ODE45'.

Current DTED data provides elevation in the vertical datum using MSL [9] and, as stated previously, aircraft elevation is reported in MSL. For this reason, prior to

propagation, Eq. (3.10) is used to transform all altitudes to HAE. As can be seen from Figure 3.6, this transformation varies based on the specific location on the globe. This analysis interrogated 58,000 geoid heights in the area of interest between N 35.1^o to N 35.3^o and W -117.3^o to W -117.5^o and found that the average geoid height to be -31.783 m with a standard deviation of 0.113 m and a maximum error of less than 0.3048 m. This set value was then added to every MSL value for both the DTED and reported aircraft altitude to provide all elevations in HAE. Prior to passing this information back to the aircraft, the local geoid undulation is subtracted from the HAE elevations to again provide MSL altitude. In this way, aircraft position and altitude is accurately compared against DTED data to provide precise information on potential terrain collisions.

3.6 Aircraft Terrain Protection

3.6.1 Protective Sphere.

As discussed previously, there have been multiple methods developed to prevent aircraft collisions with the ground, most of which require a specific setting chosen by the pilot to provide some form of audible or visual warning to initiate a manual recovery. The presented algorithm is similar in that it allows for a manual (if desired) setting for a terrain buffer, but it propagates that buffer forward in predetermined paths to anticipate impending collisions. To do this, an algorithm utilizing a sphere around the aircraft was employed with the basic equation: $x^2 + y^2 + z^2 = r^2$. This sphere assumes the aircraft is at its center and is propagated forward through multiple predetermined escape paths simulating, at each time step, where in space that aircraft would be positioned. In essence, the sphere acts as a safety buffer from terrain and can be adjusted within the algorithm based on tactical or strategic needs. The sphere itself is important because its basic dimension, the radius, will be used to evaluate whether a collision occurs with the terrain. This sphere can now be checked for 'contact' with the terrain. This requires models of the ground below using

DTED and an ability to quickly search and analyze it for each propagated path. This will be addressed in the next two sections.

3.6.2 DTED Analysis.

DTED is a result of a combined effort between NASA and the NGA. The "targeted landmass consisted of all land between 56 degrees south and 60 degrees north latitude, which comprises almost exactly 80% of Earth's total landmass" [39]. The NGA provided three products with the collected data named DTED0, DTED1, and DTED2 [39]. Typically, the level of data is referred to by the numerical suffix i.e. level 0, level 1, or level 2. For the purposes of this analysis, level 1 and level 2 will be used. It is important to note though that each lower level is simply a 'thinned' version of the one before it with level 2 being the most dense. Specifically, level 2 utilizes a post spacing of 1 arc-second which equates to 30 m spacing at the equator while the DTED post spacing for level 1 is thinned to 90 m spacing [39]. This length will decrease as distance increases North or South of the equator.

From an operational perspective, there is a benefit to utilizing level 1 over level 2. With less inherent data, level 1 allows for integration into platforms that are memory limited. Additionally, it provides for faster computations since less DTED posts will be analyzed for a given sphere radius. For these reasons, level 1 will be the default DTED data utilized. There are situations, though, that require the use of level 2 data. For example, imagine a scenario where a protective sphere with radius 145 ft is desired for a flight at or near the equator utilizing level 1 DTED. A 145 ft radius creates a sphere with a diameter of 290 ft or approximately 88.4 m. This sphere could predictably travel across the map in-between posts, thus not reporting any potential collisions with terrain that may be occurring. Additionally, it is physically impossible for more than two DTED posts to be captured and analyzed for any given iteration. For this reason, a determination must be made to mandate a minimum sphere size, or logic must be created to implement level 2 data below a specified sphere radius. This decision has both tactical and computational implications.

The current algorithm allows for future decisions on the process, by including logic to switch to level 2 DTED when a radius below 300 ft is chosen. A 300 ft radius is a strong balance between operational necessity and computational speed. First, it is uncommon for heavy or fighter type aircraft to fly below 500 ft though, in some situations, clearances to 300 ft are allowed. Additionally, a radius of 300 ft will ensure a minimum of four DTED posts are geometrically captured on each iteration as can be seen in Figure 3.7. A maximum of six posts is possible .

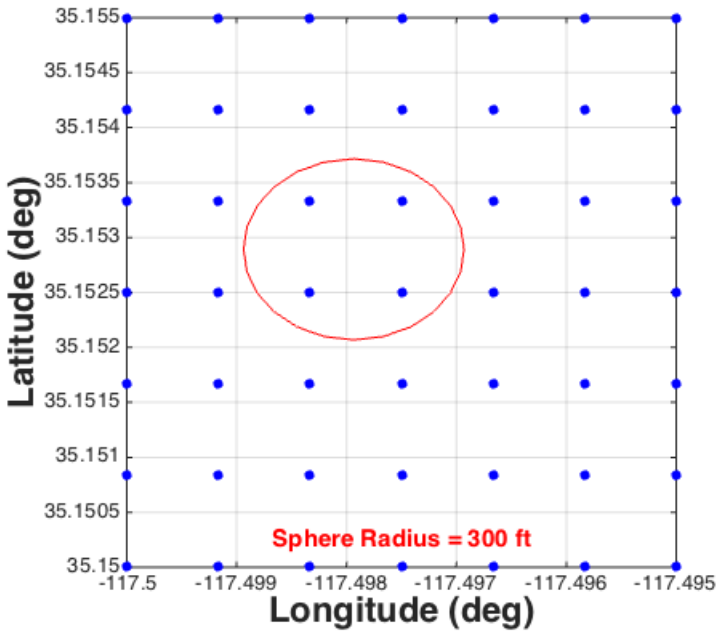

Figure 3.7: Sample Level 1 DTED Spacing with Minimum Four Captured Posts

A minimum of four captured posts is ideal because they will essentially cover a quadrant of terrain below the aircraft and will minimize missing large deviations in the height of terrain. In this way, DTED level 1 can be used in a large majority of anticipated situations, but level 2 should be available for contingency purposes. In fact,

it is recommended that DTED level 2 only be loaded on memory-limited aircraft if flight below 300 ft is anticipated or desired.

3.6.3 DTED Post Capture.

Prior to the evaluation of a potential collision with terrain, it is necessary to capture the DTED posts that are shadowed by the sphere above. To do this, an effective and computationally efficient representation of the 2-D sphere shadow on the ground had to be determined. Fortunately, degrees of latitude are consistent everywhere and can be directly correlated with the radius of the selected sphere. Unfortunately, the issue is complicated by the fact that degrees of longitude decrease in size as one travels North or South of the equator. Due to the non-uniform ellipsoidal shape of Earth, it was necessary to create a polynomial fit (5^{th} order was used for this research) to the change in distance between degrees in longitude based on a specified degree of latitude.

Table 3.1: Degree of Longitude Distance based on Latitude Position [20]

Deg Latitude	Distance (km)
0	111.32
10	109.64
20	104.65
30	96.49
40	85.39
50	71.70
60	55.80
70	38.19
80	19.39
90	0

Table 3.1 displays the data used to create the polynomial fit. This data, given at every 10° of latitude, provides a shell to formulate accurate and computationally efficient approximations of the distance between a degree of longitude at any latitude. The 5^{th} order polynomial is shown in Eq. (3.11)

$$y = -7.82\times10^{-10}x^5 + 4.86\times10^{-7}x^4 - 3.69\times10^{-6}x^3 - 0.0168x^2 - 2.16\times10^{-4}x + 111.32. \quad (3.11)$$

In this equation, x is the deg of latitude in question which will result in y, the distance between a deg of longitude in kilometers, at that latitude.

The following process is the method used to search and collect the necessary DTED. The actual algorithm to determine a potential collision is addressed in Section 3.6.4. Actually identifying the DTED posts presented a trade-off between geometric accuracy with respect to the 2-D sphere shadow and computational speed. The specific tool used to acquire the DTED posts was a rectangle (or square at the equator) and not the expected circle. The rationale for this decision stemmed from the logic required to add or remove DTED posts shadowed by the sphere. It was determined that, since DTED is already effectively gridded, it would be easier and faster to identify the posts in a quadrilateral than a circle. Additionally, the algorithm required to determine if a collision has occurred can more efficiently exclude the DTED posts than the MATLAB calculations necessary to remove posts inside the rectangle but outside the circle prior to the threshold calculation.

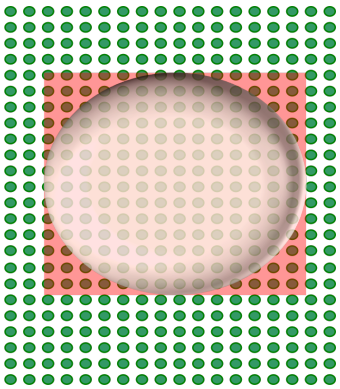

Figure 3.8: DTED Capture Logic based on Sphere Radius

Figure 3.8 graphically displays how extra DTED posts will be identified using the radius of the sphere to create a rectangle (or square at the equator) to shadow the DTED.

The DTED posts were physically identified by simply converting the radius of the sphere into degrees based on the position of each particular sphere over the terrain. For degrees latitude, the formulation was direct since there is little variation. The circumference of the Earth from pole-pole is approximately 40,007 km, therefore, each degree is 111.13 km apart as shown in Eq. (3.12).

$$\frac{40,007\ km}{360^o} = 111.13\frac{km}{deg} \tag{3.12}$$

Longitude is slightly more difficult, because as addressed previously, the shape of the earth causes a non-uniform distribution of distances between degrees. For this reason, the polynomial fit given in Eq. (3.11) is used, and it is found to be accurate within a hundredth of a kilometer. With this information, all of the DTED posts within a sphere's radius (converted to degrees based on position) of the current calculated position are gathered if they fall between the north-south distance in latitude and the east-west distance in longitude. This forms the rectangle in Figure 3.8.

3.6.4 Terrain Collision Detection Algorithm.

The next step in determining whether a collision can occur is to evaluate the identified DTED posts against the location and altitude of the sphere. To do this, an algorithm was developed (aptly named an 'inside-outside' function) that relates the position of the sphere to the DTED posts. Eq. (3.13) is the basic equation of a sphere with radius 'r' and the logical starting point for the algorithm.

$$(x-a)^2 + (y-b)^2 + (z-c)^2 = r^2 \text{ with center } [a, b, c] \tag{3.13}$$

From here, the equation is normalized by dividing by r^2 and subtracting the position of the propagated aircraft from the position of the DTED. Eq. (3.14) shows this formulation.

$$\frac{(x_{DTED} - x_{A/C})^2}{r^2} + \frac{(y_{DTED} - y_{A/C})^2}{r^2} + \frac{(z_{DTED} - z_{A/C})^2}{r^2} = 1 \tag{3.14}$$

Before this calculation can be performed, it is necessary to once again rotate reference frames. Currently, the DTED is gathered in degrees in the geodetic reference frame whereas the aircraft's propagated position is in meters in the ENU reference frame. For this reason, each DTED post is rotated into the ENU frame before this calculation is executed.

To make this computationally efficient, a matrix formulation was developed to quickly generate a solution using MATLAB.

Let:

$$Q = [(x_{DTED} - x_{A/C}),\ (y_{DTED} - y_{A/C}),\ (z_{DTED} - z_{A/C})] \tag{3.15}$$

$$N = \begin{bmatrix} \frac{1}{r^2} & 0 & 0 \\ 0 & \frac{1}{r^2} & 0 \\ 0 & 0 & \frac{1}{r^2} \end{bmatrix} \tag{3.16}$$

Then a collision occurs IF and only IF:

$$QNQ^T \leq 1 \tag{3.17}$$

If Eq. (3.17) is less than or equal to 1 for any point in the escape trajectory then a DTED post has intersected with the protective sphere. This calculation is performed for each

identified DTED post at each iteration for all specified escape paths. Once all DTED posts have been evaluated, the results of whether or not a collision occurred are determined at each iteration.

3.7 Collision Logic

3.7.1 Algorithm Priorities.

Ultimately, auto GCAS is a tool to provide backup to the pilot in times of disorientation or task saturation. To this end, the program itself must be robust, yet it cannot interfere with normal operations or put the aircraft in harm's way. Air Force Research Laboratory (AFRL) has developed three priorities that extend to the application of this algorithm. The first priority is that the auto GCAS must 'do no harm'. This means that when initiated the program does not harm the aircraft or pilot, nor does it put the aircraft in an unsafe position [36, 37].

The second priority is that auto GCAS must not impede mission operations [36, 37]. Typically, this priority addresses nuisance warnings or unnecessary activation of the system during normal operations. There are two main issues presented by this priority. First, the system assumes that the pilot is not aware, and that Auto GCAS is a last-second life-saving system [35]. This directly results in the second issue that auto GCAS will not activate until all calculated escape paths have collided with terrain. Conservatively, the program could be programmed to activate as soon as one escape path collides with the terrain. This, though, would cause numerous activations when the pilot potentially has ample room to maneuver and would definitely impede tactical operations. For this reason, the 'when' of execution leans toward a last-chance mentality much like the current F-16 auto GCAS where these priorities initially originated.

The last priority is that the program must prevent ground collisions [36, 37]. This is the 'it must work' priority and it is the focus of this research. Interestingly, this is the last priority. Placing it third means that situations could reasonably occur where collisions

with terrain happen without the activation of auto GCAS if either of the previous two priorities are not met. Ultimately though, these priorities allow for seamless integration into tactical operations without extensive retraining or integration instructions since the software should work without much, if any, pilot interaction and no workload increases. In general, "there are two potentially competing objectives when it comes to auto GCAS performance; preventing ground collisions while not impeding normal operations (nuisance potential)" [35]. Table 3.2 below displays the three priorities as outlined by AFRL.

Table 3.2: Auto GCAS Priorities

Priority	Objective
Priority 1	Do No Harm
Priority 2	Do Not Impede Ops
Priority 3	Avoid Ground Collisions

3.7.2 Algorithm Logic.

To adhere to the three stated priorities in Table 3.2, it is necessary to provide logic that analyzes each path and determines if a collision occurs. As emphasized in Priority 2, the algorithm revolves around a 'last man standing' logic tree. The main takeaway is that each path must collide with terrain before an auto GCAS activation will occur. If any path has not collided, the system will remain in standby. The algorithm looks at each path independently, as it is calculated, and determines if any DTED post penetrates a propagated sphere (satisfies Eq. (3.17)). If that occurs, the code flags the specific path and relates it to the propagation time. The time itself is specified as the time it would take the aircraft to reach that point on that specific escape path at the current and preplanned parameters. It is

important to note that the time is not the time until auto GCAS execution, but simply the time until the collision occurs. The logic is built such that only the first collision on each path is tracked. It is reasonable for a scenario to exist where the same path collides with terrain multiple times, especially if the path continues through a large land mass such as a mountain.

Once the auto GCAS system evaluates each path, it looks at the entire scenario and determines if paths have collided. A typical program run would determine if a collision occurred by evaluating each path asking the same question, "does a collision occur?" If the answer is 'yes' for each path, then the system executes. The program does this by assigning either a collision time or a value of '-1' to a path. A '-1' is a numerical placeholder to denote that no collision has occurred. If all the paths are greater than or equal to zero, then all paths have collided (they all have a collision time). In this instance, the algorithm chooses the path that collides last (at the latest time) as the executable maneuver. This is done for two specific reasons. First, choosing the path that collides last falls directly in line with the 'last man standing' logic used to determine if the algorithm should execute. Essentially, it means that this was the pilot's last avenue of escape before automatic control was initiated. Secondly, and most obviously, this path happens furthest in the future and, thus, provides for the most maneuver time for the aircraft. There is a 0.5 s time safety margin built into the algorithm so that the aircraft will actually miss the terrain once all three paths collide. This look-ahead feature helps minimize nuisance activations, allow for available reaction time (addressed in subsequent sections), and is a function of aircraft speed. For this research, 0.5 s should be acceptable for all situations. Figures 3.9 and 3.10 graphically display the projection of the TPAs and the avoidance logic.

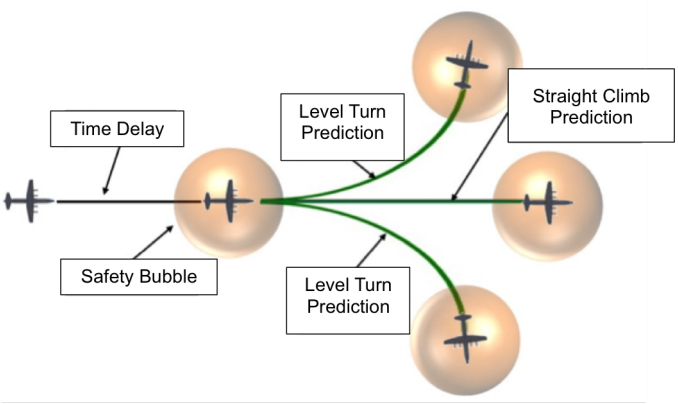

Figure 3.9: Projection of Terrain Avoidance Maneuvers

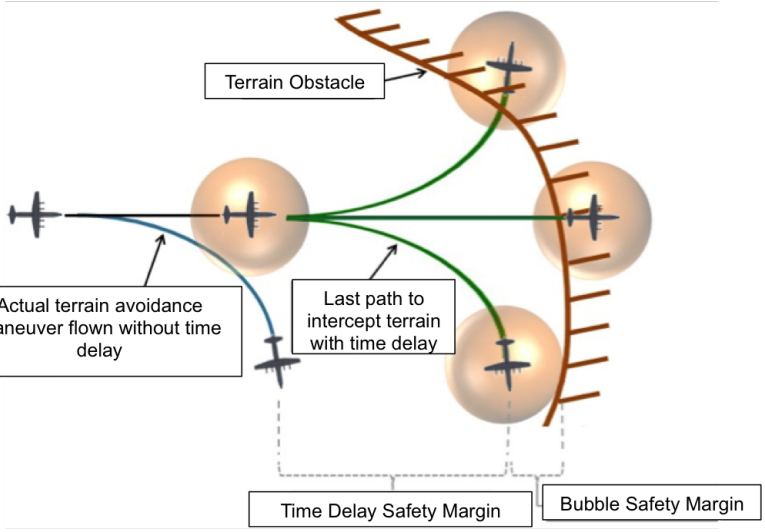

Figure 3.10: Time Safety Margin

Finally, if at any point along the decision process the system evaluates that no collision has occurred (i.e. a '-1' fills any spot in the collision matrix) then it remains in standby and

continues to run in the background with no notifications to the pilot and without control initiated on the aircraft.

3.7.3 Simulation Products.

At each reported aircraft position, the algorithm produces two products that allow for simulations and research on different terrain obstacles. These products will not be included in actual, real-time aircraft test flights, but only as a tool to evaluate the performance of the program pre/post flight or for research purposes. The first product is a collision report and the second is a graphical collision summary. The products essentially display the same information, one is textual whereas the other is graphical. Figure 3.11 shows a collision report for the first four iterations of a simulated flight.

```
Iteration 1
No Automated Path Deviation Required
Collision Report:
No Path Collided with Terrain
Elapsed time is 0.561781 seconds.

Iteration 2
No Automated Path Deviation Required
Collision Report:
No Path Collided with Terrain
Elapsed time is 0.170451 seconds.

Iteration 3
No Automated Path Deviation Required
Collision Report:
No Path Collided with Terrain
Elapsed time is 0.166622 seconds.

Iteration 4
No Automated Path Deviation Required
Collision Report:
Forward Path Collided 7.46 seconds from start
Right Path Collided 5.96 seconds from start
Elapsed time is 0.167280 seconds.

Iteration 5
Execute Left Path
Collision Report:
Forward Path Collided 3.71 seconds from start
Left Path Collided 4.46 seconds from start
Right Path Collided 3.71 seconds from start
Elapsed time is 0.170846 seconds.
```

Figure 3.11: Collision Report

As can be seen, the information reported includes whether an activation occurred and which path, if any, was executed, which paths collided with terrain and when that collision occurred, and the total elapsed time for the calculation of the algorithm. The elapsed time only includes the time necessary to determine if a collision happened. It does not include calculations that would be completed prior to the flight or plotting for simulation purposes. Therefore, it is a fairly accurate representation of the real-world processing time albeit in MATLAB. The requirement is to process at or faster than the aircraft's INS update rate. Of note, the first iteration is longer (0.561781 s) simply due to the initial MATLAB processes

when the simulation first begins. This would not be an issue during actual flight since the algorithm would already be activated.

The example in Figure 3.11 displays a few situations that are worth comment. The iteration number is equal to the number of position and state updates sent from the aircraft to the program. For example, iteration 1 is the first time the program received an update, iteration 2 is the second and so on. Each iteration includes a full run of the program, calculating each path and determining whether a collision occurs. The next line of the report states if an automatic activation was required and, if so, which path was chosen. This entails the logic used in Section 3.7.2. The next three to four lines breakdown which specific paths collide and when those collisions occur. This allows for a sanity check that the correct path was chosen or that an activation should have occurred. Iterations 4 and 5 in Figure 3.11 show the situation where two paths collide in iteration 4 and the program continues to iteration 5 where the all three paths collide and the program evaluates an impending collision.

The second product is a graphical representation of the path collision based on each iteration. This view is helpful to quickly determine which path collided with terrain. Figure 3.12 shows an example chart for the same data in Figure 3.11.

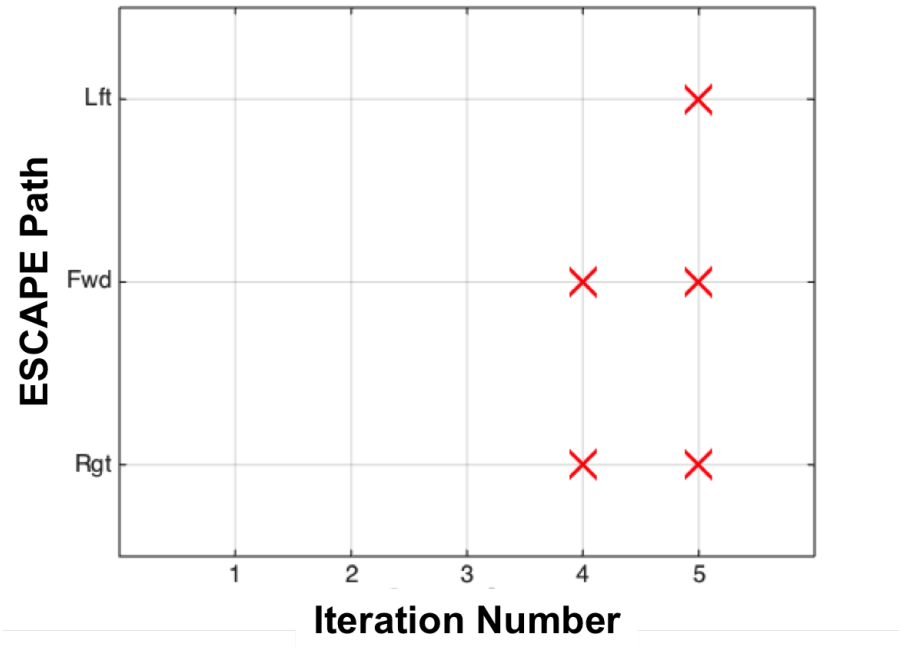

Figure 3.12: Graphical Collision Report

As can be seen from this example, there were no collisions until the 4th iteration when the right and forward paths collided with terrain. This agrees with the report shown previously and the system would intervene and make the appropriate maneuver to prevent a collision at iteration 5 by choosing the left level path. This would be path 2 from Figure 3.2. Iterations will continue for each position and state update from the flight computer for the entire flight or until activation occurs. Again, the aforementioned products are designed specifically for research or simulation purposes and will not be displayed or used in real-world flight tests.

3.8 Determination of Escape Path Time

3.8.1 Background.

With respect to aviation, there remains a gap for the characterization of terrain beyond the specifications of mountainous and non-mountainous described in Chapter 2 [15, 18].

This binary classification works well for aircraft operating in the high altitude environment above 10,000 ft. Unfortunately at lower levels, it is insufficient insofar as tactical low-level operations are concerned and especially when dealing with computer generated algorithms utilizing the terrain. The two opposing factors here are safety and computational speed. The further forward in time the program evaluates terrain the more time it takes to compute which, in turn, limits the algorithm's ability to execute in a timely manner. For these reasons, it is necessary to classify both the terrain and aircraft type differently than in the current literature and then use this classification to make calculated decisions on how far forward in time and space to propagate each escape path. These classification requirements are necessary so that aircraft and terrain can be logically grouped. Once grouped, it is possible to assign escape path times. As stated, the required methodology must focus on aircraft performance data as compared to terrain features to take advantage of climb or turn performance depending on the terrain features presented. The following section will address all of these issues as well as develop the methodology for determining an appropriate escape path propagation time based on these criteria. Finally, the system should be simple enough that pilots (or mission planners) will actually use it. The point of this research is to provide a nearly seamless integration into the cockpit with very little pilot input, not to make aviators pour over maps before each mission for a system that should work inherently. The presented classification systems and subsequent results are a step in that direction.

3.8.2 Aircraft Performance.

Chapter 2 explains the current structuring of aircraft classifications. Again, this method does not take into account the significant operational differences between the multiple heavy aircraft that operate at low altitude. To begin the classification process, it is necessary to obtain the performance characteristics of these aircraft. Specifically, low-level ground speeds are necessary so that rate and radius information can be calculated

for general performance classifications. Personal correspondence with the 418^{th} Flight Test Squadron (FLTS) and 419^{th} FLTS at Edwards AFB provided the information about the capabilities of each aircraft of interest [24]. These squadrons have specific low-level missions and are the primary flight test units for both bomber and cargo aircraft for the United States Air Force. Table 3.3 outlines mission and performance parameters for these aircraft [5, 24]. Airframes such as the B-2 Spirit and the C-5 Galaxy are purposefully absent from the table since they do not currently have a low-level mission.

Table 3.3: Military Aircraft Low-Level Flight Parameters [5, 24]

Aircraft	Airspeed (kts GS)	Altitude (ft)	Radius (ft)	Rate $\frac{deg}{sec}$
C-130	210	300-500	2,254	9.01
C-17	310	300-500	4,912	6.10
B-52	310	500	4,912	6.10
B-1	540	500	14,906	3.50

The radius and rate information presented in Table 3.3 are extrapolated from the given airspeed and the 2 g load factor requirement for the most aggressive escape path maneuver at 60° of bank. It is important to note that 2 g's was used for each aircraft as this is the g required for a level 60° turn and within the performance specifications of each aircraft in Table 3.3. The rate and radius were calculated using Eq. (3.18) and Eq. (3.19) [23] where g is gravity, n is load factor, and V is velocity from Table 3.3:

$$Radius = \frac{V^2}{g\sqrt{n^2 - 1}} \tag{3.18}$$

$$Rate = \frac{g\sqrt{n^2 - 1}}{V} \tag{3.19}$$

With this information, certain conclusions can be drawn. First, there are easily separable speed classifications: low, medium, and high, relating to the C-130, C-17/B-52, and the B-1 respectively. Speed is used as an identifier because it has significant impact on the rate and radius of a maneuver and how much ground is covered over a specific time interval. For these reasons, the aircraft will be collected into these three categories and classified as such for the purposes of this analysis. Table 3.3 will be used in two ways. First, the low-level speed will be used within the presented algorithm to determine how far over the ground the forward escape path will propagate for a given altitude climbed. Second, the radius information, a direct result of rate, will be used to ensure that a minimum 90° of turn are achieved in the lateral direction for a given escape path propagation. Since there is such a large disparity between the radii of the low, medium, and high speed aircraft, it is prudent to categorize them separately.

3.8.3 Terrain Classification.

As previously mentioned, it is necessary to provide a new terrain classification that will be both logical and easily applied in an operational setting using existing tools. In an effort to maintain some relation to the current classification structure, the gauge for mountainous terrain, $\geq$ 500 ft change in altitude in $\frac{1}{2}$ nm, will not change as defined in AFI 11-202 Vol 3 [18] though the title Upland will now be assigned to it. Table 3.4 outlines the three characterizations.

Table 3.4: Proposed Terrain Classification based on Terrain Height Delta

Terrain Class Definitions
Upland $\geq$ 500 ft per $\frac{1}{2}$ nm
250 ft per $\frac{1}{2}$ nm $\leq$ Midland $<$ 500 ft per $\frac{1}{2}$ nm
Lowland $<$ 250 ft per $\frac{1}{2}$ nm

The simplicity of the classifications is purposeful for three reasons. First, the distinction between mountainous and non-mountainous has essentially remained the same. For all Upland classifications, the same data found in 14 CFR §95.11 [15] can be used, thus still meeting the intent of military and civilian regulations. Second, the data required to determine the terrain classification is standard in most, if not all, military mission planning rooms. This data is located on FalconView programs or easily inferred from actual contour maps that are available for nearly every location on Earth. The information in Table 3.4 along with Table 3.3 provide the required information to make escape path length determinations for each class aircraft for a given terrain type.

3.8.4 Escape Path Propagation Times.

The information in Sections 3.8.2 and 3.8.3 together form a matrix of terrain and aircraft classifications that can be used to categorize appropriate escape path propagation times. Essentially, each aircraft speed classification from Section 3.8.2 will be assigned an escape path time for each terrain class from Table 3.4, thus providing adequate protection without excessive computations. Table 3.5 shows the appropriate times. These times

Table 3.5: Proposed Avoidance Path Propagation Times

Aircraft Class	Lowland	Midland	Upland
Low Speed	17.25 s	29.19 s	44.54 s
Medium Speed	17.20 s	21.14 s	30.72 s
High Speed	28.25 s	28.25 s	28.25 s

are based on surveyed data of the height of terrain above mean sea level for most of the United States as well as on aircraft performance parameters. The information assumes that either the forward path or the ability to turn 90° is the deciding factor in the actual time for propagation. This is because the lateral paths need only to propagate to 90° to avoid an

obstacle forward of the aircraft's 3-9 line and are otherwise insensitive to the slope of the terrain. With this in mind, the aircraft path propagation times were assigned based on the forward path's ability to out-climb a specific terrain obstacle. Rate and radius are important though, because they provide the information on how fast an aircraft can turn 90° and how far forward it will travel in that time. (All other flight dynamics will be modeled inherently via the equations of motion.) For example, a B-1 has a turn radius of 14,906 ft. For this high speed aircraft, a forward escape path time over the ground must not be less than the time required to make that turn. If it were, the aircraft would not have the opportunity to turn 90° to avoid an obstacle if it could not out-climb it. Equation (3.20) displays the logic for the selection of an escape path propagation time.

$$\textit{Escape Path Time} = max[t_{90^\circ}, t_{\text{fwd path}}] \tag{3.20}$$

Using data gathered from "The Average Elevation of the United States" by Henry Gannett, it was determined that only approximately 22% of the total surveyed terrain lies above 4,000-5,000 ft MSL [17]. Of this terrain, much of it can be considered heavily mountainous and most of it lies in or near the Rocky Mountains [17]. It must be mentioned that of this terrain, not all of it is necessarily mountain peaks, it includes level topography that just happens to be at high mean sea level altitudes. For example, some of the plains of Colorado lie above 4,000 ft MSL, but they would fall under the Lowland classification outlined in Table 3.4 based on their relative slope. 5,000 ft was chosen because statistically little level terrain exists at this altitude, and it typically quickly becomes more rugged above this height [17]. From here, very little terrain (19,260 sq miles) is much more than 9,000-10,000 ft in altitude [17] so, in general, an aircraft would typically not need to out-climb an obstacle that is more than 4,000 ft above the more level terrain surrounding it. In the few situations where this may be necessary, the aircraft is likely operating in an extremely mountainous area, and thus taking advantage of tactical terrain masking without being at minimum low-level altitudes. In general, so little terrain is above 10,000 ft that there is

no real need to defend against it. For this reason, within the Upland terrain category, the aircraft need only to be able to out-climb a 4,000 ft obstacle to prevent a collision.

With the 4,000 ft height established, a specific distance along the ground must be determined to define the look-ahead protection provided. To do this, the medium airspeed aircraft was selected with the understanding that the slower and faster airframes will not deviate far from this distance. Using the provided algorithm, with a 15° flight path angle limit, a 4,000 ft climb will occur within a ground distance of 2.56 nm. (It is necessary to note that very fast aircraft like the B-1 will require a specific analysis based on their increased agility, speed, and specific flight path limits.) For slow and medium speed aircraft, worst-case Midland terrain will rise at just less than 500 ft per $\frac{1}{2}$ nm. Over 2.56 nm, this is approximately 2,600 ft minimum terrain ascent. Therefore, propagated altitude for this avoidance path must reach 2,600 ft in 2.56 nm ground distance. In a similar manner for the Lowland terrain, the propagated altitude must reach 1,300 ft. In all cases though, the logic in Eq. (3.20) must be met since the aircraft must be able to turn 90° minimum. For this research, it is important to analyze exact propagation lengths because every extra second of computation slows down the algorithm, which in turn can degrade protection. By determining precise times, it is possible to create a more efficient and effective program.

3.8.4.1 Propagation Time Methodology Example.

The following example uses the above information to explain how the propagation times were chosen. The scenario will evaluate the medium speed aircraft against each of the three terrain classifications. As previously mentioned, the driving factor for this analysis is height climbed as related to horizontal distance traveled, as long as 90° of turn has been accomplished. The distance is measured as ground distance against the propagated forward path of the aircraft and the altitude is the total altitude climbed by the path during the specified time. Figure 3.13 displays the nomenclature graphically.

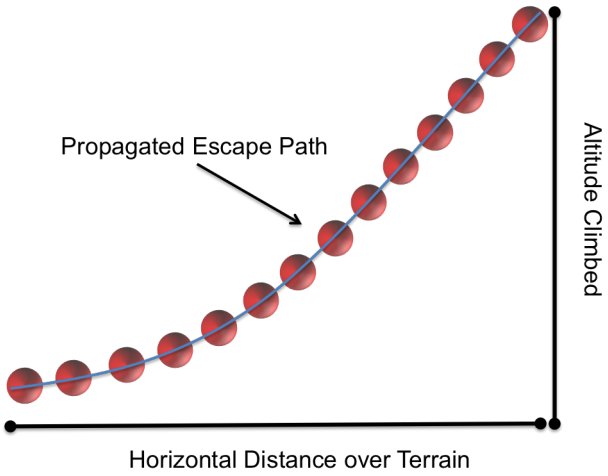

Figure 3.13: Escape Path Nomenclature

The horizontal distances and altitudes were calculated using the state equations within the presented algorithm. This ensures that the actual distances in latitude and longitude could be analyzed to determine that the appropriate ground distance was being accurately assessed. As mentioned previously, based on the information in Section 3.8.4, the propagation ground distance was based on the forward path's ability to climb 4,000 ft for Upland terrain.

It was calculated and found that 30.72 seconds should be used for the Upland scenario which correlates to 2.56 nm look-ahead and 4,001 ft altitude climbed for aircraft at medium speed. In this way, the Upland scenario shows that an aircraft traveling at 310 kts ground speed can out-climb an obstacle approximately 4,000 ft above its current altitude that is 2.56 nm away and, in the process, turn 170° for the lateral paths. Since the maximum time (Eq. (3.20)) is the time required to climb the 4,000 ft, that time is selected as the avoidance path length.

For the Midland scenario at medium speed, it was assessed that 21.14 seconds would be an appropriate look-ahead propagation time since it will out-climb an obstacle at 2,600

ft in 1.77 nm, much less than the 2.6 nm requirement. This is acceptable based on the definition of Midland found in Table 3.4 which, worst case, changes slope at just less than 500 ft per $\frac{1}{2}$ nm. At this slope, the terrain would change a maximum of 2,600 ft in 2.56 nm, which now would be avoidable with the recommended propagation timeline. Additionally for this timeframe, the aircraft turns 114° so it again meets the requirement of Eq. (3.20). For this reason, 21.14 seconds is an operationally acceptable look-ahead distance for a medium-speed aircraft operating over Midland terrain.

Finally, the Lowland scenario uses 17.20 seconds propagation time. For this case, though, the issue was not the ability to out-climb an obstacle, but to be able to out-turn an obstacle. As previously stated, the algorithm is built such that propagation paths either reach a certain altitude for protection or the lateral paths reach a minimum of 90° turn. From Table 3.4, the Lowland definition will cause a rise in terrain of just less than 250 ft per $\frac{1}{2}$ nm worst case. In this manner, an obstacle at 1,300 ft must be out-climbed in 2.56 nm which, for gradually increasing terrain, is sufficient for safe operation. This altitude can be climbed with a propagation time of approximately 11.5 seconds. Unfortunately, it will only turn 52° and not the required 90°. So in this case, the limiting factor is degrees of turn, and 17.20 seconds will be necessary for a medium speed aircraft. In general for Lowland flying, the ability to out-climb an obstacle is not a concern, but if it is, this timeline should afford the appropriate protection.

The same general logic is used for the low and high-speed aircraft as referenced in Table 3.5. The propagation length methodology is as follows: Step 1 is to determine the aircraft classification. This will typically be done once per airframe based on low-level tactical speed and turn performance much like Table 3.3. Step 2 is to determine the terrain classification explained in Section 3.8.3 and categorized in Table 3.4. Step 3 is to determine the aircraft's ability to out-climb 4,000 ft for an Upland scenario. The distance along the ground should be noted for the Upland case and applied to the Midland and Lowland worst-

case terrain rise. This will provide for minimum Midland and Lowland altitude values. They will typically be approximately 2,500 ft for a Midland scenario, or 1,250 ft for a Lowland scenario given that 90° has been accomplished. In all cases, Eq. (3.20) must be satisfied to ensure the appropriate lateral escape path turn has been propagated. It is important to note that for very fast aircraft such as the B-1, every propagation time may need to be evaluated at 90° of turn due to the very large turn radius. An example of this can be referenced in Table 3.5 for high-speed aircraft. For example, the Upland scenario for a fast aircraft like the B-1 will show that a 4,000 ft obstacle can be out-climbed in 16.75 seconds, but the aircraft will turn only 50°. An additional 11.5 seconds is required for the aircraft to reach 90°, thus 28.25 seconds is the propagation time. It is also important to note that the B-1's performance parameters were changed to a maximum of 2.4 g's and 20° of flight path angle to more accurately assess its capabilities [27].

Ultimately, the purpose of the above methodology is to provide logical protection for any aircraft operating at low-level altitudes based on their tactical airspeed and the morphology of the terrain below. This formulaic approach allows for immediate application to aircraft beyond the scope of this study (i.e. civilian airplanes) or military aircraft that are currently being designed (i.e. KC-46). As a reference, Table 3.6 shows the propagation parameters for each aircraft and all terrain types based on the times in Table 3.5.

Table 3.6: Heavy Avoidance Path Propagation Parameters [35]

Low Speed Heavy (velocity = 210 KIAS)			
	Lowland	Midland	Upland
Path Time (sec)	15.37	29.19	44.54
Altitude Climbed (ft)	1,301	2,600	4,000
Distance Covered (nm)	0.87	1.65	2.51
Deg Turned (deg)	166.0	238.1	377.0
Medium Speed Heavy (velocity = 310 KIAS)			
	Lowland	Midland	Upland
Path Time (sec)	17.20*	21.14	30.72
Altitude Climbed (ft)	2,115	2,602	4,001
Distance Covered (nm)	1.44	1.77	2.56
Deg Turned (deg)	90.2	114.3	170.2
High Speed Heavy (velocity = 540 KIAS)			
	Lowland	Midland	Upland
Path Time (sec)	28.25*	28.25*	28.25*
Altitude Climbed (ft)	7,399	7,399	7,399
Distance Covered (nm)	4.05	4.05	4.05
Deg Turned (deg)	90.3	90.3	90.3

*90° of turn was the driving factor

3.9 Sensitivity Analyses

3.9.1 Integration Methods and Limits.

The various integration methods used within this research include MATLAB's adaptive ODE45 and four fixed-step Ordinary Differential Equation (ODE) solvers using

increasing order Runge-Kutta methods. The goal for this analysis was to strike a balance between physical accuracy and computational speed. The adaptive nature of ODE45, though robust, cause additional computations that slow the algorithm. In an effort to increase speed without forfeiting accuracy, a sensitivity analysis on both integration method and integration limits was conducted. The study itself used ODE45 as the truth source forcing specific reporting points for the EOM at equally spaced time intervals. It is important to note that ODE45 will report at any time step specified by the user, but adaptive time steps are still occurring within its algorithm. With the time step specified, four different fixed step solvers were studied. They will be named ODE1, ODE2, ODE3, and ODE4 with the numeric indicating the order of the Runge-Kutta solver. These solvers are non-adaptive in nature which will allow for faster processing, though this will come at the cost of accuracy over time. For each time step, the Root Mean Square Error (RMSE) was reported over a 30 second total time interval and the solutions were plotted for comparison. Time steps of 0.1 seconds and 0.5 seconds are reported in Figures 3.14-3.17. Time steps of 0.2-0.4 seconds are included in Appendix D. In all cases, the aircraft initial condition was 3,500 ft and 350 kts starting from the same location and heading. Equations (3.3-3.7) were used to propagate the aircraft position forward in time and space using the exact same controls (forward path and level turn path) for consistency.

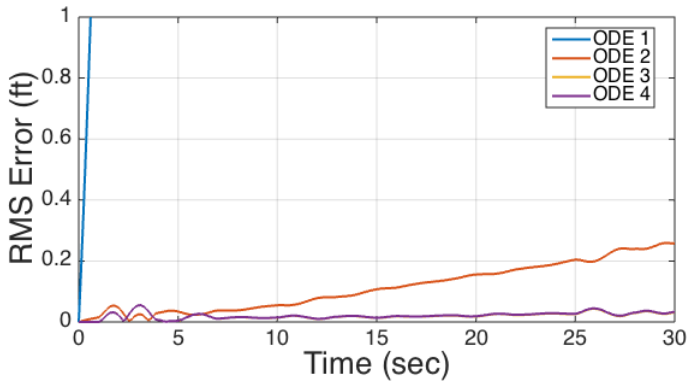

Figure 3.14: Forward Path RMSE with 0.1 s Time Step

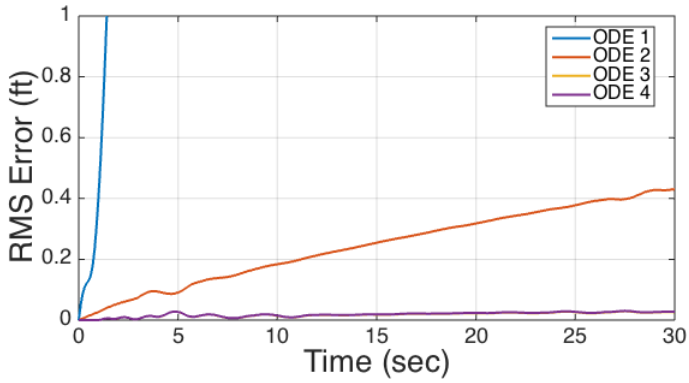

Figure 3.15: Lateral Path RMSE with 0.1 s Time Step

The analysis shows some interesting, though expected results. First, ODE1 diverges very quickly in every case for both the forward and lateral paths. For this reason, it can be excluded as an option due to its poor accuracy. ODE2 has significantly better accuracy than ODE1 and is a reasonable alternative for both paths, though it tends to diverge more quickly laterally. With a time step of 0.5 seconds for a 30 second interval, ODE2 has a total RMSE of 10.80 ft. Again, based on expected bubble sizes of 300 ft radii or larger and anticipated escape path lengths, this is an acceptable error. As can be seen in Figures 3.14-3.17 though, ODE3 and ODE4 have considerably better accuracy than ODE2 with

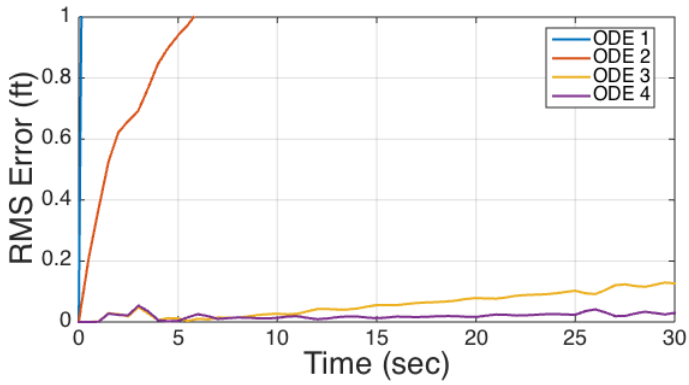

Figure 3.16: Forward Path RMSE with 0.5 s Time Step

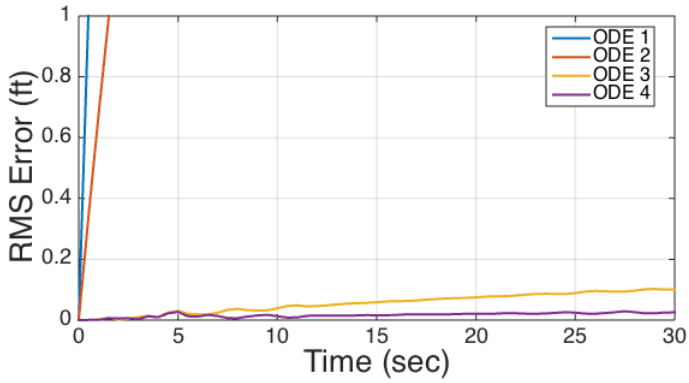

Figure 3.17: Lateral Path RMSE with 0.5 s Time Step

comparably little loss in computational speed. In all cases, ODE3 and ODE4 present less than 1 ft of error from the adaptive solution and they confer a viable alternative to the slower ODE45. Table 3.7 displays the computational speed in seconds related to each analyzed solver for a given time step. All of the ODE solvers in Table 3.7 are fixed step except for MATLAB's adaptive ODE45 which was used as a truth source baseline. Additionally, the run times are the combined time to propagate both lateral and forward paths.

Table 3.7: Computational Speeds of Fixed Step Solvers for Different Time Steps

Step/Solver	**ODE45 (truth)**	**ODE4**	**ODE3**	**ODE2**	**ODE1**
0.1 s	0.39 s	0.21 s	0.15 s	0.11 s	0.05 s
0.2 s	0.39 s	0.11 s	0.08 s	0.06 s	0.03 s
0.3 s	0.39 s	0.09 s	0.07 s	0.05 s	0.02 s
0.4 s	0.38 s	0.07 s	0.05 s	0.03 s	0.02 s
0.5 s	0.39 s	0.05 s	0.04 s	0.03 s	0.02 s

It is concluded then that ODE3, a strong balance between speed and accuracy, be used as the primary solver for this research.

3.9.2 Initial Conditions.

The initial state conditions sent to the algorithm from the aircraft can have a dramatic effect on the accuracy of the propagated solution. As a research objective, it was desired to show that the escape paths could be propagated once and then appended to the aircraft position at any point in time. The major benefit would be the savings in computational speed since the EOM would only need to be integrated once. These vectors would then be saved and rotated as required at each time step to determine whether a terrain collision had occurred. The sensitivity analysis focused on initial condition changes in flight path angle and bank. It was found that both of these parameters had a nearly immediate effect on the accuracy of the solution. The analysis made the following assumptions. First, a 300 ft bubble was assumed. Second, a medium speed aircraft was chosen with the understanding that low and high speed aircraft would bracket the results. Finally, the analysis would be concluded when the difference in altitude for the lateral path, or RMSE for the forward path, was greater than or equal to the radius of the selected bubble, 300 ft. RMSE was used for the forward path since there would not be a direct change in altitude based on a change

in either flight path angle or bank. In all cases, the truth source was an integrated solution using all the same parameters and time steps, but with 0° flight path angle and 0° bank.

For the flight path angle (γ), it was found that the lateral solution was more sensitive to changes, while the RMSE values of the forward solution were slightly less sensitive. In both cases, though, small changes in flight parameters quickly reach the threshold of usability. Table 3.8 shows the sensitivity analysis.

Table 3.8: Propagated Path Sensitivity to Initial Condition Flight Path Angle

γ (deg)	Forward RMSE (ft)	Lateral Alt Error (ft)
0.0	0.0	0.0
0.2	70.56	61.93
0.4	147.86	124.04
0.6	130.63	186.34
0.8	206.81	248.82
1.0	283.27	311.47

As can be seen, at 1.0° of flight path angle change there is a lateral altitude error of 311.47 ft. This would be outside the bubble radius indicating a significant source of error. In general, 1.0° of flight path angle would be nearly unnoticeable to the pilot and could vary quickly due to turbulence or other external forces. For these reasons, any significant climb or descents would easily negate the usability of appended escape maneuvers.

The same analysis was conducted for a change in the initial condition for bank angle (ϕ). As would be expected, this caused significant error in the lateral escape paths to occur quickly at very low angles. Table 3.9 displays the sensitivity analysis.

Table 3.9: Propagated Path Sensitivity to Initial Condition Bank Angle

ϕ (deg)	Forward RMSE (ft)	Lateral Alt Error (ft)
0.0	0.0	0.0
0.1	31.75	93.95
0.2	63.51	316.89

It is evident that at very small, unnoticeable, bank angles the lateral solution quickly diverges. For example, at 0.2° of bank, the lateral solution deviates by 316.89 ft. This further supports the claim that appended escape paths are not accurate enough for real-world use. It is thus concluded that the EOM must be propagated at each time step to report a viable solution.

3.10 Flight Test Methodology

The following sections will outline the specifics of the flight test methodology for the Have ESCAPE TMP as conducted at TPS.

3.10.1 Test Item Descriptions and Resources.

3.10.1.1 Calspan Learjet.

The Calspan VSS-equipped Learjet LJ-25D, displayed in Figure 2.6, will be employed as a platform to test the 3 and 5 TPA ESCAPE algorithms. As mentioned in Section 2.8, the VSS allows for inflight simulation of different aircraft control laws and aircraft responses in four degrees of freedom using control surface and feel actuators. The cockpit accommodates a pilot and copilot crew. There is seating in the cabin for a Test Conductor and up to two more occupants to include technical representatives or safety observers. Minimum aircrew will include the two pilots and a test conductor. A TPS student evaluation pilot will fly from the right seat where the yoke is replaced by a center stick with variable feel system components. A Calspan instructor pilot will serve as the pilot-in-command

as well as the safety pilot from the left seat. The left seat pilot controls are mechanically linked to the flight control surfaces, and provide un-augmented flight control when the VSS is disengaged. In the VSS mode, engagement and safety trip logic exists which detects failure states including aircraft states and loads, feel system, control surface parameters, and hydraulic fluid level. If a failure state or safety trip logic is satisfied, as shown in Table 3.10, hydraulic pressure is removed from the control surface and feel actuators, failures are annunciated in the cockpit, and the VSS is disengaged [13]. The VSS can also be manually disengaged by either crew member. Any VSS disengagement will always automatically return aircraft control to the safety pilot. Calspan's LJ-25D is instrumented to collect aircraft performance and state data.

Table 3.10: LJ-25D VSS Safety Trip Logic

Parameter	VSS Trip Logic
Airspeed (Above 14K ft)	325 kts & 0.79 M
Load Factor	+0.25 to 2.8
Angle of Attack	12°
Angle of Sideslip	10°

The algorithms will interface with the VSS which will directly implement the escape maneuvers. During Have ESCAPE flight test, the VSS will operate with a load-factor command and bank angle command flight control system logic. The LJ-25D does not incorporate any TAWS, GPWS, radar altimeter or any other altitude dependent systems which may interfere with the ESCAPE algorithms. When the algorithms command a maneuver to the aircraft, they send sequential, predetermined bank angle and load

factor commands to the flight control computer at 20 Hz (or any rate required by the aircraft's flight control computer) to progressively maneuver the aircraft in the intended direction. These maneuvers are commanded for up to 31 seconds, at which time the VSS is automatically disconnected and control of the aircraft is returned to the safety pilot. The pilot also has the option to manually terminate the automatic maneuver by disconnecting the Learjet's VSS. The test conductor will have the ability to monitor the activation and termination of the ESCAPE maneuvers, but the cockpit displays do not give any advance warning for these events. The pilots will be advised of any VSS disengagement through visual and audible warnings. Finally, the aircraft is equipped with an advanced Data Acquisition System (DAS) which allows for real-time collection of aircraft parameters for post-flight analysis. Table 3.11 displays the required parameters for this analysis (not all inclusive of DAS capabilities).

Table 3.11: Recorded DAS Parameters for Have ESCAPE

Name	VSS Variable Name	Units
Latitude	sensors.lat	decimal degrees
Longitude	sensors.long	decimal degrees
Altitude	sensors.h.cf	feet MSL
Heading	sensors.psi	degrees
Bank Angle	sensors.phi	degrees
Flight Path Angle	sensors.gamma	degrees
Pitch Angle	sensors.theta	degrees
Time of Decision	sensors.vss.time	seconds

3.10.1.2 Research Laptop Computer.

The ESCAPE algorithms will be run via MATLAB on a research laptop computer, which interfaces with the VSS on the Learjet. It is the physical hardware which both receives the aircraft state information as input to the running algorithm and communicates the running algorithm's commands to maneuver the aircraft. The research laptop computer is equipped with a solid state hard drive to minimize the probability of malfunctions caused by aircraft motion. The computer specifications include 64-bit Windows 8.1 Pro, 32 GB of random access memory, and an Intel Core I7-4860HQ CPU. During flight, the research laptop will be securely fastened to the test conductor's work station in the aircraft cabin. All data will be saved locally to the aircraft's hard drive for post flight analysis.

3.10.2 Test Matrix and Flight Test Predictions.

3.10.2.1 Test Matrix.

For flight test operations, it was necessary to create a test matrix that outlined the exact test points to be flown to meet the research objectives. Each point on the test matrix was specifically designed to trigger an unambiguous result or desired ESCAPE path. These terrain features were initially chosen by qualitative assessment of their shape, size, and slope based on contour lines observed on aeronautical charts. It was necessary to determine an initial point, ground track, and altitude to fly towards the terrain with consistent and repeatable geometry. Each test point was evaluated in the TPS flight sciences simulator to obtain a higher fidelity prediction of which path would be chosen during flight test. Once sufficient test points to trigger each maneuver for both 3-path and 5-path ESCAPE algorithms were found, the test points were compiled into the test point matrix found in Appendix A. Reference Section 3.3 for a full description of the ESCAPE paths. The test point matrix was then programmed into the research laptop computer in the form of a drop down menu. When a test point was selected and executed on the computer, the position and course slewing tool automatically adjusted the ESCAPE algorithm's navigation solution to

match the desired test point location and geometry. The slewing tool will be discussed in Section 3.10.2.2. A trigger time was also recorded for each test point. the trigger time was defined as the time from test point initiation to path execution, and it was used as an inflight tool to anticipate aircraft control activation. In all cases, the ESCAPE algorithms analyzed the terrain using Level 1 DTED.

3.10.2.2 Modeling and Simulation.

Prior to implementation, the ESCAPE algorithms were formatted to interface with the Calspan Learjet VSS and the Flight Sciences Simulator at TPS so that functional checks and pre-flight predictions could be accomplished. The ESCAPE algorithms then interfaced directly with the Flight Sciences Simulator (simulating the Calspan Learjet interface) so that the planned test points could be flown to predict the flight test outcome. In this way, every actual test point was evaluated prior to actual flight to document expected outcome and predicted aircraft performance. The data was then collected for comparison to actual flight data. This singular capability increased test efficiency and provided valuable data on the comparison of expected algorithm performance against actual flight test results. Additionally, this allowed the test team to visually review the test points for legitimacy before allocating expensive flight resources to them.

During flight test, low-level flight towards terrain obstacles was simulated while flying above 5,000 ft Above Ground Level (AGL) within the confines of the R-2508 complex. The low altitude flight and terrain obstacles were simulated by using a position and heading slewing tool. This tool takes the current aircraft latitude, longitude, and heading as inputs, and calculates a geographic offset and rotation to place the aircraft at a simulated latitude, longitude, and heading for a desired virtual test location. Specifically, the slewing algorithm transforms latitude, longitude, and altitude into an X, Y, Z position and translates this location to the desired X, Y, Z location wherein a transformation back to latitude and longitude is accomplished. Separately, the algorithm rotates the heading from the current

aircraft heading to the desired heading. The MATLAB SIMULINK block diagram that performs these functions is shown in Figure 3.18.

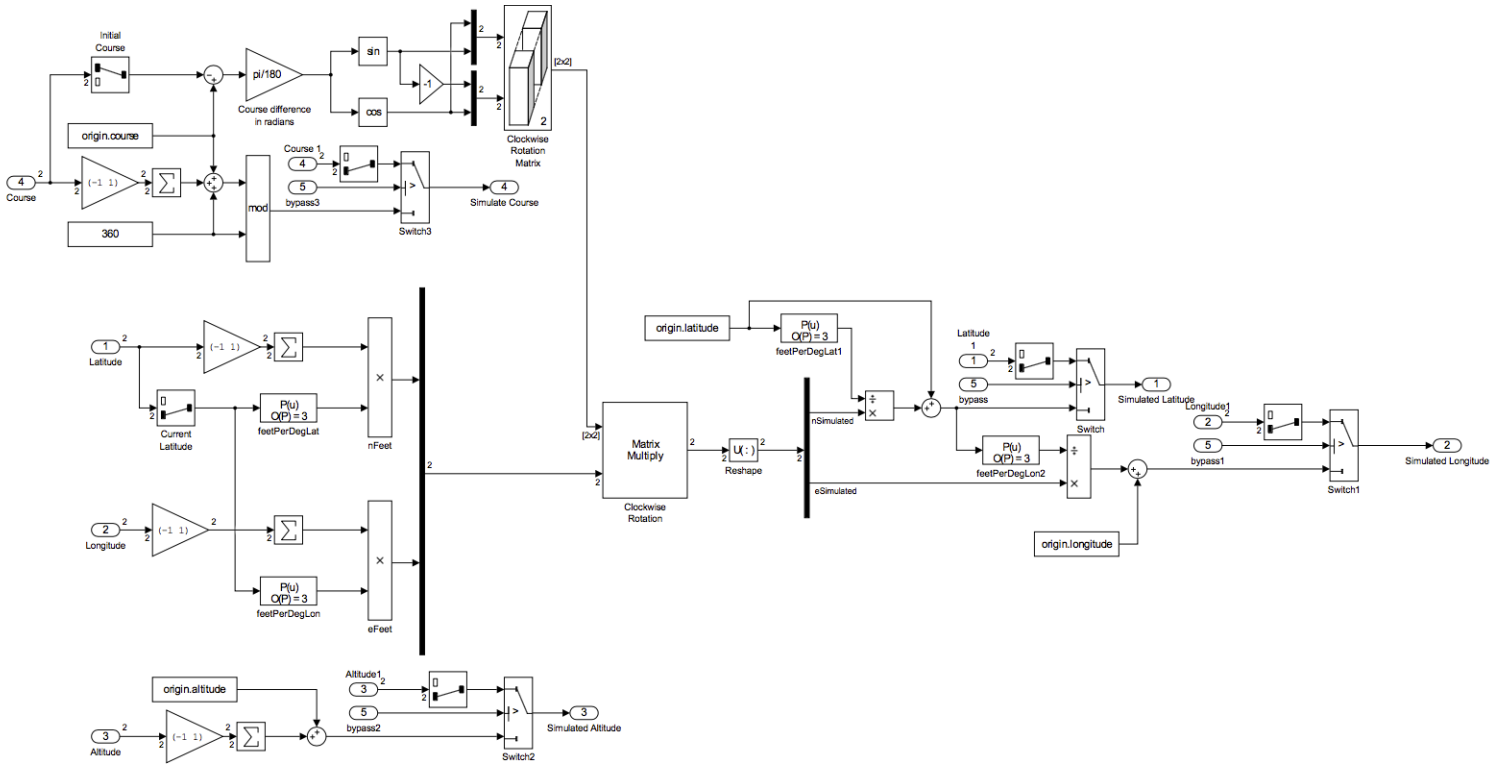

Figure 3.18: Have ESCAPE Aircraft Position Slewing Tool

Ultimately, this enabled the VSS to test the ESCAPE algorithm using terrain from any location without having to physically relocate the aircraft as long as DTED was available for that location. The slewing tool did not alter the aircraft's navigation solution, it only input the new aircraft location solution into the ESCAPE algorithm running on the research laptop which allowed the flight crew the ability to navigate accurately throughout the airspace. The tool mitigated airspace conflicts, expedited test point execution, and allowed

for safe mission operation since low-level flight was neither required nor approved by the safety board.

3.10.3 Flight Test Execution.

3.10.3.1 Aircraft Ground Checkout.

The Learjet was equipped with a ground simulation mode that was used to verify that the ESCAPE algorithms were sending the proper command vectors to the VSS. This simulation was used as a functionality check only, but it allowed a real-time determination that the algorithm, VSS, and flight controls were communicating and operating correctly prior to flight. The goals of ground checkout were as follows:

- Verify integration of the ESCAPE algorithm by ensuring information exchange between the algorithm and the VSS computer.
- With the VSS in Simulator Mode, trigger every terrain avoidance maneuver, and verify proper control surface deflection.
- Verify the operation of the DTED coordinate and elevation slewing function.
- Verify that the VSS disconnects after escape path maneuver is complete.

The ground checkout found no discrepancies, though the simulation model did not take into account aerodynamic effects or gross weight implications.

3.10.3.2 Flight Test Briefing.

A flight test briefing was to be conducted prior to each test sortie in accordance with local procedures. All crew members participating in the test mission attended the flight test briefing. The minimum crew consisted of an evaluation pilot, a Calspan safety pilot, and a test conductor. The crewmember annotated in parentheses was the individual responsible for briefing the areas below.

- Aircrew (Evaluation Pilot)

  - Weather and NOTAMs
  - Crew duties, responsibilities and Crew Resource Management (CRM)
  - Exchange of aircraft control and engaging VSS
  - Joker and bingo fuel
  - Emergency procedures

- Departure and Recovery (Evaluation Pilot)
  - Radio Frequencies
  - Airspace Management
  - Departure and recovery routing

- Specific Mission Brief (Test Conductor)
  - Test Objectives
  - Software version
  - Test hazards and general minimizing procedures
  - Go/No-Go Criteria
  - Communication plan, to include test point initiation and termination
  - Test card review

3.10.3.3 Test Execution.

During flight test, the aircraft was flown in the R-2515 airspace, at 15,000 feet pressure altitude and 310 knots groundspeed. All test points were initiated from wings level, constant altitude, unaccelerated flight. To minimize the effect of wind drift, test points were initiated with a head or tailwind to the maximum extent possible while maintaining 310 knots ground speed prior to path initiation. Once the aircraft was on conditions, the

test point was initiated and the evaluation pilot maintained a steady course, altitude, and airspeed until the ESCAPE algorithms commanded a maneuver. Since auto-throttles were not used, the evaluation pilot attempted to maintain a constant indicated airspeed with the throttles throughout the maneuver. During the level turns, the airspeed could be kept within tolerance by modulating the thrust, though airspeed was lost during all climbing maneuvers due to performance limitations of the aircraft. Flight parameters were monitored during the automatic maneuver execution to ensure that the aircraft did not enter a dangerous flight condition and to ensure the algorithms were performing as expected.

The ESCAPE algorithms analyzed the terrain by using a Level 1 DTED database created by the National Geospatial-Intelligence Agency. This database consisted of a matrix which specified terrain elevation values at regular latitude and longitude intervals. All ESCAPE paths were programmed to be executed for 31 seconds, after which the Learjet VSS automatically disengaged, causing an audible warning in the cockpit and flashing indicator lights. This indicated termination of the test run and automatically transferred control back to the safety pilot. Following each test point, handheld data were recorded to document which path was chosen, what bank angle and flight path angle were achieved, how much the speed and altitude deviated from the initial parameters, and wind data. Additionally, flight data were recorded by the research laptop and the VSS per Table 3.11.

3.10.3.4 Overall Test Conditions.

All test points were flown during day visual meteorological conditions at 15,000 feet pressure altitude and 310 knots groundspeed. The surface conditions at Edwards AFB included temperatures from 20° to 35° Celsius with light winds. The wind speed at the test point altitude varied from 0 to 22 knots.

The LJ-25D was configured with a full fuel load of 5,600 lb and test points were carried out with a fuel load varying from 4,500 lb to 1,500 lb. Three or four persons were on board the LJ-25D, two pilots, a TC, and an observer if required.

3.10.3.5 Post Flight Briefing.

Following each flight test, a post-test briefing will be carried out with all crew members to discuss the following:

- Abnormal events or emergencies
- Mission planning and products
- Test results, including data quality
- Recommendations and objectives for the next mission

3.10.4 Data Sources.

For comparison purposes, the flight test data was compared against both simulation results from the TPS Flight Sciences Simulator as well as an optimum path solution. The simulator data was obtained using the same laptop, MATLAB code, and test matrix used in flight. The data is valuable, because it controls for pilot error, aircraft aerodynamic effects, and winds which impacted actual flight data.

The optimal code, written by Suplisson as part of her PhD Dissertation [35], derives an Auto GCAS solution using a minimum control cost function and an infinite number of escape path options within the aircraft performance capabilities. For the purpose of comparison with the ESCAPE algorithms, the optimal solution was constrained to similar aircraft performance limits of 60° bank angle, 30° per second roll-rate, 2g load factor, and 15° flight path angle. To simulate the g-onset rate of the LJ-25D in its flight test configuration, the longitudinal short period natural frequency and damping ratio were adjusted in the optimal code to match the values found during flight test. The natural frequency was 1.6 rad/sec and the damping ratio was 0.4. This code implemented a constantly computed solution to minimize control inputs as an aircraft flew from one point to another. The optimal solution accounted not only for the nearest obstacle, but for all terrain within 2 nm ahead of the aircraft. The optimal solution maneuvers could apply

either the load factor or the bank angle first as required, and the amount of heading change could be of any amount. When an obstacle was encountered, it calculated an optimized solution to minimize bank and load factor inputs to avoid the terrain. In this way, the optimal solution around a terrain object is the flight path that minimizes bank and load factor commands while still avoiding the terrain by a predetermined distance. This differs from the ESCAPE solution because the optimal algorithm chooses from an infinite set of possible paths, thereby evaluating far more terrain than the ESCAPE algorithm, which only evaluates terrain beneath the 3 or 5 avoidance paths. The trade-off in the amount of examined terrain is necessary for real-time integration and allows the ESCAPE algorithm to process faster than the optimum algorithm.

Unlike the ESCAPE algorithms, the optimal solution did not use a safety bubble around the aircraft to maintain safe separation from the terrain. Instead, the aircraft was considered to be a point mass, and the optimal solution added a vertical bias to the DTED data. The collision potential was calculated based on this increased terrain elevation to ensure safe separation from the actual terrain. To guarantee that the aircraft did not fly too close to an obstacle laterally, the distance to the DTED was calculated from the aircraft position, and also from two points which were laterally offset from the aircraft by a specified distance, with one point on each side. The optimal solution attempted to keep the aircraft and the two offset points clear of the biased DTED elevation to prevent collisions.

Since the optimal solution considered the aircraft a point mass, it required a mechanism to prevent the aircraft from flying between DTED posts. This was done using the 'griddedinterpolant' function in MATLAB to create a continuous surface approximation of the discrete DTED data posts. For comparison purposes, data collected from the optimal code was obtained by inputting the same test matrix points used in actual flight. Thus, all the 'optimal' results were created after the flight tests were conducted.

Finally, it was necessary to determine a measure of nuisance since the aircraft will be physically flown at altitude away from terrain, and it will not be possible for the pilot to assess if the algorithm implements too early. For this reason, a metric named 'Available Reaction Time' was developed. The available reaction time is the amount of time that the maneuver could have been delayed while flying straight and level beyond the maneuver activation point, and still avoid a collision by an infinitely small margin. If the terrain penetrates the safety bubble, the available reaction time is based on the aircraft colliding with the terrain. If the terrain does not penetrate the safety bubble, the available reaction time is based on the bubble touching the terrain. A very large time would indicate a possible nuisance activation. The delineation between an excessively large available reaction time was not drawn since actual flight tests in the low-level environment would be required, but qualitative assessments can be made using the metric.

3.11 Data Analysis Plan

Appendix B describes the data analysis procedures for the Have ESCAPE test plan in order to analyze the data and produce the required products for analysis based on the objectives outline in Section 1.4.2. The DAP specifically details the required data parameters from the source of interest, any qualitative data required, if any, the analysis procedures, and the desired final data products. The primary data source was the Learjet VSS DAS. This system samples parameters at 200 Hz, and saves these parameters to a Microsoft Excel compatible file, which can also be imported into MATLAB. Simulator data was also gathered to predict the behavior of the ESCAPE algorithms and was processed in the same manner as the flight test data when required. The optimal solution used for comparison was derived from the optimal code designed by Suplisson's research [35]. The optimal data will be compared with the ESCAPE algorithms as described for Objective 4. The tables and graphs depicted in the DAP were used as a guide during data collection and reduction to ensure the appropriate information was being collected for the desired analysis.

Furthermore, it was used as a post-flight tool to quickly determine algorithm performance so adjustments could be made prior to the next flight test. The desired data products were used only as templates for the collected data and, in many cases, the test team expanded the products to include charts, graphs, and videos to help explain the results in more detail. The DAP, in its entirety sorted by objective and MOP, can be found in Appendix B. A thorough review of the DAP is required to understand the results presented in Chapter 4.

3.12 Summary

This chapter outlined the methodology and analytical procedures preceding the actual flight test. Within the scope of flight test, it is prudent to execute a Predict-Test-Validate type plan so that expectations can be set and outcomes assumed before expensive and/or dangerous flights are attempted. To this end, it was necessary for the test team to evaluate each test point with the test matrix and then prepare cautiously for the first flight using the tools and theory developed in this chapter. The next chapter presents the results, with analysis, of the Have ESCAPE algorithm.

IV. Results and Analysis

4.1 Overview

This chapter outlines the data, results, and analysis of the six test flights for the Have ESCAPE TMP. The flights were conducted from 31 August 2015 to 10 September 2015. The Daily Flight Test Reports for each flight can be found in Appendix C which outlines the crew, conditions of the flight, the test points flown, and any additional information pertinent to the collection of the data or the performance of the algorithm. As mentioned in Section 1.3, the flight tests focused on a worst-case scenario. The terrain used to test the ESCAPE algorithms was mountainous in nature, including vertical gradients steeper than 3,000 feet per nautical mile, and a combination of wide mountain faces and narrow valleys. Some of the mountains used as terrain obstacles had a vertical rise of 9,000 ft and a summit elevation above 13,500 ft MSL. The two main areas used for testing were the Sierra Nevada mountain range (approximately 100 nm north of Edwards AFB) and the Canadian Rockies (approximately 180 nm West of CYEG (Edmonton) airport). The specific test point locations are detailed in the test point matrix, Appendix A.

4.1.1 Chapter Outline.

This chapter will be outlined in a manner consistent with Section 1.4.2. The results and analysis for each objective and associated MOPs will be independently analyzed to determine appropriate algorithm adequacy, performance, and comparison with the optimal solution.

As a reminder, the overall test objective was to compare three and five path limited option Automatic Ground Collision Avoidance System solutions for heavy-type aircraft against optimally derived ground avoidance solutions.

The specific test objectives were to:

1. Evaluate the 3 TPA Solution

2. Evaluate the 5 TPA Solution

3. Determine Acceptable Algorithm Parameters

4. Compare 3 and 5 TPA Solutions with the Optimal Solutions

The DAP located in Appendix B, organized by objective, contains the procedures and processes used to analyze the data for the results presented herein.

4.2 Specific Test Objective 1: Evaluate the 3-TPA Solution.

4.2.1 MOP 1: Algorithm Path Selection.

The 3-TPA path selection data were analyzed by observing the aircraft response during simulation and comparing it to the aircraft response during flight test. The evaluation criteria were satisfied if the chosen escape path matched the simulation results. During flight test, the algorithm's decision logic was also monitored from the research laptop, to confirm that the algorithm was commanding the correct path.

The 3-TPA path selection results are presented in Table 4.1. The data showed that the 3-TPA ESCAPE algorithm chose the expected path 19 times out of 21 test runs. This shows that the algorithm results were repeatable and predictable. This predictability and repeatability of the flight test results demonstrate the algorithm's effectiveness, in that it was able to perform consistently from one flight to another.

Table 4.1: 3-TPA Path Selection

Algorithm: 3-TPA Test Dates: 31 Aug-10 Sep 15
Pressure Altitude: 15,000 ft Airspeed: 310 kts Groundspeed

Test Point	Result	Number of Test Runs	Forward Path	Left Path	Right Path
6	Forward Path	7	5	2	
6	Left Path	7		7	
8	Right Path	7			7

The cases where the algorithm chose an unpredicted path were caused by small variations in the test point setup parameters, from the execution of the position slewing tool, to the execution of the escape maneuver. Since the algorithm logic was based on the safety bubble contacting any single DTED post, a very small change in lateral or vertical position could have made the difference between hitting a DTED post much earlier in the projected trajectory; or missing the DTED post which was hit during simulation. Sources of error which may have led to a different path being selected include pilot technique to maintain a constant heading and altitude and variable winds which may have caused the aircraft to drift away from the desired flight path. Analysis of the aircraft ground track during the test point setup revealed that all cases where the ground track was more than 0.5° from the planned course led to a different path being selected. Although this track error was within the tolerance specified in the test point matrix, it proved to be enough to consistently trigger a different escape path. The other flight parameters specified in the test point matrix were maintained within tolerance, and no other correlation was noticed between test point flight parameters and path selection.

4.2.2 MOP 2: 3-TPA Aircraft Response.

The 3-TPA aircraft response data were analyzed by plotting the time history of the load factor (N_z) and bank angle (ϕ) for the commanded values and the achieved values. The time history of the altitude and the flight path angle were also plotted to compare with the expected values. From the time history plots, the maximum parameter deviation was noted for the transitory period and for the steady-state period. The transitory period was defined as the time during which the bank angle or load factor was commanded to change with time. The steady-state period was defined as the period of time during which the bank angle and load factor were commanded to remain steady with time. The evaluation criteria were satisfied if the aircraft flew within 0.1 g of the commanded load factor, within 5° of the commanded bank angle, maintained altitude within 100 feet during level maneuvers,

and maintained the flight path angle of 15° within 3° of the predicted value during climbing maneuvers.

The 3-TPA aircraft response results are summarized in Table 4.2, which represents the largest deviation from the desired value of the aircraft state, as observed over the course of four separate flights, for both the transitory period and the steady-state period. Negative values indicate that the aircraft state was less than desired, while positive values indicate that the aircraft state was greater than desired. To compare data between flights and to observe trends, sample time history plots are presented in Figures 4.1 to 4.3, which show data for test point 6. Additional time history plots are presented in Appendix D for test points 7 and 8.

Table 4.2: Maximum Deviation from Desired Aircraft States for 3-TPA

Algorithm: 3-TPA Test Dates: 31 Aug-10 Sep 15
Pressure Altitude: 15,000 ft Airspeed: 310 kts Groundspeed

	Transitory Period				Steady-State Period			
Test Point	Bank Angle*	Load Factor	Altitude	Flight Path Angle	Bank Angle*	Load Factor	Altitude	Flight Path Angle
6 (FWD)	N/A	-0.30 g	N/A	N/A	+1.3°	-0.09 g	N/A	-4.3°
7 (Left)	-21.3°	-0.29 g	-23 ft	+0.2°	+0.8°	-0.05 g	+710 ft	-5.9°
8 (Right)	-22.6°	-0.42 g	+12 ft	+0.3°	+1.5°	-0.05 g	+973 ft	-7.3°

(red indicates values outside expected performance)
*Bank Angles represent magnitude, negative values mean less bank than commanded.

Figure 4.1 shows that the bank angle was maintained within tolerance during the execution of the forward path maneuver (test point 6). Figure 4.2 shows that the load factor was found to lag the commanded value during transitory periods and to overshoot the desired value, but it subsequently stabilized within evaluation criteria during the steady-state periods. The amount of lag in the load factor was a function of aircraft fuel load

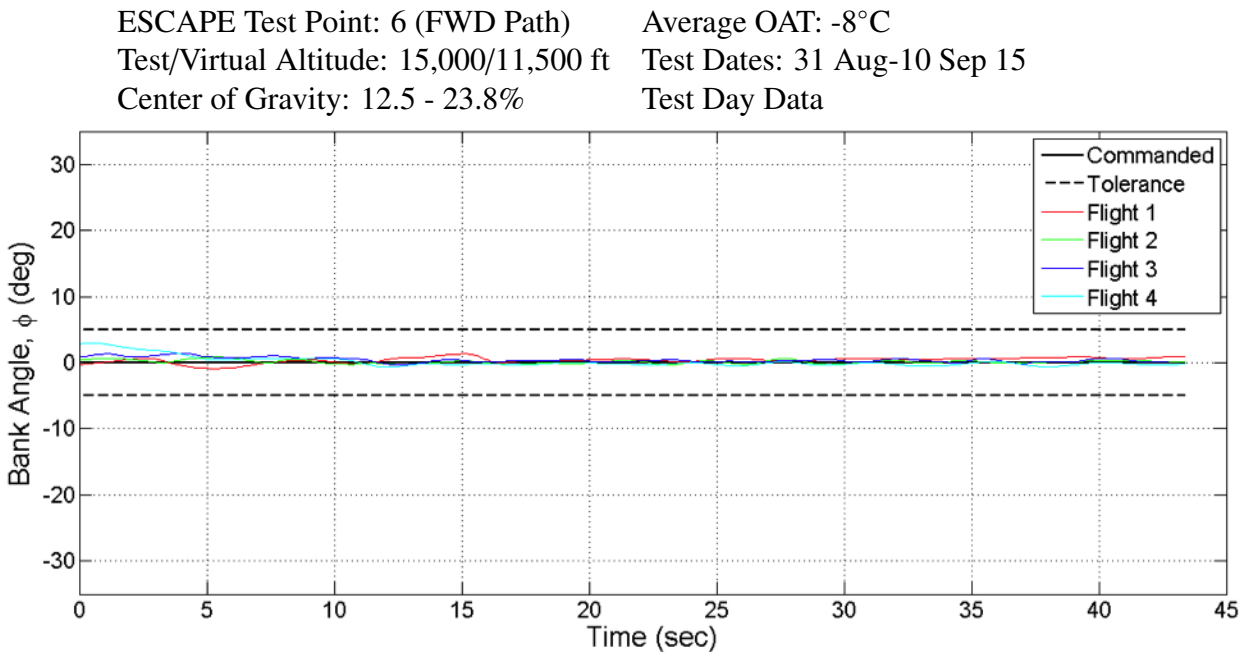

Figure 4.1: Bank Angle vs Time for Test Point 6, Forward Path

and center of gravity, where greater fuel weight and forward center of gravity resulted in increased lag. The algorithm did not directly command the flight path angle, but it established the climb angle by commanding a pre-calculated load factor applied over a period of time.

Figure 4.3 shows that although the initial flight path angle was within evaluation criteria, there was variance of approximately 3° between test runs, caused by differences in aircraft weight and center of gravity location. In all cases, the flight path angle decreased throughout the maneuver, and in one out of four test runs, the final flight path angle was less than 12°. Maximum continuous power was applied during the climb, but the aircraft was thrust limited and could not maintain its airspeed. As the airspeed decreased, the VSS attempted to maintain the commanded load factor by increasing the angle of attack. The angle of attack remained below 12° in all cases and did not cause any VSS safety trips. This indicated that the climb angle was not impeded by the loss of airspeed or by

ESCAPE Test Point: 6 (FWD Path) Average OAT: -8°C
Test/Virtual Altitude: 15,000/11,500 ft Test Dates: 31 Aug-10 Sep 15
Center of Gravity: 12.5 - 23.8% Test Day Data

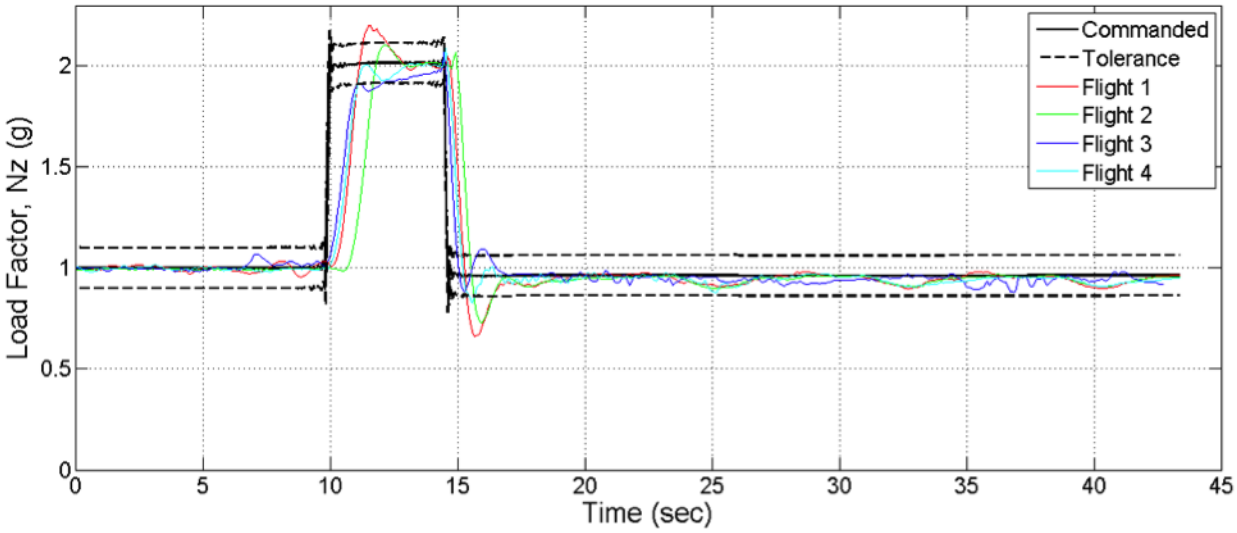

Figure 4.2: Load Factor (N_z) vs Time for Test Point 6, Forward Path

the lift limit, but rather by an inadequate commanded load factor. In fact, the flight path angle was maintained at 15° during the climbing turn maneuvers which will be discussed in Objective 2, because more load factor was being commanded, even though the airspeed was decreasing throughout the maneuver. The inability to maintain a steady climbing flight path angle without artificial limiters in place was a continuing issue. It was a direct result of the open loop nature of the flight path angle control being subjugated to an N_z that was theoretically designed for a single flight condition. It did not adapt for changes in aircraft parameters such as gross weight and center of gravity.

In the case of test point 6, two of the test runs impacted the simulated terrain as will be discussed in the next section. This indicates that an inability to precisely hold a flight path angle was detrimental to the algorithm's performance.

The time history plots for test points 7 and 8 (left and right level paths respectively) are presented in Appendix D Figures D.7 through D.12. During execution of the left and right

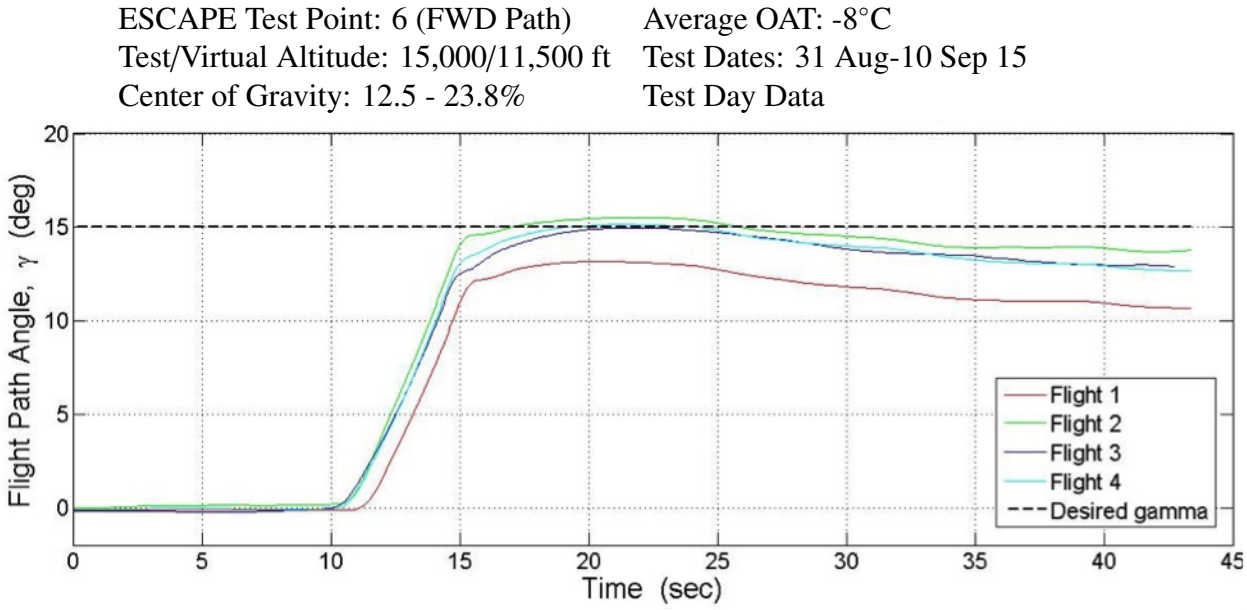

Figure 4.3: Flight Path Angle (γ) vs Time for Test Point 6, Forward Path

level turn maneuvers, the steady-state bank angle and load factor were maintained within tolerance of the commanded values. During the transitory period, both the load factor and the bank angle lagged the commanded value by an average of 0.25 seconds. This lag, along with small variations in bank angle and load factor, affected the aircraft's ability to maintain a constant altitude during the turn. The algorithm attempted to maintain a constant altitude by adjusting the commanded load factor based on the bank angle as per:

$$N_z = \frac{1}{\cos \mu} \tag{4.1}$$

However, the lag caused by aircraft dynamics caused errors in the expected N_z to ϕ relation, and this prevented the aircraft from maintaining level flight. During and shortly after the roll-in, the aircraft descended as much as 80 ft due to insufficient commanded load factor during the transitory period. Once the load factor reached its steady-state value, the aircraft began to climb and the final altitude varied from 100 ft to 973 ft above the starting altitude dependent upon gross weight and center of gravity parameters.

The aircraft's inability to maintain the desired flight path angle, and the lag between the commanded parameters and the actual parameters prevented the aircraft from flying the maneuvers as planned. Since the algorithm's collision predictions assumed that the aircraft would fly the maneuvers as planned, the inability to maintain the desired flight parameters could affect the ESCAPE algorithm's effectiveness against the terrain which will be discussed thoroughly in the next section.

4.2.3 MOP 3: 3-TPA Ground Miss Distance.

The 3-TPA ground miss distance was calculated using a MATLAB script which accepted the aircraft virtual navigation solution (downstream of the position and course slewing tool) as an input, and returned the terrain miss distance as an output. The script determined the minimum miss distance by using the Root Mean Square (RMS) error equation to calculate the distance between the aircraft and the DTED posts at every iteration point of the navigation solution for the duration of the escape maneuver. Eq. (4.2) shows the calculation.

$$RMS_{error} = \sqrt{(X_{DTED} - X_{AC})^2 + (Y_{DTED} - Y_{AC})^2 + (Z_{DTED} - Z_{AC})^2} \tag{4.2}$$

The minimum miss distance was the least of these values. This script was validated by taking sample data to plot the aircraft trajectory over a DTED map, and confirming that the miss distance was correct. The evaluation criterion was satisfied if the distance between the navigation solution and the DTED was more than the specified safety bubble radius at all points of the escape flight path. Though a distance found to be inside the bubble radius would not necessary indicate an impact with terrain, the fact that the aircraft model assumes a point mass makes further interpretation of the distance irrelevant. The specifics of the analysis can be further referenced in Appendix B.

The 3-TPA ground miss distance results are presented in Table 4.3, tabulated with one test run per container. The flight test results are also presented graphically in 3-dimensional plots presented in Appendix D Figures D.13 and D.14, which show where the turning paths

intersected the terrain. The data show that in all cases but one, the aircraft impacted the simulated terrain. The two primary causes for the ground impacts are the achieved flight path angle, and the open-loop path selection logic. Of note, the available reaction time is not included in Table 4.3 because the values are all essentially zero since no time was practically available before impact (even in the case with a 39 ft miss distance).

Table 4.3: 3-TPA Ground Miss Distance

Algorithm: 3-TPA Test Dates: 31 Aug-10 Sep 15
Pressure Altitude: 15,000 ft Airspeed: 310 kts Groundspeed

Ground Miss Distance (ft)				
Test Point	Flight 1	Flight 2	Flight 3	Flight 4
6 (FWD)	0	39	0	0
7 (Left)	0	0	0	0
8 (Right)	0	0	0	0

The algorithm assumed that the aircraft would be able to climb at a constant flight path of 15°, and the maneuver initiation point is based on this assumption. As discussed in the previous section, the aircraft was not able to maintain 15° of flight path angle for the duration of the maneuver, which resulted in less altitude gained than predicted, and the aircraft could not out-climb the terrain obstacle. This caused the aircraft to impact the terrain in three out of four test runs, as illustrated in Figure 4.4. The only case where test point 6 did not impact the ground is the second test run, which produced the highest flight path angle, due to the aircraft weight and center of gravity location. Even in this case, the average flight path angle was lower than planned, and the aircraft missed the ground by only 39 feet. The important point though, is that the aircraft must meet or exceed the algorithm's expected performance or terrain clearance cannot be guaranteed.

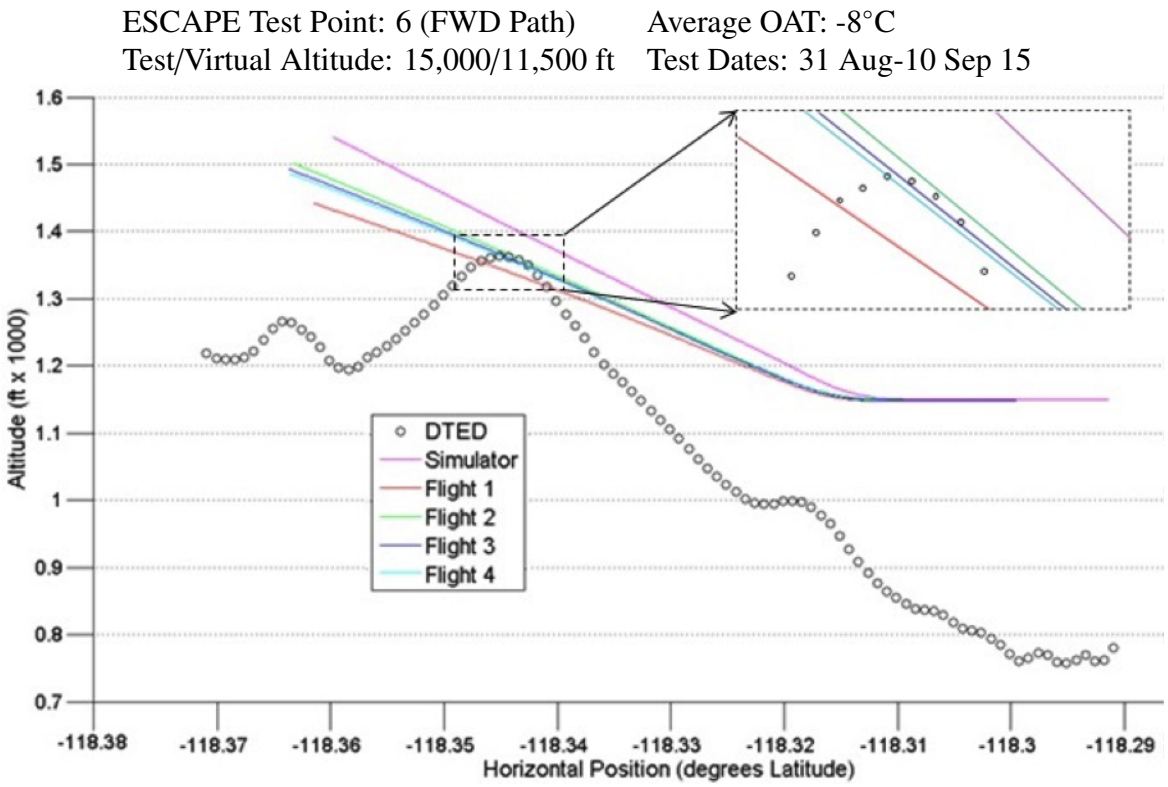

Figure 4.4: Planned vs Achieved Flight Path Angle for Test Point 6, Forward Path

Another cause for ground impact during test points 7 and 8 was the fact that the algorithm stops scanning terrain once it implements a maneuver. In order to avoid nuisance activations, the algorithm did not command any maneuvers until it predicted that all projected escape paths would impact the terrain. Once every projected path impacted the terrain, the algorithm determined which path offered the longest time of flight prior to impact, and commanded the aircraft to fly that maneuver with a time delay safety margin to avoid actual impact. The algorithm assumed that the escape path which offered the longest time of flight prior to impact would offer the best chances to avoid the terrain by taking advantage of the time delay safety margin and the bubble safety margin. However, in some cases, such as the one depicted in Figure 4.5, the safety margins would have to increase to impractical values in order to protect the aircraft using this logic, since the left level turn

would have resulted in a collision even if it had been initiated 50 iterations earlier than the actual initiation point. (To be clear, this issue is somewhat artificial in nature since the aircraft was slewed to a location deep in the mountains, where realistically, it may not have been practical (or possible) to physically fly the aircraft without causing an activation that would have cleared the terrain. In any case, the presented problem shows a limitation in the algorithm's performance that can be directly addressed.) The algorithm logic is illustrated in Figure 4.5, using data from test point 7.

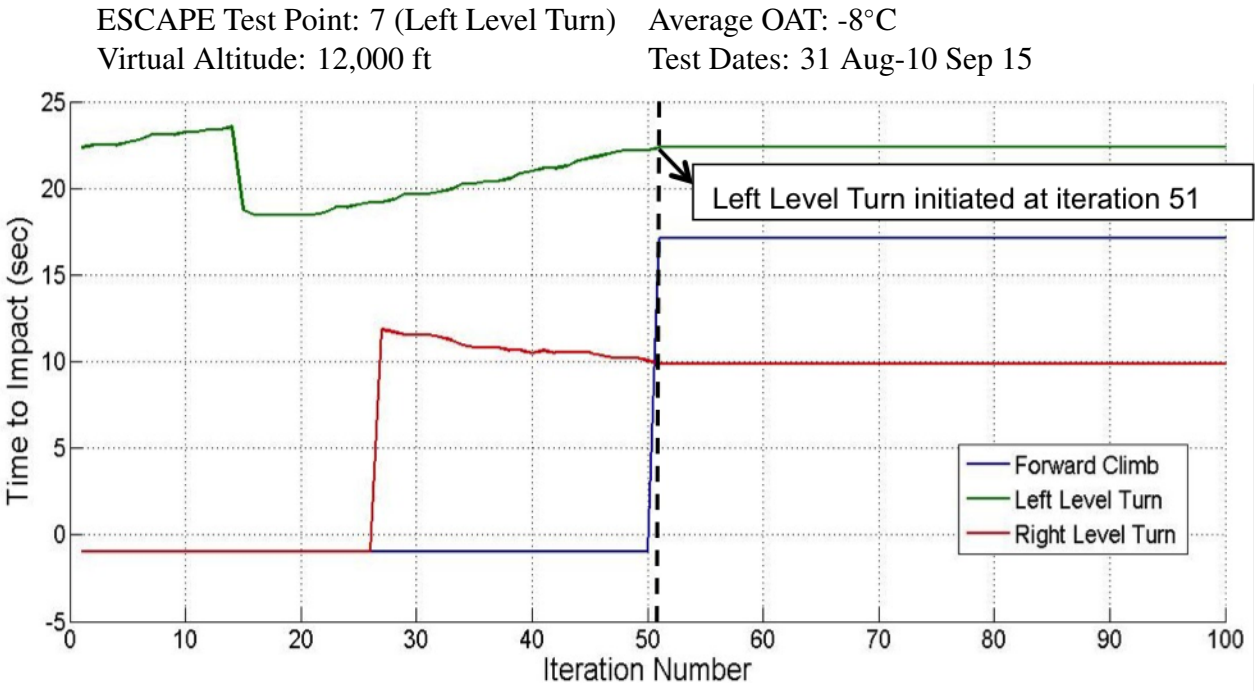

Figure 4.5: Ground Impact Predictions for Test Point 7

Figure 4.5 shows that as of the first iteration, the left level turn was predicted to intercept the terrain after 23 seconds time of flight, a byproduct of the slewed position. After 26 iterations, the right level turn was predicted to intercept the terrain after 12 seconds, and the left level turn was still predicted to intercept the terrain after 20 seconds. After 50 iterations, the forward climb was predicted to intercept the terrain after 17 seconds,

the right level turn was predicted to intercept the terrain after 10 seconds, and the left level turn was predicted to intercept the terrain after 22 seconds. At this point, the algorithm commanded the left level turn because it offered the longest time of flight prior to impact. However, the left level turn was predicted to impact the terrain for more than the last 50 iterations, corresponding to more than 1.5 seconds. This caused the aircraft to choose an escape path which predicted that a collision would occur even if the maneuver had been initiated well prior to the expiration of the time delay safety margin.

With this flight test result, additional simulator test points were flown to evaluate the possibility of allowing the algorithm to continue to evaluate the terrain during the actual execution of one of the TPAs. This was done by simply restarting the algorithm immediately upon TPA execution. Through this limited analysis, it was found that the algorithm would alter its flight path and TPA choice during execution and avoid the terrain. Through this rudimentary experimentation, the algorithm proved to be even more robust. Unfortunately, it was not possible to test these points in flight due to flight safety restrictions for software changes to the ESCAPE paths. This does, however, show promise for future research and testing.

Although the effects of wind on the flight test data were not specifically analyzed, a logical assumption would be that it also had an effect on the ground miss distance. Theoretically, a no wind assumption would reduce the accuracy of the predicted turn radius. This would cause the downrange travel to be smaller than predicted with headwind, and longer than predicted with tailwind. Additionally, the turn radius would vary throughout the turn, depending on whether the aircraft was flying into or away from the wind.

Another factor which affected the ground miss distance was the lag between the command vector and the aircraft response. The load factor and bank angle time history plots showed that on average, the aircraft's load factor and bank angle started to increase approximately 0.25 seconds after the command vector was initiated, which is equivalent to

half of the time delay safety margin, or 130 ft of downrange travel at a groundspeed of 310 kts. For this reason, aircraft performance, inertia, and center of gravity have a direct affect on the algorithm's performance and must be accounted for within the time delay safety margin. Since this lag is typically very small, on the order of a tenth of a second, it need be only evaluated at a worst-case condition and applied throughout the individual aircraft's flight envelope.

4.2.4 Specific Test Objective 1 Conclusion.

The 3-TPA path selection was found to be dependable throughout flight test. The predictability and robustness of the three path ESCAPE algorithm was demonstrated in flight test through the consistency with which it chose the escape paths for a given situation based on expected simulation results.

The 3-TPA aircraft response did not consistently hold specified parameters due to the lag in the load-factor onset, and due to the inability to maintain the desired flight path angle. The ability to control the aircraft using pre-determined load factor and bank angle commands was demonstrated in flight test, but should be improved to be able to consistently achieve the desired aircraft response.

Finally, the algorithm processing needs to be updated to allow for a closed-loop anlaysis of the terrain during maneuver execution. The current algorithm stops evaluating terrain once a TPA has been chosen. It is recommended that it continue to evaluate the terrain which would require aircraft initial state information to be constantly fed into the path control logic. With these additions, the ESCAPE algorithm effectiveness should provide increased protection in even the most challenging terrain.

4.3 Specific Test Objective 2: Evaluate the 5-TPA Solution.

4.3.1 MOP 1: Algorithm Path Selection.

The 5-TPA path selection data were analyzed by observing the aircraft response during simulator sessions and comparing it to the aircraft response during flight test. The

evaluation criteria were satisfied if the chosen escape path matched the simulation results. During flight test, the algorithm's decision logic was also monitored from the research laptop, to confirm that the algorithm was commanding the correct path.

The 5-TPA path selection results are presented in Tables 4.4. The data showed that for all 43 test points, the five path algorithm chose the predicted escape path. This shows that the algorithm results were repeatable and predictable. This predictability and repeatability of the flight test results demonstrate the algorithm's effectiveness, in that it was able to perform consistently from one flight to another.

Table 4.4: 5-TPA Path Selection

Algorithm: 5-TPA Test Dates: 31 Aug-10 Sep 15
Pressure Altitude: 15,000 ft Airspeed: 310 kts Groundspeed

Test Point	Result	Number of Test Runs	Forward Path	Left Path	Right Path	Left-Up Path	Right-Up Path
9	Left-Up Path	6				6	
10	Forward Path	6	6				
11	Forward path	7	7			6	
12	Forward Path	6	6				
13	Right-Up Path	6					6
38	Left-Up Path	4				4	
39	Left-Up Path	4				4	
40	Right-Up Path	4					4

Prior to flight test, the test team attempted to find test points which would trigger each of the five different escape paths. When the test team simulated test points 10 and 11 on their personal computers, the left and right paths were triggered, respectively. However, when these test points were simulated in the TPS flight sciences simulator using the research laptop, both of these test points triggered the forward path. The different outcome is explained by the difference in processing power. The personal laptops could not run the algorithm as rapidly; which provided less overlap in the safety bubbles, and a greater distance traveled between iterations of the algorithm's predictions. The test team attempted

to find new test point parameters which would force the 5-TPA solution to choose the left and right level turn maneuvers by performing simulation against cliff faces, valleys, and box canyons and approached these terrain features at various angles and altitudes. In fact, the test team created a MATLAB script that ran thousands of iterations over hundreds of hours on personal (slower processor) computers. After extensive analysis and simulation, no such test point was found that triggered a level turn in the flight science simulator. The fact that the test team could not find any scenario to trigger the level turn paths with the 5-TPA solution indicated that whenever 15° climbing maneuvers, straight ahead or turning were available, there were few situations where a level turn was advantageous.

Since the algorithm appeared to favor the climbing maneuvers over the level turn maneuvers, the 3-TPA test points were repeated while using the 5-TPA solution to determine if the algorithm would still choose the same paths when given additional options. The results of this experiment are shown in test points 38 to 40 which mirror test points 6 to 8, but with the 5-TPA algorithm as seen in the test matrix in Appendix A. This experiment showed that in all three cases, the 5-path algorithm chose climbing turn maneuvers, which were not previously available. In the case of test points 39 and 40 (level turns in the 3-TPA algorithm), the 5-TPA solution chose a maneuver which was in the same direction as the 3-TPA solution, but it assessed that the climbing turn was a better option than the level turn. With respect to terrain avoidance alone, these preliminary results seem to suggest that climbing maneuvers are distinctly favored over level maneuvers. Of note, this does not take into account mission related scenarios that would benefit from level maneuvers.

4.3.2 MOP 2: 5-TPA Aircraft Response.

The 5-TPA aircraft response data were analyzed by plotting the time history of the load factor (N_z) and bank angle (ϕ) for both the commanded values and the actual achieved values. The time history of the altitude and the flight path angle were also plotted to compare with the expected values. From the time history plots, the maximum parameter

deviation was found for the transitory period and for the steady-state period, precisely as outlined in Section 4.2.2 with the same evaluation criterion.

The 5-TPA aircraft response results are summarized in Table 4.5, which represents the largest deviation from the desired value of the aircraft state, as observed over the course of four separate flights for both the transitory period and the steady-state period. Negative values indicate that the aircraft state was less than desired, while positive values indicate that the aircraft state was greater than desired. To compare data between flights and to observe trends, sample time history plots for test point 9 are presented in Figures 4.6 through 4.8. Additional time history plots for test point 13 are presented in Appendix D Figures D.15 through D.17. This section will discuss the results of test points 9 and 13, which represent the left-up and right-up maneuvers respectively. The other test points resulted in the forward path, which yielded similar results to test point 6, discussed within Objective 1.

Table 4.5: Maximum Deviation from Desired Aircraft States for 5-TPA

Algorithm: 5-TPA Test Dates: 31 Aug-10 Sep 15
Pressure Altitude: 15,000 ft Airspeed: 310 kts Groundspeed

	Transitory Period				Steady-State Period			
Test Point	Bank Angle*	Load Factor	Altitude	Flight Path Angle	Bank Angle*	Load Factor	Altitude	Flight Path Angle
9 (Left-Up)	-26°	-0.21 g	N/A	N/A	-1.5°	-0.09 g	N/A	+1.5°
13 (Right-Up)	-24°	-0.22 g	N/A	N/A	+2.5°	-0.09 g	N/A	+4.1°

(red indicates values outside expected performance)
*Bank Angles represent magnitude, negative values mean less bank than commanded.

ESCAPE Test Point: 9 (Left-Up) Average OAT: -8°C
Test/Virtual Altitude: 15,000/6,800 ft Test Dates: 31 Aug-10 Sep 15
Center of Gravity: 12.5 - 23.8% Test Day Data

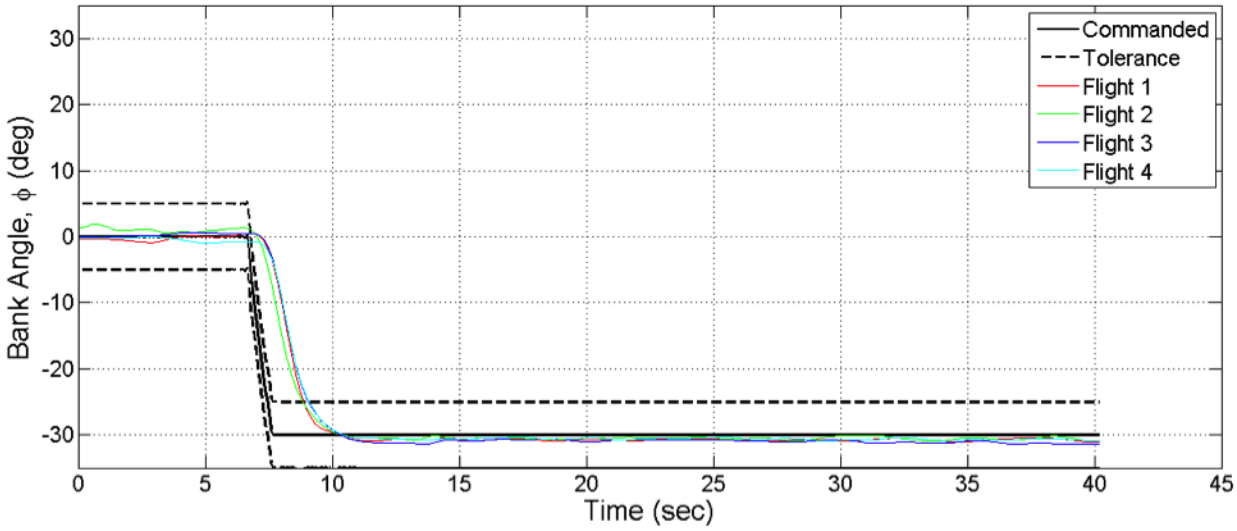

Figure 4.6: Bank Angle vs Time for Test Point 9, Left-Up Path

ESCAPE Test Point: 9 (Left-Up) Average OAT: -8°C
Test/Virtual Altitude: 15,000/6,800 ft Test Dates: 31 Aug-10 Sep 15
Center of Gravity: 12.5 - 23.8% Test Day Data

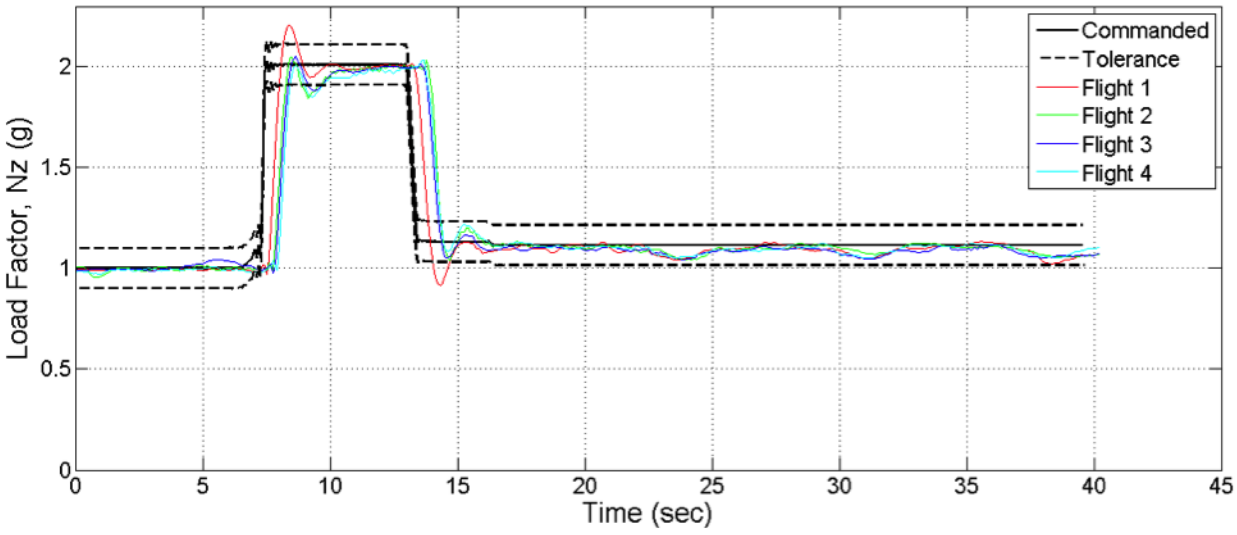

Figure 4.7: Load Factor vs Time for Test Point 9, Left-Up Path

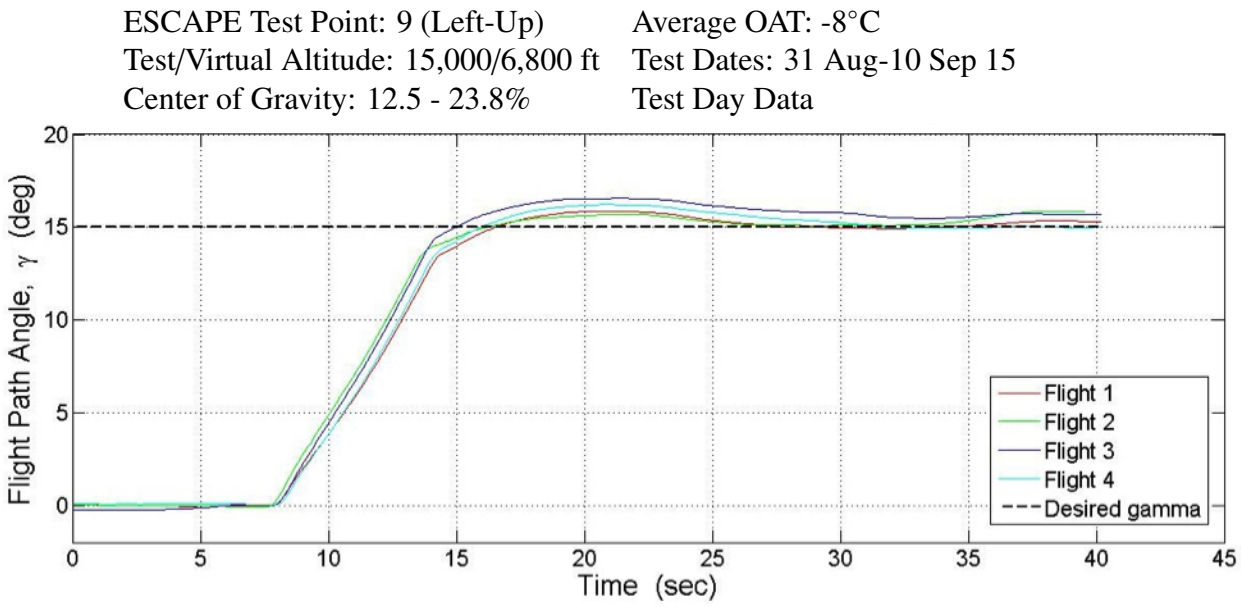

Figure 4.8: Flight Path Angle vs Time for Test Point 9, Left-Up Path

Figures 4.6 and 4.7 show that the bank angle and the load factor both lagged the commanded value during the transitory period. Similar to the straight ahead pull-up and the level turns discussed within Objective 1, the flight path angle was set and maintained by modulating the load-factor over a period of time. In all cases, the climbing turns achieved an initial flight path angle which was within tolerance, varying between 13.5° and 16.1° as shown in Figure 4.8. This indicates that the duration of the 2-g command was adequate for the tolerances of this test. During the steady-state period, the bank angle and load factor were held within tolerance, with only fluctuations within the bounds specified in Table 4.5. Unlike the straight ahead climb, the flight path angle remained above 15° during the climbing turns because the commanded load factor was slightly more than required to maintain the desired climb angle, but the VSS limited the flight path angle to 15°. This was a byproduct of a VSS limiter that was put in place for the climbing turn maneuvers to prevent a VSS safety trip which was unnecessary for the straight ahead climbs. The result of this limiter showed the necessity for precise flight path angle control.

4.3.3 MOP 3: 5-TPA Ground Miss Distance.

The 5-TPA ground miss distance data were analyzed using a MATLAB script which accepted the aircraft virtual navigation solution (downstream of the position and course slewing tool) as an input, and returned the terrain miss distance and available reaction time as outputs. All algorithm processing is exactly the same as the three path algorithm.

The 5-TPA ground miss distance results are presented in Table 4.6, tabulated with one test run per container. The flight test results are also presented graphically in 3-dimensional plots shown in Figure 4.9 and Appendix D Figure D.18. In both cases, they show that

ESCAPE Test Point: 9 (Left-Up) Average OAT: -8°C
Test/Virtual Altitude: 15,000/6,800 ft Test Dates: 31 Aug-10 Sep 15
Center of Gravity: 12.5 - 23.8% Test Day Data

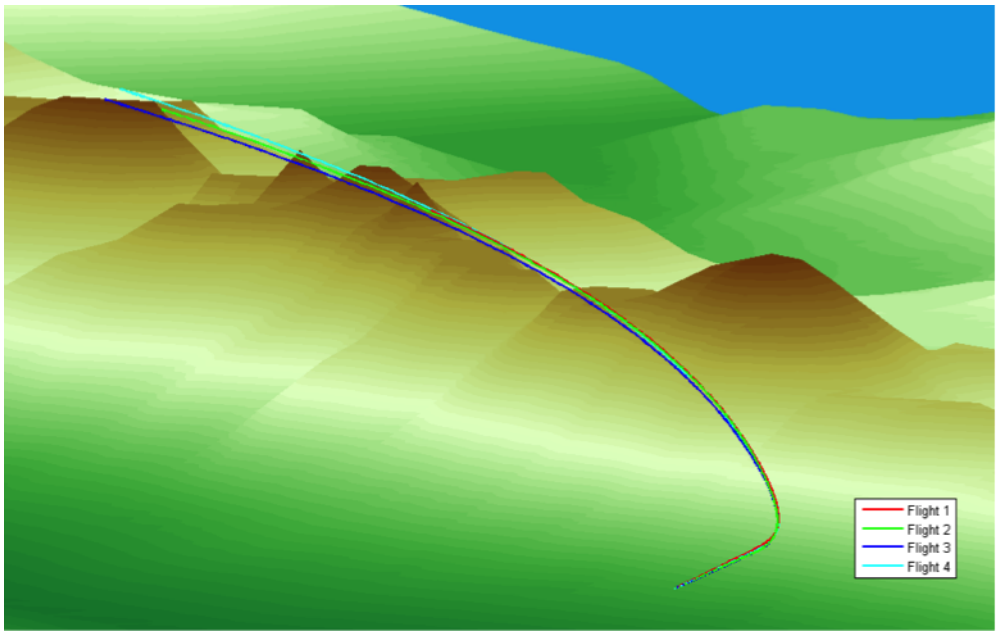

Figure 4.9: 3D Presentation of Flight Test Data, Test Point 9, Left-Up Path

the climbing turn paths do not intersect the terrain. The Ground Miss Distance was the distance between the aircraft and the terrain at the closest point of approach. As previously mentioned, the available reaction time, a measure of nuisance, was the amount of time that

the maneuver could have been delayed while flying straight and level beyond the maneuver activation point, and still avoid a collision by an infinitely small margin. For all cases, a 300 ft bubble was used, so any miss distance less than 300 ft represents a terrain clearance inside the bubble. The data showed that all test runs for test points 9 and 13 (left up and right up paths) did not impact the simulated terrain, while all test runs except one for test points 10 (desired left, actual forward), 11 (desired right, actual forward), and 12 (forward) did impact the simulated terrain with the same analysis as Objective 1 since flight path angle was not adequately maintained. This reduced climb performance caused the aircraft to impact the terrain in all but one test run. As previously discussed, points 10 and 11 were attempted level paths with the 5-path algorithm, but with actual processing speeds, the algorithm always chose to climb.

As previously discussed, the climbing turn maneuvers successfully maintained 15° of flight path angle throughout the maneuver. This allowed the aircraft to maintain a sufficient climb gradient to avoid the obstacles.

The variance in the ground miss distance data and the available reaction time computation was a result of the same factors as discussed for Objective 1, namely variations in wind and the lag between the command vectors and the aircraft response. Again, all of the issues presented in Objective 1 were also evident in Objective 2, except that the algorithm had success in all cases when the flight path angle was maintained during the maneuver which is evident in Table 4.6 for the climbing turn ESCAPE paths.

4.3.4 Specific Test Objective 2 Conclusion.

Similar to Objective 1, the path selection logic was found to be robust for the 5-TPA algorithm. The predictability and robustness of the 5-TPA solution were similar to those of the 3-TPA solution. Difficulty in finding terrain to trigger the level paths indicated that climbing paths may be more desirable than level paths. Such terrain may exist, but it has proven itself to be difficult to find.

Table 4.6: 5-TPA Miss Distance and Available Reaction Time

Algorithm: 5-TPA Test Dates: 31 Aug-10 Sep 15
Pressure Altitude: 15,000 ft Airspeed: 310 kts Groundspeed

	Ground Miss Distance				Available Reaction Time			
Test Point	Flight 1	Flight 2	Flight 3	Flight 4	Flight 1	Flight 2	Flight 3	Flight 4
9 (Left-Up)	197	304	240	133	0.18	0.02	0.11	0.30
10 (Fwd)	0	0	0	0	0	0	0	0
11 (Fwd)	0	251	0	0	0	0.03	0	0
12 (Fwd)	0	0	0	0	0	0	0	0
13 (Right-Up)	189	185	258	47	0.14	0.14	0.12	0.10
38 (Left-Up)	264	254	No Data	178	0.18	0.17	No Data	0.12
39 (Left-Up)	239	No Data	No Data	235	0.01	No Data	No Data	0.01
40 (Right-Up)	373	249	356	329	0.14	0.12	0.11	0.05

Once again, similar to the 3-TPA algorithm, the 5-TPA solution created an aircraft response that did not meet expectations for the forward path due to the lag in the load factor and bank angle caused by center of gravity and weight changes in the aircraft. The climbing turn maneuvers, however, showed that direct control of the flight path angle (γ) would result in improved performance and terrain protection.

This added protection for the climbing turn maneuvers resulted in 100% saves from the terrain for the test points that resulted in those maneuvers. For that reason, it is recommended that further research focus on methods to more precisely control the

flight path angle since load factor control alone is unpredictable with changing aircraft parameters.

The specific recommendations for Objectives 1 and 2, which are very similar, will be presented in Chapter 5.

4.4 Specific Test Objective 3: Determine Algorithm Parameters.

The third specific test objective was to determine acceptable algorithm parameters by analyzing the algorithm's performance with various safety bubble sizes against Level 1 DTED and determining the overall processing time required to run the algorithms.

4.4.1 MOP 1: Bubble Size for Level 1 DTED.

The test points for this MOP were similar to those used for specific objectives 1 and 2, with the only difference being the variation in bubble radius of 100 ft, 200 ft, and 300 ft as seen in Appendix A for test points 14-37. Three different bubble sizes were analyzed to determine the level of protection provided against Level 1 DTED. The path selection was then annotated to determine the effect of the changing bubble size. The relationship between bubble size and miss distance was not evaluated during this analysis because the results of Objectives 1 and 2 revealed that too many other factors affected the miss distance to be able to draw useful conclusions about this relationship. It is safe to assume though, that a reduction in bubble size will result in less terrain miss distance and less available reaction time which will ultimately reduce algorithm effectiveness. Once the recommendations outlined in Chapter 5 are addressed, it would be prudent to reevaluate miss distances with varying bubble size.

The three and five path selection results are presented in Tables 4.7 and 4.8 respectively. The data show that there was more variability in path selection as bubble size decreased. Though some of this could be attributed to minor deviations in heading or wind, there were situations where a 100 ft bubble flew between DTED posts without triggering an ESCAPE maneuver. The tabulated results in the "No Path" column denote

scenarios where a collision was either completely undetected or was detected after having flown through a terrain feature. Additionally, smaller bubble sizes allowed for fewer DTED posts to be analyzed during an iteration, which could have affected path selection for a given terrain feature because a different DTED post could have tripped the algorithm logic. For example, Test Point 17 displays a situation where the left path was expected, but in one-third of the cases, the algorithm chose a dissimilar path. In this scenario, a different path was chosen simply by reducing the bubble size to 100 ft. In this way, the chosen bubble size is directly related to algorithm performance based on the desired level of DTED. Of note, most military platforms currently only have the capability to carry Level 1 DTED.

Table 4.7: 3-TPA Bubble Size Effects

Algorithm: 3-TPA Test Dates: 31 Aug-10 Sep 15
Pressure Altitude: 15,000 ft Airspeed: 310 kts Groundspeed

		Number of Chosen Paths for Bubble Size				
Test Point	Bubble Size (ft)	Expected Path	Left	Fwd	Right	No Path
14	100	No Path	2	0	0	3
15	200	Left Path	4	1	0	0
16	300	Fwd Path	2	5	0	0
17	100	Left Path	4	1	1	0
18	200	Left Path	5	0	0	0
19	300	Left Path	7	0	0	0
20	100	Right Path	0	0	6	0
21	200	Right Path	0	0	5	0
20	300	Right Path	0	0	7	0

(red indicates different path chosen than expected.)

It is much easier to understand this concept graphically. As depicted in Figures 3.7 and 4.10, the minimum number of DTED posts that can be collected by a 300 ft, 200 ft and 100 ft bubble size were 4, 1, and 0 respectively. This was determined for Level 1 DTED with a post spacing of approximately 295 ft. Although it was not used for this project, Level

Table 4.8: 5-TPA Bubble Size Effects

Algorithm: 5-TPA Test Dates: 31 Aug-10 Sep 15
Pressure Altitude: 15,000 ft Airspeed: 310 kts Groundspeed

		Number of Chosen Paths for Bubble Size						
Test Point	Bubble Size (ft)	Expected Path	Left	Left-Up	Fwd	Right-Up	Right	No Path
23	100	Right Path	0	0	0	0	3	2
24	200	Left-Up	0	4	0	0	0	0
25	300	Left-Up	0	4	0	0	0	0
26	100	No Path	0	0	1	0	0	3
27	200	Fwd Path	0	0	4	0	0	0
28	300	Fwd Path	0	0	6	0	0	0
29	100	Right Path	0	0	2	0	1	1
30	200	Fwd Path	0	0	3	0	0	0
31	300	Fwd Path	0	0	7	0	0	0
32	100	Left-Up	0	1	2	0	0	0
33	200	Fwd Path	0	0	4	0	0	0
34	300	Fwd Path	0	0	6	0	0	0
35	100	Right-Up	0	0	0	0	4	0
36	200	Right-Up	0	0	0	0	4	0
37	300	Right-Up	0	0	0	0	5	0

(red indicates different path chosen than expected.)

2 DTED also exists, and provides a post spacing of approximately 98 feet. Based on this analysis, Level 1 DTED is sufficient for a 300 ft radius, Level 2 DTED is recommended for a 200 ft radius, and Level 2 DTED is *required* for a 100 ft radius. This would allow at least 1 DTED post to be identified providing for some terrain analysis at each bubble iteration.

In general, the amount of DTED analyzed for both the three and five path algorithms was increased by increasing bubble size. This was evident in Tables 4.7 and 4.8 as the predictability of the 300 ft and 200 ft bubble sizes was generally more consistent than the 100 ft size for both algorithms. In all cases, higher fidelity DTED would allow more posts to be identified per iteration for a given bubble size which will increase the level of protection provided by the algorithm.

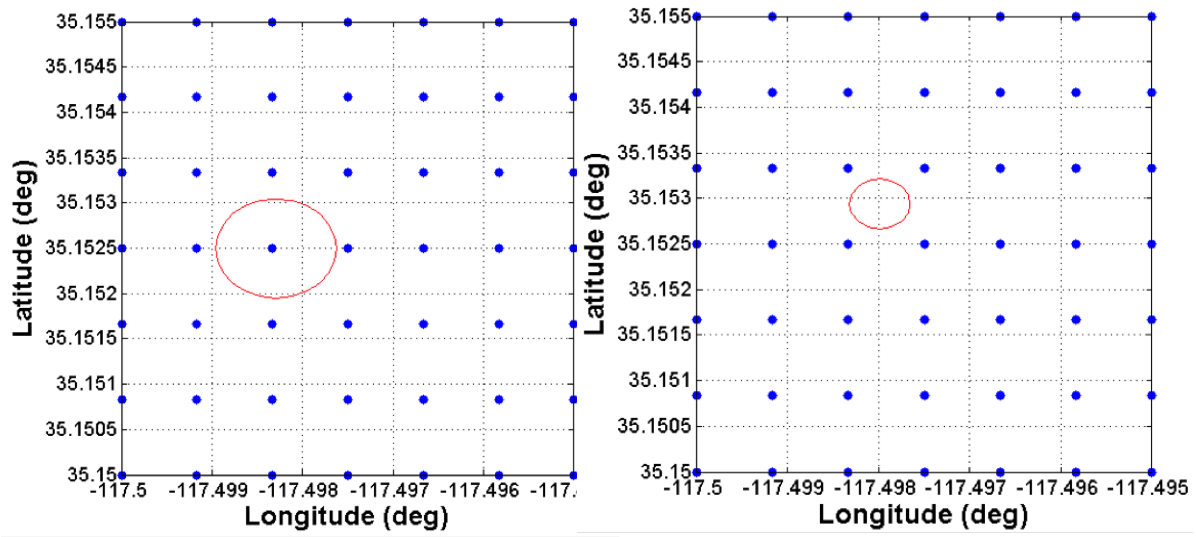

(a) 200 ft Radius Bubble

(b) 100 ft Radius Bubble

Figure 4.10: Minimum Post Identification for Level 1 DTED

4.4.2 MOP 2: Algorithm Processing Time.

For every test point flown, the MATLAB Tic-Toc functions were used to measure and record the time required to process each iteration of the ESCAPE algorithms to include solving the equations of motion for each projected flight path and conducting the collision prediction. All test points were flown a minimum of four times and data were recorded each time to increase statistical significance. The same research laptop and software were used, and nonessential user background processes were eliminated when possible to decrease variability. The computer was a commercial off the shelf laptop with a standard Windows 8.1 Pro operating system. Operating system software was not modified or trimmed down to meet the specific purposes of the test program.

A total of 14,695 data points were collected during flight test. Since the algorithms were being processed at 12.5 Hz, the data were analyzed for serial correlation, and the data within each test point were found to be correlated. To obtain independent data points, the

data were decimated by a factor of 30 prior to statistical analysis. Box plots were generated using MATLAB to show the distribution of the data. The evaluation criteria were satisfied if the algorithm processing time was sufficiently quick to provide an overlap in the safety bubbles from one iteration to the next and if the processing time was always less than the algorithm's time safety margin of 0.5 seconds.

Figures 4.11 and 4.12 show the results of the statistical analysis of the overall processing time for all flights. The results from this analysis are representative of the full capabilities of the algorithm and the research laptop. These results are summarized in Table 4.9 for the 3 and 5 path algorithms' average and maximum processing time.

3-TPA	Data Basis: Flight Test
Simulink 8.5	Altitude: 14,500-18,500
MATLAB 8.5.0.197613 (R2015a)	Dates: 31 Aug - 10 Sep 2015
Windows 8.1 Pro	Test Day Data

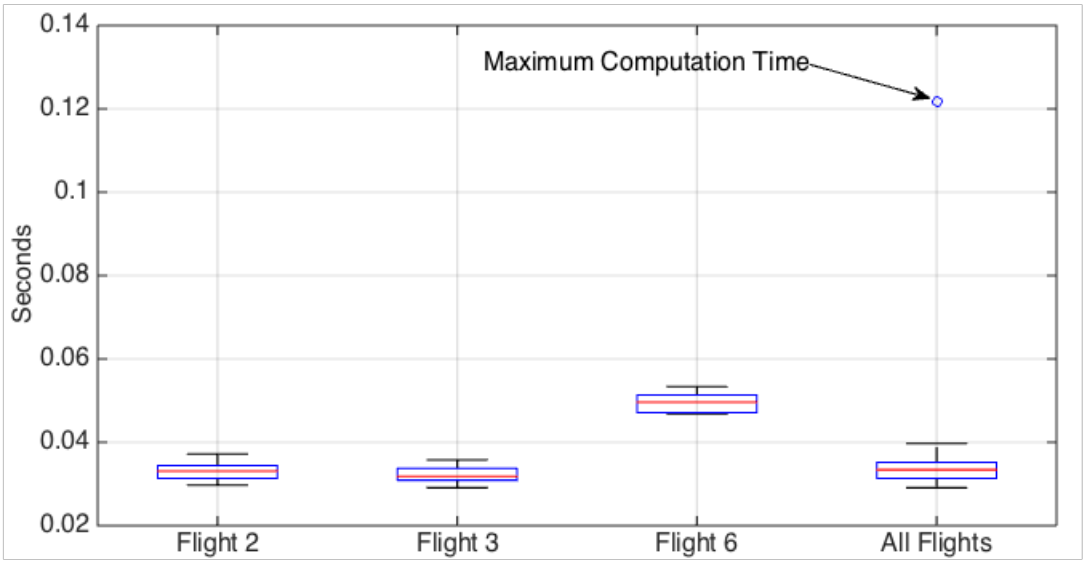

Figure 4.11: Overall Processing Time for the 3-TPA Algorithm

5-TPA	Data Basis: Flight Test
Simulink 8.5	Altitude: 14,500-19,100
MATLAB 8.5.0.197613 (R2015a)	Dates: 31 Aug - 10 Sep 2015
Windows 8.1 Pro	Test Day Data

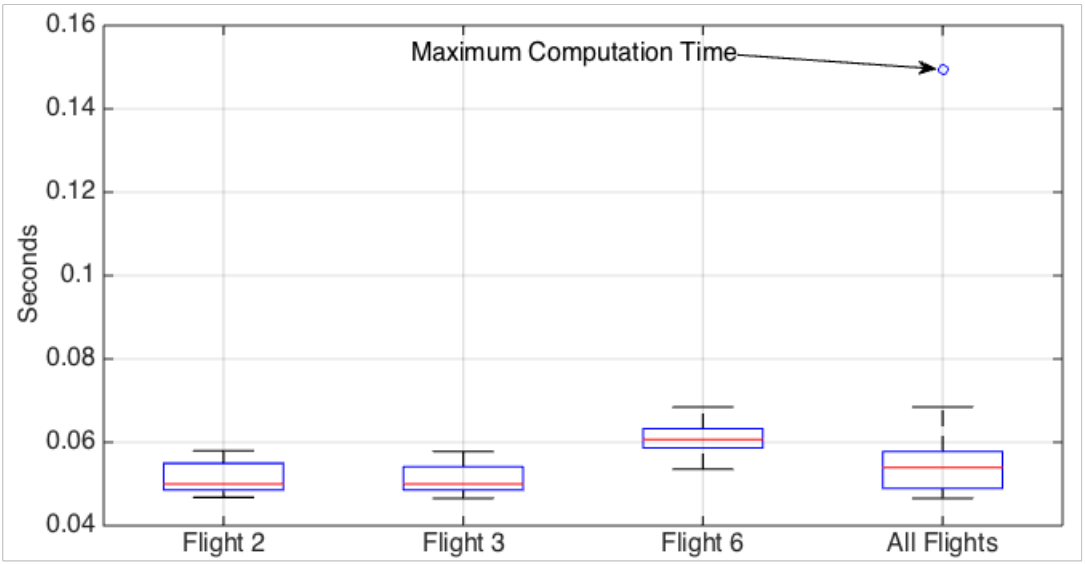

Figure 4.12: Overall Processing Time for the 5-TPA Algorithm

The data show that the longest observed processing time for one iteration was 0.1494 seconds. At 310 knots ground speed, the aircraft traveled at 523.22 ft/s which corresponds to 78 feet in 0.1494 seconds. Therefore, the maximum algorithm processing time was sufficiently fast to provide an overlap between the safety bubble from one iteration to the next. Both algorithms' maximum processing times were well below the time safety margin of 0.5 seconds. Of note, the maximum processing times are outliers. Specifically, they are 13.13 and 17.46 standard deviations from the mean, for the 3-TPA and 5-TPA solutions respectively. Of the 3,570 data points for the 3-TPA solution, only 262 points fell above the 95-percentile, 0.0512 seconds, in the fourth quartile. Of the 7,107 data points for the 5-TPA solution, only 512 points fell above the 95-percentile, 0.0637 seconds, in the fourth quartile.

The three path algorithm was on average 34% faster than the five path algorithm. In general, it was possible to run at more than five iterations per second. In fact, all test points were flown at 12.5 Hz and could theoretically have been run at 28.25 Hz (3-TPA) and 18.55Hz (5-TPA), but were limited by VSS capabilities.

Table 4.9: Overall Processing Time for both Algorithms

Description	Time (sec)
Average Processing Time per Iteration (3-TPA Algorithm)	0.0354
Average Processing Time per Iteration (5-TPA Algorithm)	0.0539
Maximum Processing Time per Iteration (3-TPA Algorithm)	0.1217
Maximum Processing Time per Iteration (5-TPA Algorithm)	0.1494

4.4.3 Specific Test Objective 3 Conclusion.

With respect to varying bubble size, additional research will be required to determine the minimum radius for a given aircraft and mission. This will be a function of the aircraft's expected altitude, computing memory available to store the DTED, and processing power. With these parameters determined, an appropriate bubble size could be selected. In this way, the analysis supports that varying bubble sizes is practical and possible for military utility but should be flexible for different aircraft and mission sets. Additionally, the correct level of DTED must be used for proper terrain protection based on the chosen size.

The overall algorithm processing time was satisfactory for both the 3-path and 5-path algorithms. The algorithm processing time was always sufficiently quick to provide an overlap in the safety bubbles and was never more than the time delay of 0.5 seconds. This suggests that the computing power is readily available to effectively run the ESCAPE algorithms in real time to provide terrain clearance at expected operating speeds.

4.5 Specific Test Objective 4: Compare the 3 and 5-TPA solution with the Optimal Solution

The fourth specific test objective was to compare the 3-TPA and 5-TPA solutions with the optimally derived solution by comparing the algorithm's path selection, ground miss distance, and available reaction time of each solution.

4.5.1 MOP 1: Proper Path Selection.

The flight test data collected for this MOP were compared with the optimal code explained in Section 3.10.4 and focused on test points 6-13 from the Test Matrix in Appendix A. The test points that produced this data were then simulated with Suplisson's optimal code to determine the optimum solution response. The resulting direction of turn, flight path angle, bank angle, and N_z, were recorded. The ESCAPE algorithm solutions were compared to the optimal solutions at the ESCAPE algorithm's activation point.

The aircraft response obtained in flight test was compared to the optimum escape solution to qualitatively evaluate if the ESCAPE algorithms chose the similar path. Since the optimum code could choose from an infinite number of escape paths bounded by 60° angle of bank and a 2-g load factor, qualitative comparison regions were used to find a similar ESCAPE algorithm (non-optimal) path. These regions were numbered in the same manner as the Have ESCAPE paths and remained consistent for both the three and five path ESCAPE algorithms, which helped determine the usefulness of the 5-path algorithm.

- Region 1 was described by a flight path ranging from a straight ahead climb, to a 45° oblique 2-g climbing turn to a maximum of 15° flight path angle.
- Regions 2 and 3 were described by a flight path ranging from a level 2-g turn to a 5° oblique climbing turn.
- Regions 4 and 5 were described by a flight path ranging from a 5° climbing turn, to a 45° climbing turn, to a maximum of 15° flight path angle.

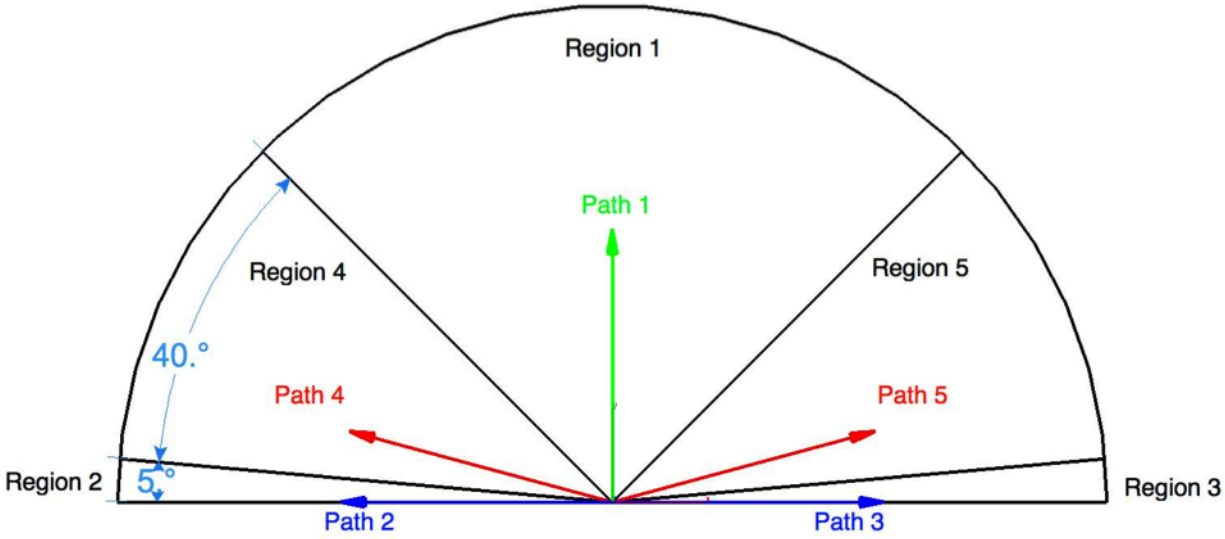

Figure 4.13: Qualitative Comparison Regions

These comparison regions are summarized in Figure 4.13, as seen from the tail of the aircraft and looking forward. The ESCAPE algorithm's solutions and optimal solutions were deemed similar if the flight test result and the optimum solution both fell within the same comparison region.

The qualitative comparisons between the 3-TPA or 5-TPA algorithms and the optimum algorithm are detailed in Tables 4.10 and 4.11 and Figures 4.14 to 4.25. The data showed the optimal solution always fell within region 1, which matched the flight test results of test points 6, 10, 11, and 12, but did not match the results of test points 7, 8, 9, and 13.

Figure 4.14 shows that the bank angle response obtained in flight test (test point 6, 3-TPA) was centered around a 0° bank condition (straight ahead climb) while the optimum solution commanded approximately 9° of right bank within approximately 2.5 seconds of initiation, then returned to a wings level attitude over the next 25 seconds.

Figure 4.15 shows that the N_z response obtained in flight test (test point 6, 3-TPA) achieved the commanded load factor of 2-g while executing the straight ahead climb and

Table 4.10: 3-TPA Optimal Path Selection Comparison Table

Test Point	3-TPA Chosen Path	Optimally Chosen Region	Result
6	1	1	Similar
7	2	1	Different
8	3	1	Different

Table 4.11: 5-TPA Optimal Path Selection Comparison Table

Test Point	5-TPA Chosen Path	Optimally Chosen Region	Result
9	4	1	Different
10	1	1	Similar
11	1	1	Similar
12	1	1	Similar
13	5	1	Different

then unloaded to a load factor of 1-g within approximately 5 seconds of activation. The optimum solution commanded an approximate load factor of 1.4-g in approximately 1.2 seconds, followed by a return to 1-g over the next 15 seconds.

Figure 4.16 shows that the flight path angle response obtained in flight test (test point 6, 3-TPA) achieved the desired 15° in approximately 7 seconds but failed to maintain that flight path angle over the length of the maneuver. The optimum solution commanded a 15°

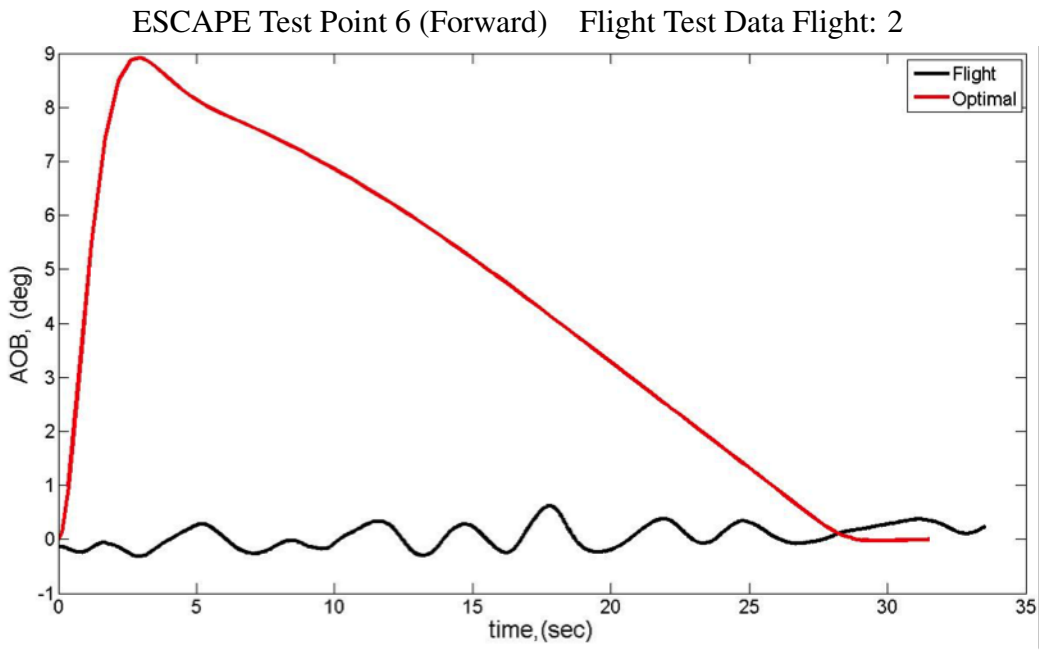

Figure 4.14: Flight Test Angle of Bank vs Optimal Angle of Bank

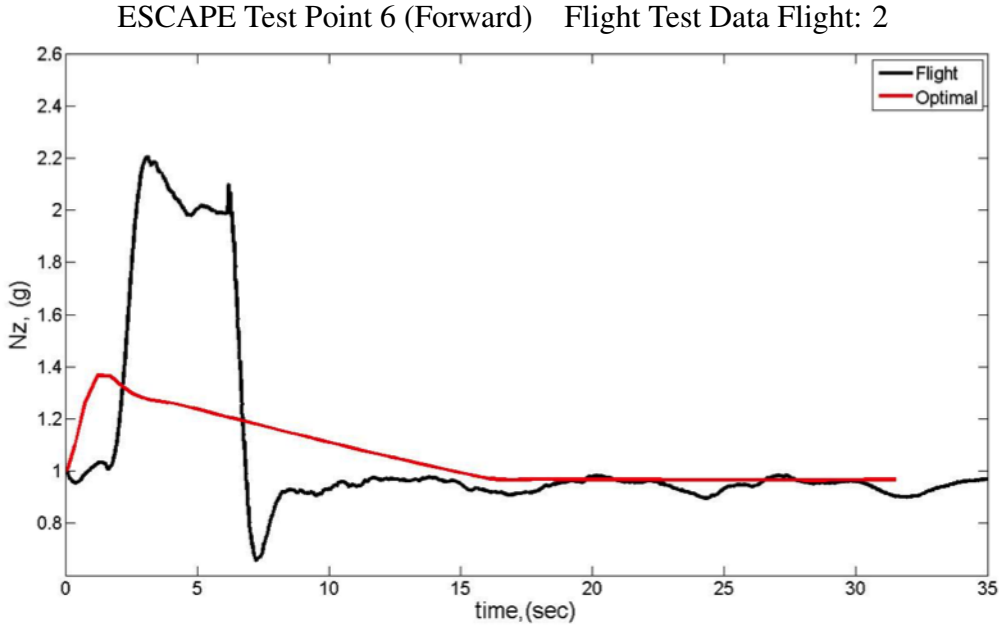

Figure 4.15: Flight Test N_z vs Optimal N_z

flight path angle in approximately 15 seconds and maintained the flight path angle until maneuver termination.

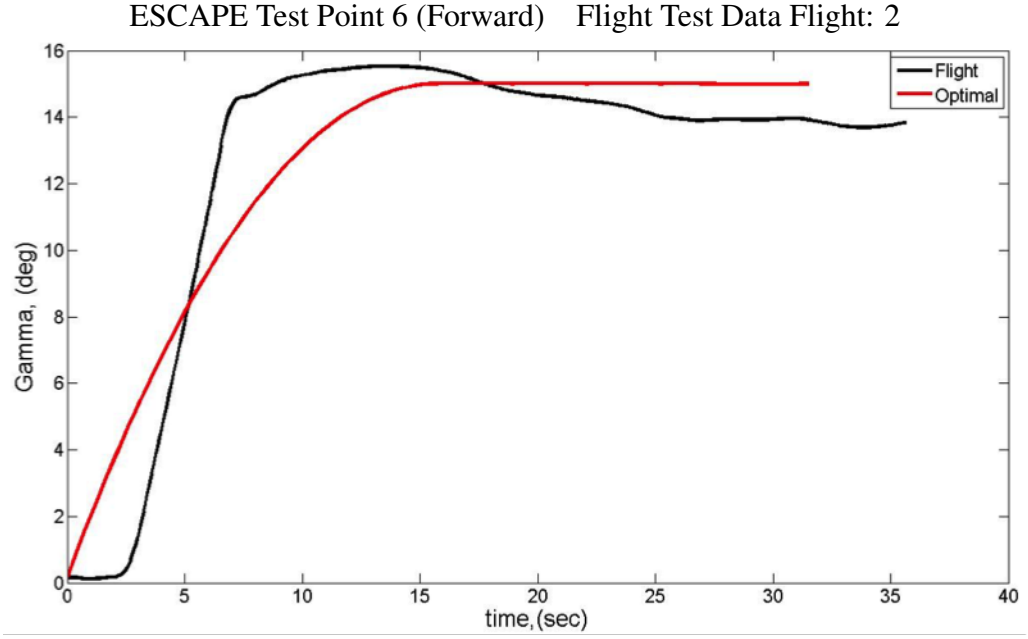

Figure 4.16: Flight Test Flight Path Angle vs Optimal Flight Path Angle

Figure 4.17 shows the flight test response and the optimal solution for test point 6 (3-TPA) in a 3D depiction. Although test point 6 resulted in similar results when using the qualitative comparison regions, when angle of bank, N_z, and flight path angle responses are coupled for the optimum solution, its motion can be described as a climbing right jink (a climb combined with slight change in direction of flight). Similar results were obtained in test points 10, 11, and 12 (5-TPA).

Figure 4.18 shows that the bank angle response obtained in flight test (test point 7, 3-TPA) achieved the commanded 60° of left bank within 6.5 seconds of initiation and maintained that commanded bank until maneuver termination. The optimum solution commanded 9° of right bank within 2.5 seconds, and then returned to a wings level attitude over the next 23 seconds.

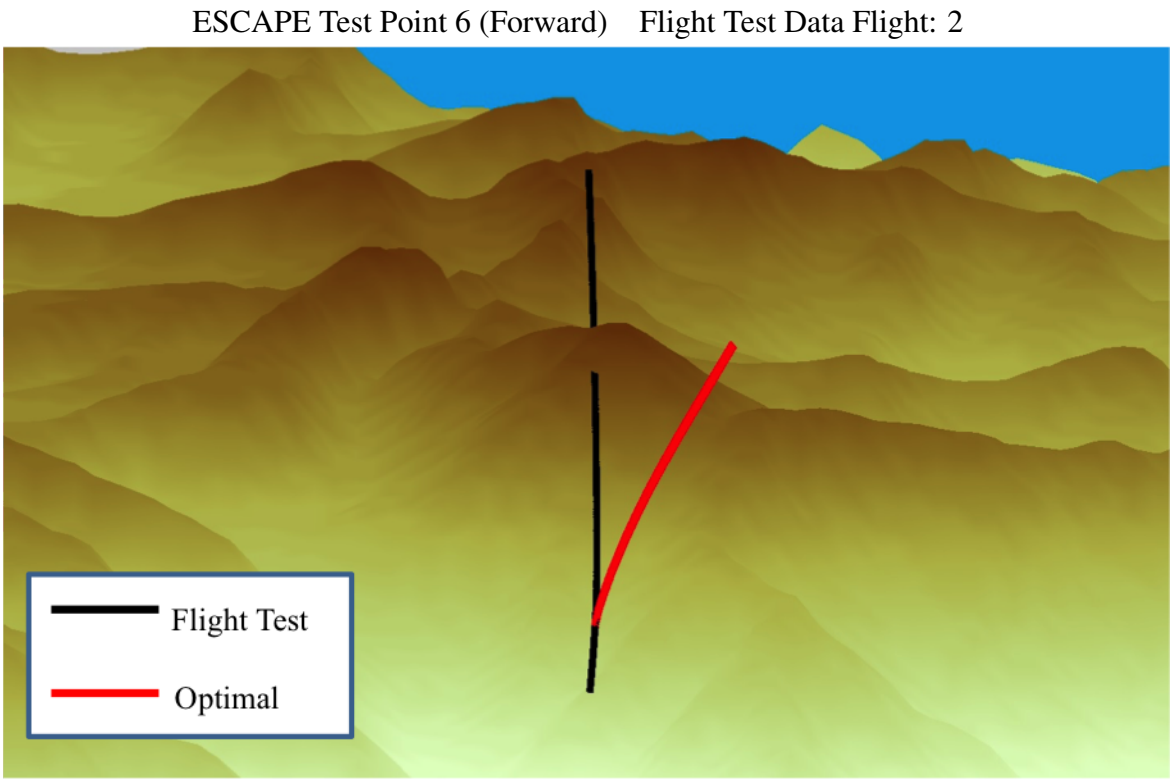

Figure 4.17: Test Point 6 3-TPA and Optimal Flight Path

Figure 4.19 shows that the N_z response obtained in flight test (test point 7, 3-TPA) achieved the commanded load factor of 2-g within 5 seconds of initiation while executing a commanded level turn and maintained a load factor of 2-g until maneuver termination. The optimum solution commanded an approximate load factor of 1.3-g within 1.2 seconds, and then returned to a load factor of 1-g over the next 15 seconds.

Figure 4.20 shows that the flight path angle response obtained in flight test (test point 7, 3-TPA) drifted from 0° over time, although a level turn was intended. The optimum solution commanded a 15° flight path angle in approximately 18 seconds and maintained this flight path until maneuver termination.

Figure 4.21 shows the flight test path and the optimal solution path for test point 7 (left level, 3-TPA) in a 3D depiction. Test points 7 and 8 (right level, 3-TPA) resulted in different

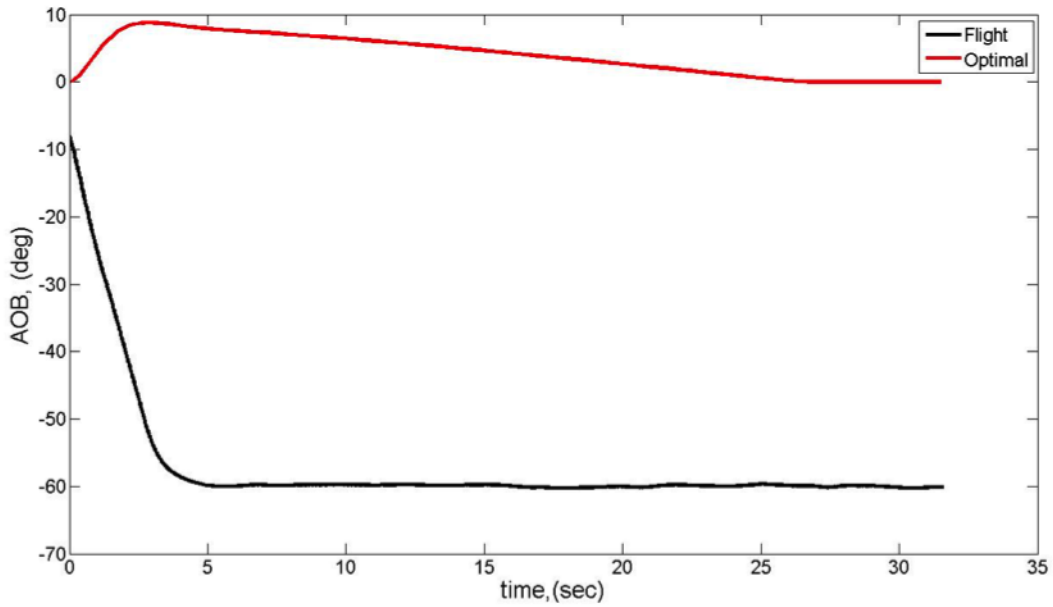

Figure 4.18: Flight Test Angle of Bank vs Optimal Angle of Bank

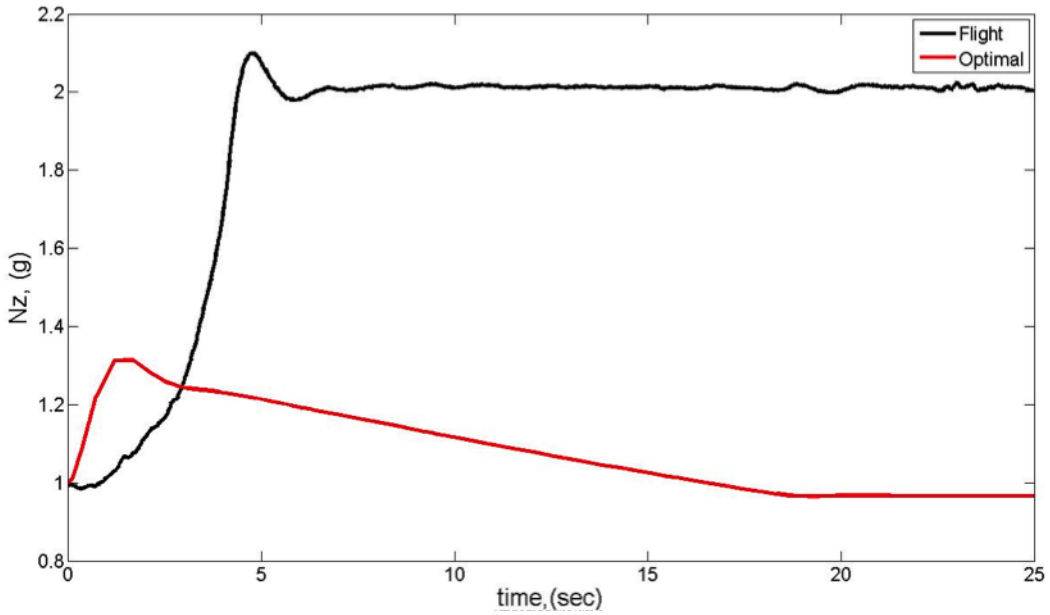

Figure 4.19: Flight Test N_z vs Optimal N_z

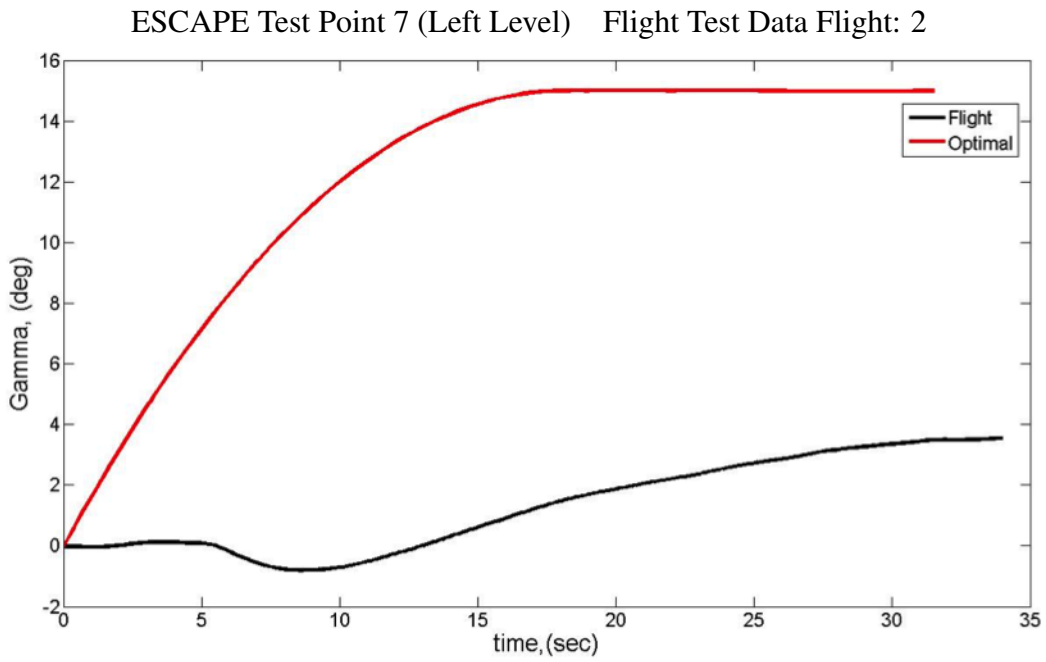

Figure 4.20: Flight Test Flight Path Angle vs Optimal Flight Path Angle

terrain avoidance maneuvers when using the qualitative comparison regions. In test point 7, the 3-TPA solution chose a level left turn to miss the terrain while the optimum solution chose a climbing right jink. Test point 8 (Appendix D, Figures D.19 through D.22) showed similar results to test point 7, with one exception. In test point 8, the 3-TPA algorithm chose a right level turn, and the optimum solution again chose a climbing right jink. The difference in direction of turn between the 3-TPA and optimal solutions could be attributed to the differences in terrain analysis. Since the 3-TPA algorithm was only analyzing the terrain along the pre-planned maneuver paths, it did not see maneuvers that the optimal solution had available. In both cases where the 3-TPA algorithm chose a level turn, the optimum solution chose a climbing jink (a climb combined with slight change in direction of flight).

Figure 4.22 shows that the bank angle response obtained in flight test (test point 13, 5-TPA) achieved the commanded 30° of right bank within 4 seconds of initiation and was

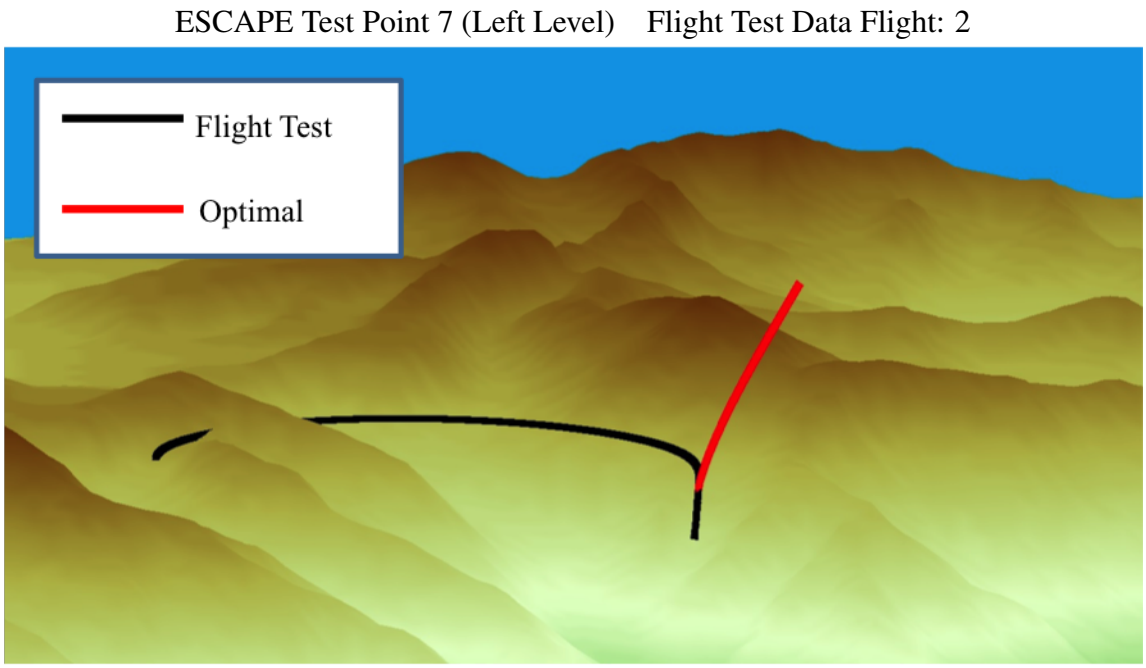

Figure 4.21: Test Point 7 3-TPA and Optimal Flight Path

centered on 30° until maneuver termination. The optimum solution commanded 3° of left bank within 2.5 seconds, and then returned to a wings level attitude over the next 19 seconds.

Figure 4.23 shows that the N_z response obtained in flight test (test point 13, 5-TPA) achieved the commanded load factor of 2-g while executing the climbing right turn and then unloaded to a load factor of 1-g within approximately 8 seconds of activation. The optimum solution commanded an approximate load factor of 1.5-g within 1.2 seconds, and then returned to a load factor of 1-g over the next 10 seconds.

Figure 4.24 shows that the flight path angle response obtained in flight test (test point 13, 5-TPA) achieved the desired 15° in approximately 10 seconds but overshot and maintained approximately 16° until maneuver termination. The optimum solution commanded a 15° flight path angle in approximately 10.5 seconds and maintained the flight path angle until maneuver termination.

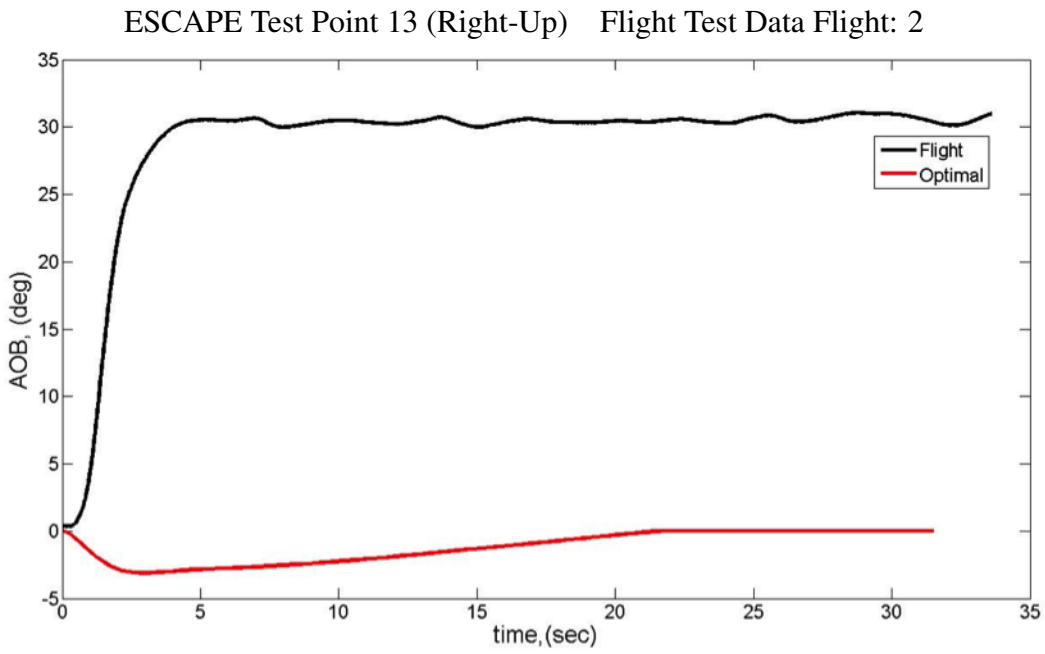

Figure 4.22: Flight Test Angle of Bank vs Optimal Angle of Bank

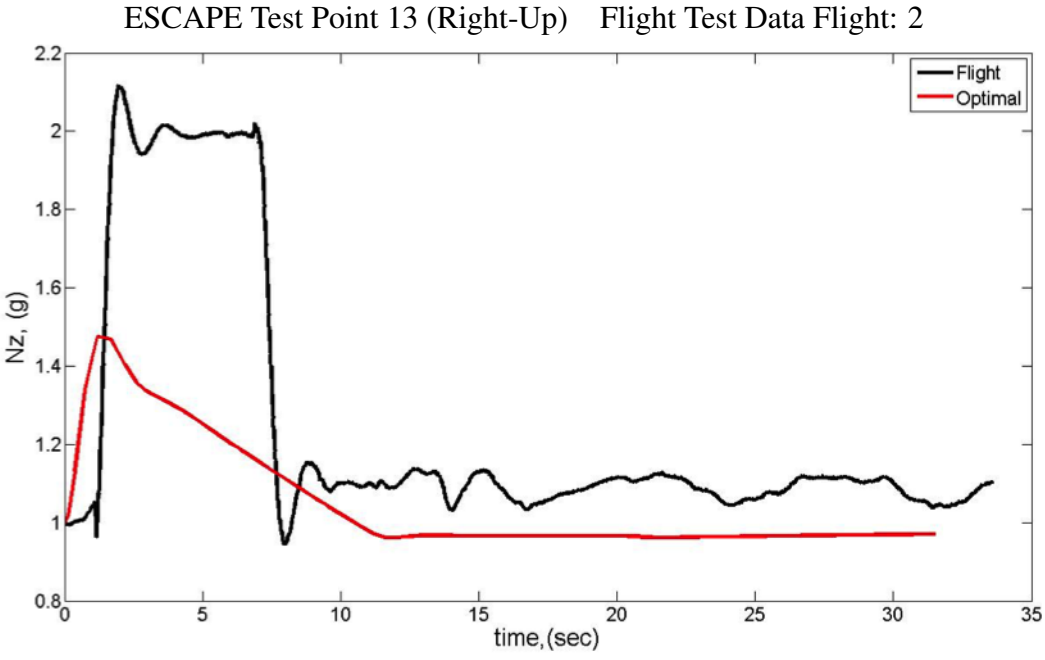

Figure 4.23: Flight Test N_z vs Optimal N_z

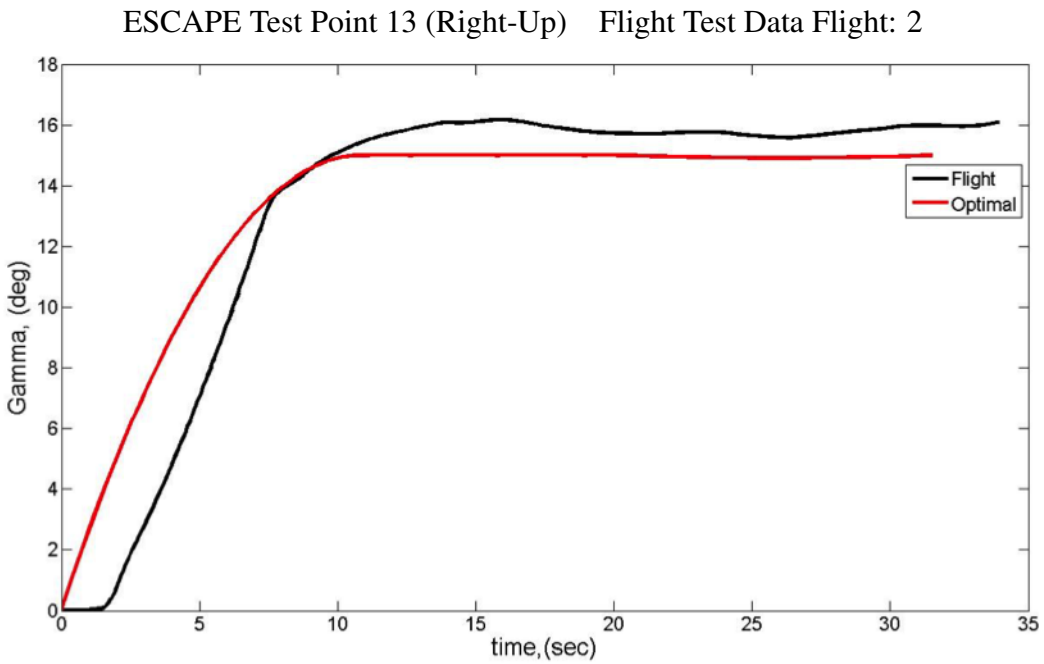

Figure 4.24: Flight Test Flight Path Angle vs Optimal Flight Path Angle

Figure 4.25 shows the flight test path and the optimal solution path for test point 13 in a 3D depiction. (Of note, for this test point the test day winds were later included in the optimal solution and resulted in the optimal path leaning 3° to the right, much closer to the flight test result. Though this is not graphically depicted, it suggests that wind effects could cause even better agreement between the two paths.) Test point 9 also resulted in different terrain avoidance maneuvers when using the qualitative comparison regions. In test point 9 (Appendix D, Figures D.23 through D.26), the 5-TPA solution chose a climbing right turn to miss the terrain, while the optimal solution chose a climbing right jink with up to 18° angle of bank. Again, the difference in direction of turn between the 5-TPA and optimal solutions could be attributed to the differences in terrain analysis. Additionally, the optimal solution penalized aircraft control, so the solution would tend to minimize bank and load factor inputs to minimize the penalty. For this reason, the ESCAPE algorithms tended to execute larger control movements than the optimal solution. (Note: The optimal solution was a minimum control maneuver.)

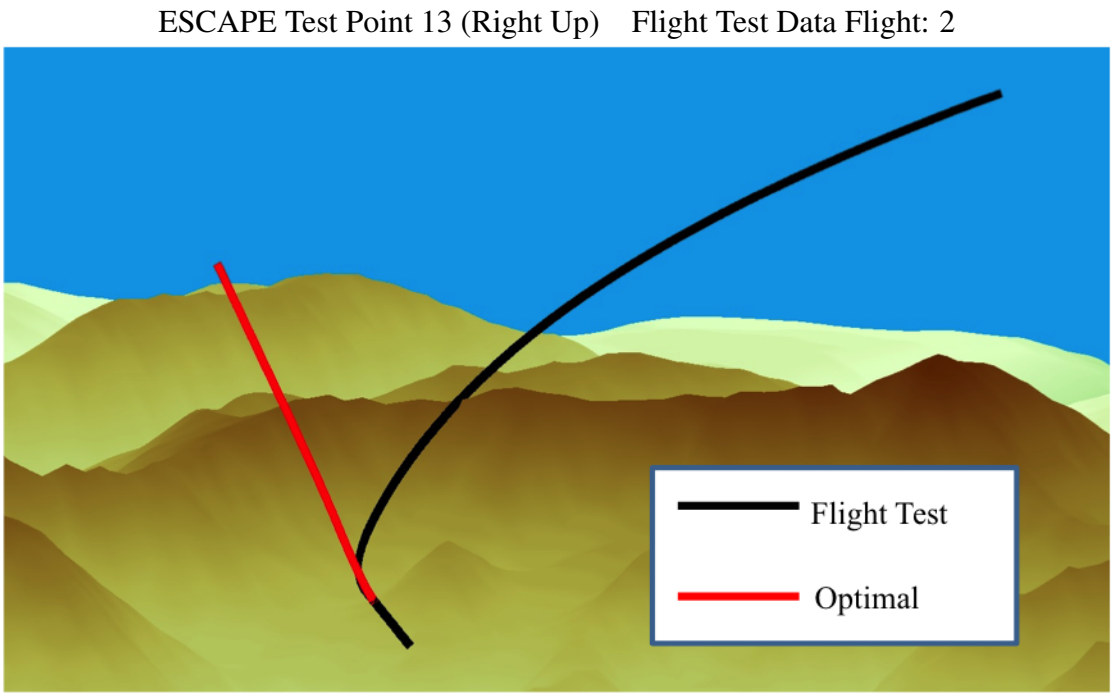

Figure 4.25: Test Point 13 5-TPA and Optimal Flight Path

In all cases the optimum solution chose a terrain avoidance maneuver within region 1. While evaluating the 5-TPA solutions, terrain features forcing a level turn were not found, as discussed in Objective 2. The tendency for both the ESCAPE algorithm's solution as well as the optimal solution to climb when given an option to make a level turn suggests that if a terrain avoidance maneuver has the ability to climb, it should execute a climbing maneuver. Further, the tendency of the optimal solution to remain within region 1 for all evaluated terrain features x of the chosen flight path angle of 15°. This flight path angle is aggressive for large, climb limited aircraft and may have impacted the results of the optimal solution to remain within region 1 by allowing the ability to out-climb terrain. A reduction in flight path angle to lower values may force the optimal solution closer to regions 2 and 3. These decreased flight path angles may be required for heavier gross weights or lower performing aircraft. Additionally, the 5-TPA solution may choose more climbing turns and

less straight ahead climbs, and the 3-TPA solution may choose more level turns under the same logic.

4.5.2 MOP 2: Terrain Miss Distance and Activation Time Differences between the Optimal and Chosen Path.

The same optimal data used to determine the similar path selection was used to determine and compare the terrain miss distance and available reaction time. The optimal solution data provided to the test team described the minimum control maneuver required to miss the terrain from the same point of activation as the ESCAPE algorithms. The data provided from the optimal solution was input into the same miss distance processing techniques used to calculate the distances for the actual flight test data as explained in Appendix B. To draw conclusions from the data provided, the optimal algorithm's available reaction time was qualitatively assessed by comparing the optimal solution's response to the 3 and 5-TPA response. If the optimal solution response was less aggressive in load factor, bank angle, and flight path angle, then the optimal solution could have continued to fly towards terrain until the maximum allowable bank and load factor was required. This meant the available reaction time for the optimal solution was greater than the 3 or 5-TPA solution. The differences between the flight test data and the optimal solution data provided a measure of how closely the ESCAPE algorithms matched the optimal code. Large differences in the data could indicate a potential for nuisance activations or the need for additional escape path options.

The terrain miss distance and available reaction time of the 3 and 5-TPA ESCAPE algorithms and optimal algorithm are detailed in Tables 4.12 and 4.13. Table 4.12 shows that the 3-TPA solution had zero miss distance. These results are specifically discussed in Section 4.2.3. The optimum solution's ground miss distance was 300 feet for all runs. At the common activation point, the optimum solution commanded a maneuver that required less load factor and less bank angle than the ESCAPE maneuvers. The reduced load factor

and angle of bank indicate that the optimum solution could have continued further along the initial flight path before requiring a terrain avoidance maneuver at the maximum allowable load factor. For example, in any given scenario, a last possible avoidance maneuver would be triggered by the max allowable load factor and maximum allowable bank. Since the optimal solution penalizes such large control motions, it tended to initiate a maneuver sooner, reducing control movements. Therefore, the optimum solution's available reaction time was greater than the 3-TPA solution's available reaction time in all cases. Table 4.13 shows that the 5-TPA solution had available reaction times ranging from 0 seconds to 0.59 seconds and miss distances ranging from 0 feet to 304 feet. These results are specifically discussed in Section 4.3.3. The optimum solution's ground miss distance was 300 feet for all runs. At the common activation point, the optimum solution again commanded a maneuver that required less load factor and less bank angle than the ESCAPE maneuvers. Therefore, the optimum solution's available reaction time was greater than the 5-TPA solution's available reaction time in all cases as anticipated.

Table 4.12: 3-TPA Miss Distance vs Optimal Solution

	Optimal Solution		3-TPA Solution
Test Point	Miss Distance (ft)	Available Reaction(< or > 3-TPA) (sec)	Miss Distance (ft)
6	300	>	0
7	300	>	0
8	300	>	0

The possibility of increased nuisance activations from the 3 and 5-TPA solutions is indicated by the optimal solution's available reaction time being greater than the ESCAPE algorithms' available reaction time. Additionally, the optimal solution chose a less aggressive maneuver commanded over a longer period of time to miss the terrain when

Table 4.13: 5-TPA Miss Distance vs Optimal Solution with Available Reaction Time

	Optimal Solution		3-TPA Solution	
Test Point	Miss Distance (ft)	Available Reaction(< or > 3-TPA) (sec)	Miss Distance (ft)	Available Reaction Time (sec)
9	300	>	304	0.30
10	300	>	0	0
11	300	>	251	0.03
12	300	>	0	0
13	300	>	185	0.14

compared to the 3 and 5-TPA ESCAPE algorithm which chose a more aggressive maneuver over a shorter period time (a direct by-product of preplanned maximum performance avoidance maneuvers). This was expected as the 3-TPA and 5-TPA solutions have limited number of terrain avoidance maneuvers, and they are not evaluating as much terrain as the optimum solution. Overall, it was expected that the optimal code would include a longer available reaction time based on it implementing at the same point as the ESCAPE algorithms. As previously stated, the optimal solution was locating the optimum path with minimum control to avoid the terrain, thus it had more available options than the ESCAPE algorithms. The identical activation point was necessary, though, so that the optimal code comparison would be relevant with respect to initiation point. The results in Table 4.13 show that the current available reaction time for the ESCAPE algorithms is either 0 or close to it indicating that nuisance activations would be unlikely. The main issue is creating a non-zero available reaction time which would be possible by implementing the ESCAPE algorithms *during* maneuver execution as explained in Sections 4.2.3 and 4.3.3.

4.5.3 Specific Test Objective 4 Conclusion.

In conclusion, the comparison of path selection between the ESCAPE algorithm's solutions and the optimal solution showed different results when using the qualitative comparison regions. The optimal solution climbed within region 1 (Figure 4.13) for all

test points, while the ESCAPE algorithm's solutions maneuvered within other regions. This, along with the inability to force a level turn with the 5-TPA solution, suggests that climbing turns are more useful when executing terrain avoidance maneuvers and additionally questions the usefulness of level turns.

For that reason, if a 3 path algorithm is chosen, it is recommended that it use climbing turns and a straight ahead climb. There are situations, though, where level turns may be tactically relevant for survival from non-terrain threats and, thus, they should not be systematically ruled out for military use. Additionally, as outlined in Section 4.2.3, the aggressive 15° climb angle may not be possible for heavier, thrust limited aircraft and may drive different performance outcomes for TPA selection.

4.6 Conclusion

This chapter outlined the results of the Have ESCAPE flight tests through an analysis of both flight and simulation data. The complete list of recommendations will be outlined in Chapter 5 based on the information provided herein. The intent of the analysis was two fold. First, it was necessary to determine the effectiveness of the algorithm and determine any weaknesses in its execution. As with all flight test, the overarching goal is to find a way to "break" any system intended to autonomously operate the aircraft. More specifically, it is necessary to stress the system within its specified operating range. The unique capabilities of the VSS enabled Learjet allowed for worst-case analysis of the algorithm within a relatively safe environment. Secondly, these results allowed the ability to present very specific updates to the algorithm that will make it more robust in challenging environments while presenting future research goals. The following chapter will outline those recommendations and present a path forward for Have ESCAPE 2.

V. Conclusions and Recommendations

5.1 Overview

As outlined in Chapter 1, the goal of this research was to determine, design, test, and analyze an algorithm to provide automatic terrain avoidance protection for heavy type aircraft. The impetus for this research stemmed from an Air Force mandate to reduce the number of controlled flight into terrain accidents that have remained a statistically significant contributor to aviation loss of life and assets. This research leveraged, as a truth source, the creation of optimal ground collision avoidance processes that had been developed by Suplisson at AFIT. To this end, an algorithm was developed through the creation of preplanned avoidance maneuvers using 3-DOF EOM. This algorithm quickly propagated the aircraft's position forward in time so that the terrain ahead could be evaluated using DTED to determine whether a collision was imminent and take control of the aircraft if necessary. Once developed, this research was flight tested as a TMP under the project name Have ESCAPE at the United States Air Force Test Pilot School using the Calspan VSS Learjet. The following paragraphs summarize the research and emphasize the conclusions and recommendations developed in Chapter 4. Additionally, the author will present his advice for direction on future research to continually develop the software in an efficient and productive manner.

5.2 Research Questions Response

In Section 1.2, numerous research questions were posed to guide the analysis while delineating goals for flight test and requesting specific answers to heavy Auto GCAS issues. This section will summarize the answers to those questions based on the findings of this research.

- **Can raw DTED be used as a collision evaluation tool for an Auto GCAS algorithm?**

  Yes. Raw DTED can be effectively used as an evaluation tool, but it must be used with caution. As mentioned in Section 2.3.2, DTED is spaced by a predetermined distance based on the level of DTED chosen. As long as the bubble size is large enough to identify DTED posts at each iteration, there will be sufficient information to protect the aircraft from terrain. This is specifically addressed in Section 4.4.1.

- **Is the bubble propagation method adequate for terrain collision prevention?**

  Yes. As long as the requirements of Section 4.4.1 are met, the bubble propagation method is viable. The accuracy of this technique is directly linked to the accuracy of the 3-DOF EOM. For the shorter propagation times used in this research (31 seconds), and for the desired aircraft dynamics, the model has shown to be effective in calculating future aircraft position.

- **How long should the ESCAPE paths be propagated forward, and is it a function of the type of terrain encountered?**

  Section 3.8 addresses this topic, and it was found that it is directly related to aircraft performance and terrain. For this reason, aircraft were grouped into three performance categories, low speed, medium speed, and high speed (Section 3.8.2). The terrain was subsequently grouped into three categories as well, lowland, midland, and upland (Section 3.8.3). Using Equation (3.20), it was found that the aircraft must either turn 90° or out-climb the terrain obstacle to effectively avoid a collision. For this reason, based on performance and terrain, the algorithm propagation lengths will change to fit a specific aircraft.

- **How many ESCAPE paths should be propagated?**

  Based on this research, it was found that three paths should be sufficient for heavy aircraft terrain avoidance as long as each path utilizes a climb. Section 4.5.1 explains this finding. In short, it was determined that the optimal solution, minimizing aircraft control, will always initiate some amount of climbing maneuver. For this reason, a 5-path algorithm utilizing level and climbing turns was determined to be excessive. The research points to a 3-path algorithm that utilizes climbing turns vice level turn avoidance paths.

- **For heavy-type aircraft, are the ESCAPE paths performance dependent?**

  The ESCAPE paths are highly dependent upon aircraft performance, especially when determining maximum flight path angle (γ). As will be addressed in Section 5.3, the aircraft TPAs should be directly linked with specific aircraft performance capabilities. Additionally, this performance may vary based on real-time weight and center of gravity changes, therefore, acceptable performance parameters that are achievable throughout the aircraft's operating envelope should be chosen when determining the ESCAPE paths.

- **Is the 3-DOF EOM model and subsequent control adequate for this Auto GCAS algorithm?**

  Yes. This research has found that for the speeds, propagation lengths, and desired aircraft performance required of the algorithm, the presented 3-DOF EOM model from Section 3.2.1 is acceptable. Quantitatively, this is shown in Sections 4.2.1 &

4.3.1 since the predicted path selection consistently matched the path selected during flight test. This suggests that the predicted aircraft location matched closely to the actual aircraft location. In this way, the EOM accurately identified the future location of the aircraft based on the specified control.

- **Can the algorithm be adequately implemented in real-time?**

  Yes. Section 4.4.2 directly answers this question. The research shows that both three and five path propagation times are well within limits of acceptability based on aircraft speed and algorithm time delay. The ESCAPE algorithm was found to run sufficiently fast to allow for bubble overlap in all cases, which means that there would be no gaps in terrain evaluation along the aircraft's expected trajectory.

- **Should the algorithm evaluate terrain at all times?**

  Yes. This is addressed within recommendation 2 in Section 5.3. In short, continued terrain analysis will prevent ground collisions in the rare cases where the algorithm chooses a terrain path that will subsequently cause an impact. Additionally, this will allow for increased flexibility within the algorithm without detrimental processing costs or nuisance activations.

- **Is the optimal path a 'better' solution than preplanned trajectories?**

  The answer to this question depends on the context. For real-time implementation, the optimal algorithm is currently too slow. The path it chooses, though, is always the best path for minimizing control while avoiding the terrain. It is apparent that once processing speed advances to allow for optimal path integration, it will be the better

solution for terrain avoidance. For current Auto GCAS algorithms, the preplanned trajectories are sufficient and can consistently defeat terrain. For this reason, they are the better option now.

5.3 Recommendations and Guidance for Future Research

All of the stated objectives of Section 1.4.2 were fulfilled through the application and flight test of this research. The collected data led to specific recommendations to improve the robustness of the algorithm. In general, this will be done by providing more thorough terrain protection through the application of updated control schemes, increased algorithm run times, and flexibility with initial aircraft states among others. The intent is to suggest guidance for future research and flight tests so that true heavy aircraft Auto GCAS can become a reality. (The author put these recommendations in his opinion of priority order.)

1. **Update the aircraft EOM entry parameters to allow for a variable aircraft initial state and apply this technique to the ESCAPE paths.**

   Guidance for Future Research:

   The current algorithm structure only accepts an aircraft flying in straight and level, unaccelerated flight. The TPAs also assumed that the aircraft was beginning the maneuver from straight and level, unaccelerated flight. From a flight test perspective, this allowed for a manageable test plan that could be executed within the scope of a TMP. However, it is not practical for actual flight, and this recommendation is a logical step forward for the algorithm. This suggestion would require sending the current aircraft state information to the ODE solver and propagating new ESCAPE paths at each iteration. The potential downside of this will manifest itself in computing speed. Fortunately, Section 4.4.2 has shown that current computing power should not be a limiting factor, though additional research on that matter will

be required. Once integrated, this recommendation will allow the algorithm to be flexible in a realistic flight environment.

2. **Investigate the behavior and robustness of the ESCAPE paths during maneuver execution by commanding continued terrain analysis after initial path selection.**

   Guidance for Future Research:

   This recommendation follows directly from Sections 4.2.3 and 4.3.3 and the fact that the ESCAPE algorithm did not prevent collisions from terrain in all instances. In some specific cases, the algorithm will actually choose a path that may eventually impact terrain since that path has the longest time until impact. Though the current command logic is ideal for minimizing nuisance activations, it does present the possibility of a collision when the algorithm stops analyzing the terrain and only commands the maneuver. Initial testing has shown that an "eyes-open" technique is both possible and effective, though it will require recommendation 1 to be complete for total effectiveness. In this way, the algorithm will attain the capability to update its maneuver selection during the execution of a previously chosen TPA.

3. **Adjust the command strategy to consistently achieve and maintain the desired parameters during TPA execution.**

   Guidance for Future Research:

   This recommendation is purposefully vague since there are three probable techniques for solving the problem. First, it may be possible to use closed-loop control on both bank angle (ϕ) and load factor (N_z) to maintain the required flight path. The benefit of this technique is that it allows for the same, proven 3-DOF EOMs to be used that are currently included in this algorithm. The potential issue with this technique is that it becomes very difficult to command a specific flight path angle using only bank angle and load factor with constantly changing aircraft weight and center of gravity.

This was proven to be an issue as detailed in Section 4.2.2. The second solution is to command flight path angle (γ) directly. This technique would be the simplest to apply, but it may require new EOMs that allow for actual control of the flight path angle. It is unknown whether a 3-DOF model exists that would allow for this type of control in a computationally efficient manner. The third solution, a possible compromise, is to use the current EOMs while installing flight path angle limiters within the ODE solvers so that climb angles or turns can be controlled precisely.

4. **Investigate a 3-TPA solution that uses climbing turns vice level turns.**

   Guidance for Future Research:

   For the sole purpose of avoiding terrain, the flight test data of Section 4.5 show that, in nearly all cases, the Have ESCAPE algorithm will choose to climb for terrain when given the option to stay level. Additionally, it was shown that the optimal solution, when minimizing control, will typically climb to avoid terrain as well. For this reason, it is assessed that climbing turns are more relevant to optimal terrain avoidance. However, this does not take into account mission related priorities that could require staying close to the terrain. Ultimately, this becomes a trade-off between mission requirements and terrain avoidance which is beyond the scope of the research. In the end, if a 3-path algorithm is desired, it is recommended that the lateral paths climb.

5. **Include wind effects in the ESCAPE algorithm predictions.**

   Guidance for Future Research:

   As stated in Section 3.2.1, the EOMs within the Have ESCAPE algorithm currently set winds to zero. It is recommended that future research introduce real-time winds into the existing equations. Fortunately, the Calspan Learjet VSS has the capability of inputting this information into the algorithm. Obviously, wind can have a major

effect on aircraft direction of travel and performance so this inclusion is both prudent and necessary for long-term success of heavy aircraft Auto GCAS.

6. **Collect performance capabilities for intended aircraft and update the TPA solutions to reflect those capabilities.**

   Guidance for Future Research:

   Flight test found that 15° nose-high was too large of a flight path angle for the learjet to maintain airspeed during the ESCAPE maneuver. Though some loss of airspeed may be desired and practical, only a few heavy aircraft can even attain that flight path. For this reason, it is recommended that a lower flight path angle, 5°-7°, be evaluated to better represent very large, under-powered aircraft. It is predicted that the algorithm will more often choose lateral paths when a shallower angle is commanded.

7. **Research the benefit of reducing aircraft speed during turning escape path execution to create a smaller turn radius and increase terrain miss distance.**

   Guidance for Future Research:

   This recommendation should allow for a smaller turn radius which will ultimately increase distance from terrain. It is important to note that this recommendation must be executed with caution since a reduced speed will lower the aircraft's stall margin and prevent pilot initiated aggressive maneuvering if required post-activation. Ultimately, auto-throttles would be desirable to execute this speed reduction automatically, but it should be functionally possible with a test pilot flying predetermined speeds.

8. **Recommend DTED Level 1 for 300 ft bubble radii and DTED Level 2 for 200 ft and 100 ft bubble radii.**

Guidance for Future Research:

There is no specific guidance for future research based on this finding. It is simply a reiteration from Section 4.4.1 since it directly affects safety of flight and should not be lost within the mass of the document.

5.4 Conclusion

Although the field of Auto GCAS is just now gaining traction in the aviation community, the primary goal has always been to increase flight safety. With faster processing, digital flight control systems, and high fidelity terrain characterization, there is no need for another aircraft to fly under its own power into terrain. It is this author's hope that, in the near future, all aircraft are equipped with an effective, automatic ground avoidance system. The research included within this document is a small step in that direction and hopefully, future Have ESCAPE flight tests will provide the necessary data to make that goal a reality.

Appendix A: Have ESCAPE Test Matrix

Figure A.1 (located after the test matrix) displays the Have ESCAPE path numbering schematic.

Table A.1: Have ESCAPE Test Matrix

Test Point	Description	TPA	Sim Path	Bubble Size	Latitude	Longitude	CRS Heading	Altitude	Trigger Time	Note
0	Learjet ωn and ζ	NA	NA	NA	NA	NA	NA	NA	NA	Learjet stability Parameters
1	Escape Path Test Run	NA	1	300	NA	NA	NA	NA	NA	Manual Execution
2	Escape Path Test Run	NA	2	300	NA	NA	NA	NA	NA	Manual Execution
3	Escape Path Test Run	NA	3	300	NA	NA	NA	NA	NA	Manual Execution
4	Escape Path Test Run	NA	4	300	NA	NA	NA	NA	NA	Manual Execution
5	Escape Path Test Run	NA	5	300	NA	NA	NA	NA	NA	Manual Execution
6	Terrain Test	3	1	300	36.7	-118.291	270	11500 ft	10 Sec	
7	Terrain Test	3	2	300	36.6987	-118.2988	272.6	12000 ft	8 Sec	
8	Terrain Test	3	3	300	36.6931	-118.3013	189	12500 ft	9 Sec	
9	Terrain Test	5	4	300	53.3597	-118.7143	340	6800 ft	8 Sec	
10	Terrain Test	5	1*	300	36.65	-118.25	270	10500 ft	8 Sec	*Desired path 2
11	Terrain Test	5	1*	300	53.3396	-118.6518	70	6800 ft*	9 Sec	*Desired path 3
12	Terrain Test	5	1	300	36.7824	-118.3136	223	10500 ft	9 Sec	
13	Terrain Test	5	5	300	36.5724	-118.2619	237	12500 ft	7 Sec	
14	Bubble Size - Terrain	3	3*	100	36.7	-118.291	270	11500 ft	> 20	*Slipped through DTED, no trigger
15	Bubble Size - Terrain	3	2*	200	36.7	-118.291	270	11500 ft	12 Sec	*Desired path 1
16	Bubble Size - Terrain	3	1	300	36.7	-118.291	270	11500 ft	10 Sec	
17	Bubble Size - Terrain	3	2	100	36.6987	-118.2988	272.6	12000 ft	10 Sec	
18	Bubble Size - Terrain	3	2	200	36.6987	-118.2988	272.6	12000 ft	10 Sec	
19	Bubble Size - Terrain	3	2	300	36.6987	-118.2988	272.6	12000 ft	8 Sec	
20	Bubble Size - Terrain	3	3	100	36.6931	-118.3013	189	12500 ft	10 Sec	
21	Bubble Size - Terrain	3	3	200	36.6931	-118.3013	189	12500 ft	10 Sec	
22	Bubble Size - Terrain	3	3	300	36.6931	-118.3013	189	12500 ft	9 Sec	

(Continued on the next page)

Test Point	Description	TPA	Sim Path	Bubble Size	Latitude	Longitude	CRS Heading	Altitude	Trigger Time	Note
23	Bubble Size - Terrain	5	3*	100	53.3597	-118.7143	340	6800 ft	10 Sec	*Desired path 4, slipped through DTED
24	Bubble Size - Terrain	5	4	200	53.3597	-118.7143	340	6800 ft	8 Sec	
25	Bubble Size - Terrain	5	4	300	53.3597	-118.7143	340	6800 ft	7 Sec	
26	Bubble Size - Terrain	5	-*	100	36.65	-118.25	270	10500ft	> 20 Sec	*Slipped through DTED, no trigger
27	Bubble Size - Terrain	5	1*	200	36.65	-118.25	270	10500 ft	7 Sec	*Desired path 2
28	Bubble Size - Terrain	5	1*	300	36.65	-118.25	270	10500 ft	8 Sec	*Desired path 2
29	Bubble Size - Terrain	5	3*	100	53.3396	-118.6518	70	6800 ft*	13 Sec	*Slipped through DTED
30	Bubble Size - Terrain	5	1*	200	53.3396	-118.6518	70	6800 ft*	10 Sec	*Desired path 3
31	Bubble Size - Terrain	5	1*	300	53.3396	-118.6518	70	6800 ft*	9 Sec	*Desired path 3
32	Bubble Size - Terrain	5	4*	100	36.7824	-118.3136	223	10500 ft	12 Sec	*Desired path 1, Slipped through DTED
33	Bubble Size - Terrain	5	1	200	36.7824	-118.3136	223	10500 ft	9 Sec	
34	Bubble Size - Terrain	5	1	300	36.7824	-118.3136	223	10500 ft	9 Sec	
35	Bubble Size - Terrain	5	5	100	36.5724	-118.2619	237	12500 ft	8 Sec	
36	Bubble Size - Terrain	5	5	200	36.5724	-118.2619	237	12500 ft	7 Sec	
37	Bubble Size - Terrain	5	5	300	36.5724	-118.2619	237	12500 ft	7 Sec	
38	TPA-3 points as TPA-5	5	4	300	36.7	-118.291	270	11500 ft	15 Sec	
39	TPA-3 points as TPA-5	5	4	300	36.6987	-118.2988	272.6	12000 ft	11 Sec	
40	TPA-3 points as TPA-5	5	5	300	36.6931	-118.3013	189	12500 ft	11 Sec	
41	Terrain Test	5	5*	300	53.3	-118.6	184	6562 ft	11 Sec	*Desired path 3

Note: All test point tolerances: ±2° course, ±15 kts ground speed, ±2° flight path angle, ±3° bank angle, ±50 ft altitude

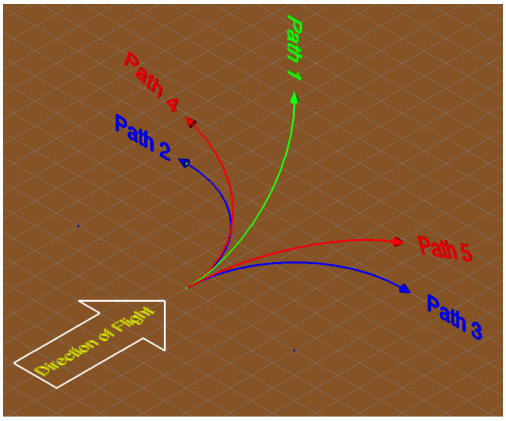

Figure A.1: Have ESCAPE Path Numbering (Section 3.3)

Appendix B: Data Analysis Plan

The remainder of this page intentionally left blank.

Objective	1 & 2 – Evaluate the 3-TPA and 5-TPA Solutions
MOP	1 – Expected Path Analysis

Required Data Parameters

Description	Name	Units	Source
Time	sensor.vss_time	Seconds	DAS and Laptop
Latitude	sensors.lat	Decimal degree	DAS and Laptop
Longitude	sensors.long	Decimal degree	DAS and Laptop
Altitude	sensors.h_sensor	Feet	DAS and Laptop
Heading	sensors.psi	Degree	DAS and Laptop
True Airspeed, V_t	sensors.v_cf_sensor	Feet per second	DAS
Bank Angle, ϕ	sensors.phi_sensor	Degree	DAS
Pitch Angle, θ	sensors.theta_sensor	Degree	DAS
Angle of Attack, α	sensors.alpha_cf_sensor	Degree	DAS
Flight Path Angle, γ	sensors.gamma	Degree	DAS
Z-axis acceleration	sensors.nz_sensor	Gravity, g	DAS
Safety Bubble Radius		Feet	ESCAPE Algorithm
Chosen ESCAPE Path			ESCAPE Algorithm
Latitude of Decision		Decimal degree	ESCAPE Algorithm
Longitude of Decision		Decimal degree	ESCAPE Algorithm
Wind Direction		Degree	Research Laptop
Wind Speed		Knots	Research Laptop
Course		Degree	DAS

Qualitative Data Required

Description		Source
Pilot Comments		Handheld Data, noted by FTE on flight cards
Data Quality	Maneuver Quality Determination	Pilot & FTE (real time) FTE (post-flight)
	Data gathering effectiveness and procedure if data are unusable	Determine if effective real-time. If unusable or unsure, repeat test point.
	Repeats	None planned, but approved, fuel allowing.
Analysis Procedure	The analysis for this MOP compares the results of simulation to the results of flight test. For each test run, the ESCAPE algorithm will command one of 5 pre-determined maneuvers: Maneuver 1 – Constant altitude, 60^o bank angle, left turn	

Maneuver 2 – Wings level, 15° flight path angle, straight ahead climb
Maneuver 3 – Constant altitude, 60° bank angle, right turn
Maneuver 4 – 30° bank angle, 2g pull until 15° flight path angle, left turn
Maneuver 5 – 30° bank angle, 2g pull until 15° flight path angle, right turn

To ensure a valid comparison between the simulation and the flight test, the aircraft states must be compared at the start of the test run, and at the maneuver initiation point. To be considered similar, the aircraft states must match within the following tolerances:

Aircraft State	Tolerances
Latitude	± 0.00025 deg
Longitude	± 0.00025 deg
Altitude	± 50 ft
Course	± 2 deg
Ground Airspeed	± 15 kts
Bank Angle	± 3 deg
Flight Path Angle	± 2 deg

The determination of which maneuver was chosen by the algorithm will be done by observing the aircraft response and matching it to the corresponding maneuver description or by observing the output data from the algorithm, which will specify which maneuver was commanded.

If the maneuver commanded in flight test matches the maneuver commanded in simulation for a given test run, the evaluation criteria will be satisfied. If the maneuvers do not match, the test run will be further analyzed to determine why the algorithm did not perform as expected. The investigation should focus on factors such as, but not limited to, effects of wind, DTED fidelity, quality of test run (pilot inputs, accelerations, turbulence, etc.) and navigation solution drift.

Data Products	A table will be generated depicting the aircraft states at the beginning of the test run and at the maneuver initiation point, as well as the simulation results and the flight-test results. An example is given below:

Parameters	Test Run 1	Test Run 2	Test Run 3
Chosen Escape Maneuver			
Simulation Result			
Flight Test Result			
Initial Point			
Latitude			
Longitude			
Altitude			
Heading			
Airspeed			
Maneuver initiation point			
Latitude			
Longitude			
Altitude			
Heading			
Airspeed			
Test Run Tolerance			
In tolerance? Comments:			

Objective	1 & 2 – Evaluate the 3-TPA and 5-TPA Solutions
MOP	2 – Aircraft Response to the Control Vector

Required Data Parameters

Description	Name	Units	Source
Latitude	sensors.lat	Decimal degree	DAS and Laptop
Longitude	sensors.long	Decimal degree	DAS and Laptop
Altitude	sensors.h_sensor	Feet	DAS and Laptop
Heading	sensors.psi	Degree	DAS and Laptop
True Airspeed, V_t	sensors.v_cf_sensor	Feet per second	DAS
Bank Angle, ϕ	sensors.phi_sensor	Degree	DAS
Pitch Angle, θ	sensors.theta_sensor	Degree	DAS
Angle of Attack, α	sensors.alpha_cf_sensor	Degree	DAS
Flight Path Angle, γ	sensors.gamma	Degree	DAS
Z-axis acceleration	sensors.nz_sensor	Gravity, g	DAS
Safety Bubble Radius		Feet	ESCAPE Algorithm
Chosen ESCAPE Path			ESCAPE Algorithm
Latitude of Decision		Decimal degree	ESCAPE Algorithm
Longitude of Decision		Decimal degree	ESCAPE Algorithm
Wind Direction		Degree	Laptop
Wind Speed		Knots	Laptop
Command Vector		Degree	ESCAPE Algorithm
Course		Degree	DAS

Qualitative Data Required

Description	Source
Pilot Comments	Handheld Data, noted by FTE on flight cards

Data Quality	Maneuver Quality Determination	Pilot & FTE (real time) FTE (post-flight)
	Data gathering effectiveness and procedure if data are unusable	Determine if effective real-time. If unusable or unsure, repeat test point.
	Repeats	None planned, but approved, fuel allowing.

Analysis Procedure

The analysis for this MOP compares the maneuvers commanded by the ESCAPE algorithm to the VSS, with the maneuvers achieved during flight test.

Using DAS data of Bank Angle, Pitch Angle and Z-Axis Acceleration, a time history plot will be created to depict the actual aircraft performance. On the same plot, the time history of the commanded state values will also be depicted. By comparing the time history of the actual and commanded aircraft states, the difference between the two will be quantified during the transitory periods, and during the steady state periods.

The transitory period is defined as the period of time during which the bank angle or flight path angle is commanded to change with time. The steady state period is

<table>
<tr><td></td><td>defined as the period of time during which the bank angle and flight path angle are commanded to be steady with time.

Using similar methods, the altitude will be analyzed for level turns (maneuvers 1 and 3) and the flight path angle will be analyzed for climbing maneuvers (maneuvers 2, 4 and 5).</td></tr>
<tr><td>Data Products</td><td>Time history plots will be created showing commanded aircraft state values, and achieved aircraft state values. A table showing the difference between the commanded value and the achieved value for the aircraft state of interest could also be created. An example is given below.

<table>
<tr><th>Parameter</th><th>Test Run 1</th><th>Test Run 2</th><th>Test Run 3</th></tr>
<tr><td>Transitory Period</td><td></td><td></td><td></td></tr>
<tr><td>Δ Bank Angle</td><td></td><td></td><td></td></tr>
<tr><td>Δ Load Factor</td><td></td><td></td><td></td></tr>
<tr><td>Δ Altitude</td><td></td><td></td><td></td></tr>
<tr><td>Δ Flight Path Angle</td><td></td><td></td><td></td></tr>
<tr><td>Steady State Period</td><td></td><td></td><td></td></tr>
<tr><td>Δ Bank Angle</td><td></td><td></td><td></td></tr>
<tr><td>Δ Load Factor</td><td></td><td></td><td></td></tr>
<tr><td>Δ Altitude</td><td></td><td></td><td></td></tr>
<tr><td>Δ Flight Path Angle</td><td></td><td></td><td></td></tr>
<tr><td colspan="4">Pilot Comments:</td></tr>
<tr><td colspan="4">Test Run 1:

Test Run 2:

Test Run 3:</td></tr>
</table>
</td></tr>
</table>

Objective	1 & 2 – Evaluate the 3-TPA and 5-TPA Solutions
MOP	3 – Terrain Miss Distance

Required Data Parameters

Description	Name	Units	Source
Latitude	sensors.lat	Decimal degree	DAS and Laptop
Longitude	sensors.long	Decimal degree	DAS and Laptop
Altitude	sensors.h_sensor	Feet	DAS and Laptop
Heading	sensors.psi	Degree	DAS and Laptop
True Airspeed, V_t	sensors.v_cf_sensor	Feet per second	DAS
Bank Angle, ϕ	sensors.phi_sensor	Degree	DAS
Pitch Angle, θ	sensors.theta_sensor	Degree	DAS
Angle of Attack, α	sensors.alpha_cf_sensor	Degree	DAS
Flight Path Angle, γ	sensors.gamma	Degree	DAS
Z-axis acceleration	sensors.nz_sensor	Gravity, g	DAS
Safety Bubble Radius		Feet	ESCAPE Algorithm
Chosen ESCAPE Path			ESCAPE Algorithm
Latitude of Decision		Decimal degree	ESCAPE Algorithm
Longitude of Decision		Decimal degree	ESCAPE Algorithm
Wind Direction		Degree	Laptop
Wind Speed		Knots	Laptop

Qualitative Data Required

Description		Source
Pilot Comments		Handheld Data, noted by FTE on flight cards
Data Quality	Maneuver Quality Determination	Pilot & FTE (real time) FTE (post-flight)
	Data gathering effectiveness and procedure if data are unusable	Determine if effective real-time. If unusable or unsure, repeat test point.
	Repeats	None planned, but approved, fuel allowing.

Analysis Procedure

The analysis for this MOP finds the closest distance between the aircraft and the terrain throughout the maneuver flown by the aircraft.

The analysis will be carried out using a MATLAB® code which accepts the aircraft's navigation solution (Latitude, Longitude, Altitude) as an input, and returns the terrain miss distance as an output. The code will use the following logic to complete the analysis:

The navigation solution will be overlaid onto the DTED database to confirm that the flight path is entirely contained within the DTED being analyzed.

For each point in the navigation solution, the code will calculate the horizontal distance and vertical distance to each DTED post. Using the Pythagorean theorem and as shown in Figure A1, the slant distance to each DTED post, d_{An},

will also be calculated. This allows the code to find d_{Min}, the minimum distance from terrain for that point of the navigation solution.

Once this calculation is complete for each point of the navigation solution, the overall minimum distance from terrain, D_{Min}, can be identified.

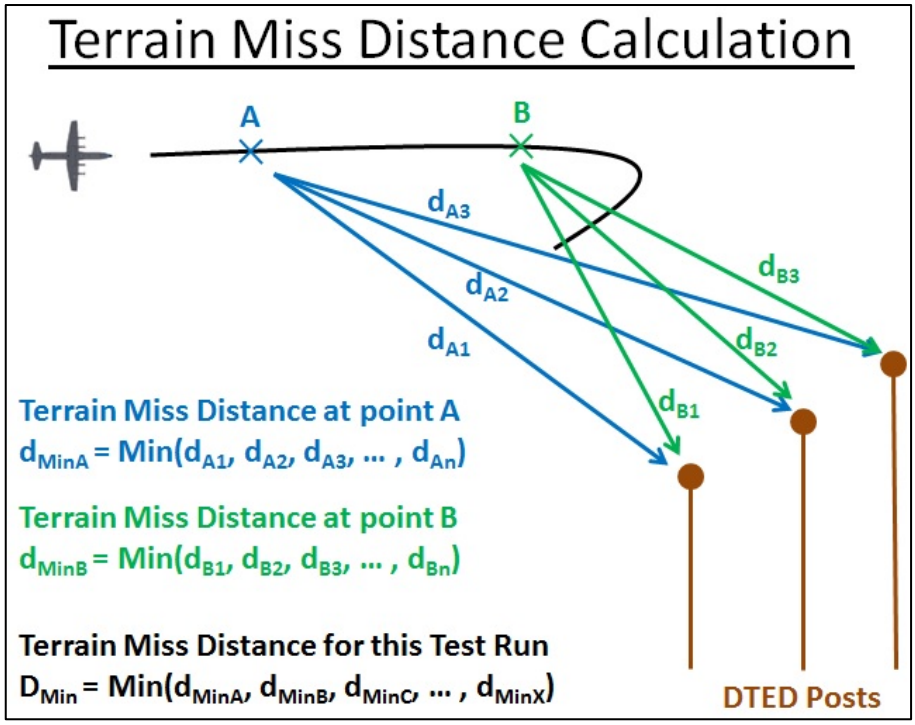

Once the terrain miss distance has been calculated, the available reaction time will be calculated. The available reaction time is defined as the maximum amount of time that the aircraft could have flown straight and level beyond the maneuver activation point and still avoid a collision by an infinitely small distance. The available reaction time will be determined by finding the minimum horizontal distance between the aircraft flight path and the closest DTED post, when measured in the direction of the initial flight path.

$$Available\ Reaction\ Time\ = \frac{Min.\,horizonal\ distance\ from\ DTED\ to\ Flt\ Path}{Ground\ speed}$$

Data Products

A table depicting the chosen path, miss distance and available reaction time will be created. An example is shown below:

Test Run	Chosen Path	Miss Distance (ft)	Available reaction time (sec)	Notes & Pilot Comments
1				
2				
3				

Objective	3 – Determine Acceptable Algorithm Parameters
MOP	1 – Bubble Size for Level 1 DTED Resolution

Required Data Parameters

Description	Name	Units	Source
Latitude	sensors.lat	Decimal degree	DAS and Laptop
Longitude	sensors.long	Decimal degree	DAS and Laptop
Altitude	sensors.h_sensor	Feet	DAS and Laptop
Heading	sensors.psi	Degree	DAS and Laptop
True Airspeed, V_t	sensors.v_cf_sensor	Feet per second	DAS
Bank Angle, ϕ	sensors.phi_sensor	Degree	DAS
Pitch Angle, θ	sensors.theta_sensor	Degree	DAS
Angle of Attack, α	sensors.alpha_cf_sensor	Degree	DAS
Flight Path Angle, γ	sensors.gamma	Degree	DAS
Z-axis acceleration	sensors.nz_sensor	Gravity, g	DAS
Safety Bubble Radius		Feet	ESCAPE Algorithm
Chosen ESCAPE Path			ESCAPE Algorithm
Latitude of Decision		Decimal degree	ESCAPE Algorithm
Longitude of Decision		Decimal degree	ESCAPE Algorithm
Wind Direction		Degree	Laptop
Wind Speed		Knots	Laptop

Qualitative Data Required

Description		Source
Pilot Comments		Handheld Data, noted by FTE on flight cards
Data Quality	Maneuver Quality Determination	Pilot & FTE (real time) FTE (post-flight)
	Data gathering effectiveness and procedure if data are unusable	Determine if effective real-time. If unusable or unsure, repeat test point.
	Repeats	None planned, but approved, fuel allowing.

Analysis Procedure	The analysis for this MOP determines whether or not the algorithm functions properly for various safety bubble radii. This analysis will be carried out by observing the aircraft response and ESCAPE algorithm outputs, when a test run is repeated multiple times, while keeping all parameters constant except the safety bubble radius. If the aircraft response changes based on the safety bubble radius, the flight path will be analyzed to determine if the bubble has flown between DTED posts, or if a DTED post lies between two successive bubbles due to the lack of overlap. This will be done by plotting the time history of the aircraft's navigation solution in MATLAB® , and overlaying the DTED Data on the same plot. By zooming-in on the flight path and surrounding DTED posts, the analyst will determine if the navigation solution is located below the surface of the digital terrain.

<table>
<tr><td></td><td>The maneuver initiation point with the new bubble size will also be compared to the data from Objectives 1 and 2, to determine if the maneuver was initiated later than the Available Reaction Time margin. If so, then the bubble size did not allow the algorithms to trigger the maneuver in time to avoid a collision.</td></tr>
<tr><td>Data Products</td><td>A table showing the results of a given test run geometry for various safety bubble size will be created. An example is shown below.

Algorithm:3TPA Test dates: 17 Sep 15
Pressure Altitude: 15,000ft Airspeed:200 kt
<table><tr><th rowspan="2">Test point</th><th colspan="3">Bubble Size (ft)</th></tr><tr><th>100</th><th>200</th><th>300</th></tr><tr><td>1</td><td></td><td>L*</td><td>L</td></tr><tr><td>2</td><td></td><td>R</td><td>R</td></tr><tr><td>3</td><td>C</td><td>C</td><td>C</td></tr></table>*chosen path. L-left turn, R-right turn, C – climb, CL-climbing left turn, CR-climbing right turn.
: No algorithm activation</td></tr>
</table>

Objective	3 – Determine Acceptable Algorithm Parameters
MOP	2 – Processing Time

Required Data Parameters

Description	Name	Units	Source
Total time for 1 iteration of the ESCAPE Algorithm for both 3 path and 5 path algorithms	ESCAPE_AlgorithmTime	Seconds	MATLAB

Qualitative Data Required

Description		Source
Pilot Comments		N/A
Data Quality	Maneuver Quality Determination	CSO & FTE (real time) CSO & FTE (post-flight)
	Data gathering effectiveness and procedure if data are unusable	Determine if effective real-time. If unusable or unsure, repeat test point.
	Repeats	Yes, for statistical significance as per Section 2.

Analysis Procedure	The analysis for this MOP calculates the average and maximum processing time of the ESCAPE algorithm for both 3-TPA and 5-TPA solutions. The same laptop must be used for both simulation and inflight execution; this is critical for accurate data. Ensure all non-critical processes are disabled prior to testing the ESCAPE Algorithm executions. Determine the averages and maximums of the ESCAPE Algorithm's execution times for both the 3-path and 5-path algorithms measured in seconds from both simulator and flight data. This data will be collected automatically by a time counter function within the MATLAB software. Since the algorithms will be processed at 12.5 Hz, the test team will randomly pick 4 algorithm iterations to make up the data sample for analysis. This will prevent using correlated data points for the statistical analysis. The analysis will be performed using MATLAB to determine the maximum time and average time required to execute the ESCAPE algorithms. A box-plot will also be produced to depict the difference in time required for each algorithm.
Data Products	A box plot and a table showing the results of the 3-path and 5-path algorithms' average and maximum processing times will be created. An example is shown below.

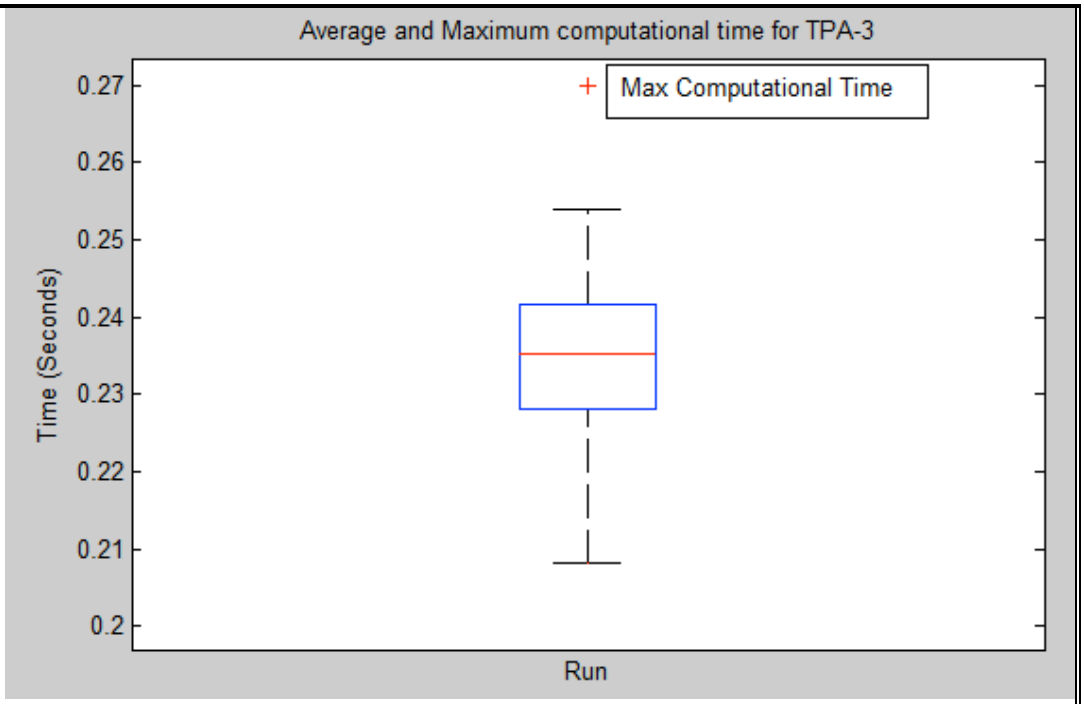

Metric	Value
Average time to execute ESCAPE Algorithm 3-TPA	Seconds
Average time to execute ESCAPE Algorithm 5-TPA	Seconds
Maximum time to execute ESCAPE Algorithm 3-TPA	Seconds
Maximum time to execute ESCAPE Algorithm 5-TPA	Seconds

Objective	4 – Compare 3-TPA & 5-TPA with Optimal Solution
MOP	1 – Proper Path Selection

Required Data Parameters

Description	Name	Units	Source
Latitude	sensors.lat	Decimal degree	Laptop and Optimum
Longitude	sensors.long	Decimal degree	Laptop and Optimum
Altitude	sensors.h_sensor	Feet	Laptop and Optimum
Heading	sensors.psi	Degree	Laptop and Optimum
True Airspeed, V_t	sensors.v_cf_sensor	Feet per second	DAS and Optimum
Bank Angle, ϕ	sensors.phi_sensor	Degree	DAS and Optimum
Pitch Angle, θ	sensors.theta_sensor	Degree	DAS and Optimum
Angle of Attack, α	sensors.alpha_cf_sensor	Degree	DAS and Optimum
Flight Path Angle, γ	sensors.gamma	Degree	DAS and Optimum
Z-axis acceleration	sensors.nz_sensor	Gravity, g	DAS and Optimum
Safety Bubble Radius		Feet	ESCAPE Algorithm
Chosen ESCAPE Path			ESCAPE Algorithm
Latitude of Decision		Decimal degree	ESCAPE Algorithm
Longitude of Decision		Decimal degree	ESCAPE Algorithm
Wind Direction		Degree	Laptop
Wind Speed		Knots	Laptop
Optimal Path Bank Angle		Degree	Optimal Code
Optimal Path Climb Angle		Degree	Optimal Code

Qualitative Data Required

Description		Source
Pilot Comments		Handheld Data, noted by FTE on flight cards
Data Quality	Maneuver Quality Determination	Pilot & FTE (real time) FTE (post-flight)
	Data gathering effectiveness and procedure if data are unusable	Determine if effective real-time. If unusable or unsure, repeat test point.
	Repeats	None planned, but approved, fuel allowing.

Analysis Procedure

The analysis for this MOP compares the results of flight test with the results from the optimally derived solution.

For each flight test data point, the test run parameters will be loaded into the optimum code to derive the equivalent optimum escape maneuver. The optimum escape maneuver will be defined by its flight path angle, bank angle, and direction of turn.

The aircraft response obtained in flight test will be compared to the optimum escape maneuver to qualitatively evaluate if the ESCAPE algorithms chose the proper path. Since the optimum code can choose from an infinite number of

<table>
<tr><td></td><td>escape paths, qualitative comparison regions will be used to find an equivalent ESCAPE algorithm (non-optimal) path.

For each test run, the chosen path will be compared to the optimum solution by comparing average bank angle, load factor, flight path angle, direction of turn, and comparison regions described above. Based on this comparison, the ESCAPE team will decide whether or not the algorithms chose the similar path.</td></tr>
<tr><td>Data Products</td><td>Provide tabular data to summarize if the flight test results and optimal solutions were within the same comparative flight path region for qualitative similarity. A notional example is shown below.

<table>
<tr><th>Test point</th><th>Comparative Region for 3-TPA Solution</th><th>Comparative Region for Optimal Solution</th><th>Result</th></tr>
<tr><td>1</td><td>1</td><td>1</td><td>Similar</td></tr>
<tr><td>2</td><td>2</td><td>3</td><td>Different</td></tr>
<tr><td>3</td><td>3</td><td>3</td><td>Similar</td></tr>
<tr><td>4</td><td>1</td><td>1</td><td>Similar</td></tr>
</table>
</td></tr>
</table>

Objective	4 – Compare 3-TPA & 5-TPA with Optimal Solution
MOP	2 – Terrain Miss Distance & Available Reaction Time vs Optimal Code

Required Data Parameters

Description	Name	Units	Source
Latitude	sensors.lat	Decimal degree	Laptop and Optimum
Longitude	sensors.long	Decimal degree	Laptop and Optimum
Altitude	sensors.h_sensor	Feet	Laptop and Optimum
Heading	sensors.psi	Degree	Laptop and Optimum
True Airspeed, V_t	sensors.v_cf_sensor	Feet per second	DAS and Optimum
Bank Angle, ϕ	sensors.phi_sensor	Degree	DAS and Optimum
Pitch Angle, θ	sensors.theta_sensor	Degree	DAS and Optimum
Angle of Attack, α	sensors.alpha_cf_sensor	Degree	DAS and Optimum
Flight Path Angle, γ	sensors.gamma	Degree	DAS and Optimum
Z-axis acceleration	sensors.nz_sensor	Gravity, g	DAS and Optimum
Safety Bubble Radius		Feet	ESCAPE Algorithm
Chosen ESCAPE Path			ESCAPE Algorithm
Latitude of Decision		Decimal degree	ESCAPE Algorithm
Longitude of Decision		Decimal degree	ESCAPE Algorithm
Wind Direction		Degree	Laptop
Wind Speed		Knots	Laptop

Qualitative Data Required

Description		Source
Pilot Comments		Handheld Data, noted by FTE on flight cards
Data Quality	Maneuver Quality Determination	Pilot & FTE (real time) FTE (post-flight)
	Data gathering effectiveness and procedure if data are unusable	Determine if effective real-time. If unusable or unsure, repeat test point.
	Repeats	None planned, but approved, fuel allowing.

Analysis Procedure	The analysis for this MOP compares the results of flight test with the results from the optimally derived solution. For each flight test data point, the test run parameters will be loaded into the optimum code to derive the equivalent optimum escape maneuver. From the optimum escape maneuver, the test team will determine the minimum terrain miss distance and the available reaction time, using similar techniques as described for MOP 3 of Objectives 1 & 2. The miss distances and available reaction time from the optimal solution will be compared to the flight test results for 3-TPA and 5-TPA solutions.

<table>
<tr><td>Data Products</td><td>Tabular data will be provided to summarize the Terrain Miss Distances and Available Reaction Time between the 3-TPA, 5-TPA, and optimal escape path solutions. A notional example is shown below.

Test points: 1-3 Test dates: 17 Sep 15
Pressure Altitude: 15,000ft Airspeed: 200 kts
<table><tr><th>Test Point</th><th>Algorithm</th><th>Miss Distance (ft)</th><th>Distance Difference (ft)</th><th>Available Reaction Time (sec)</th><th>Reaction Time Difference (sec)</th></tr><tr><td>1</td><td>3TPA</td><td>500</td><td>250</td><td>2.5</td><td>-1.5</td></tr><tr><td>2</td><td>5TPA</td><td>200</td><td>-50</td><td>2.0</td><td>-2.0</td></tr><tr><td>3</td><td>Optimal</td><td>250</td><td>-</td><td>4.0</td><td>-</td></tr><tr><td></td><td colspan="5">Pilot comment:</td></tr></table></td></tr>
</table>

Appendix C: Daily Flight Test Reports

The remainder of this page intentionally left blank.

DAILY/INITIAL FLIGHT TEST REPORT

1. AIRCRAFT TYPE	2. SERIAL NUMBER
LJ-25D	N203VS

3. CONDITIONS RELATIVE TO TEST

A. PROJECT / MISSION NO	B. FLIGHT NO / DATA POINT	C. DATE
Have ESCAPE	Flight #1	31 Aug 2015
D. FRONT COCKPIT *(Left Seat)*	**E. FUEL LOAD**	**F. JON**
Thomas / Trombetta	5,299	998TMP00
G. REAR COCKPIT *(Right Seat and rest of crew)*	**H. START UP GR WT / CG**	**I. WEATHER**
Kita / Kemper	15,000	SKC / Winds 220/15 @ 15k ft / 20° C
J. TO TIME / SORTIE TIME	**K. CONFIGURATION / LOADING**	**L. SURFACE CONDITIONS**
0900L / 2.0 hrs	Clean	Dry
M. CHASE ACFT / SERIAL NO	**N. CHASE CREW**	**O. CHASE TO TIME / SORTIE TIME**
N/A	N/A	N/A

4. PURPOSE OF FLIGHT / TEST POINTS

The purpose of this flight was to test the Have ESCAPE 3 and 5 path algorithms IAW the approved test plan. Maneuvers were flown at 15,000' MSL and 310 kts ground speed. Test points 0-22 were flown (reference Test Point Matrix)

5. RESULTS OF TESTS *(Continue on reverse if needed)*

Conditions: The mission was flown in clear skies and no turbulence. Winds aloft indicated 220/15 kts at 15,000 ft PA.

Ground Block: The mission laptop computer had to be restarted and the IP address needed to be manually entered for initial VSS integration. Once complete, the ESCAPE algorithm was interfacing correctly with the VSS.

Takeoff: Uneventful.

Mission Results: The first data point included an analysis of the longitudinal modes of motion (Test point 0). To do this, a hand flown pitch doublet was executed and the number of overshoots and period were determined. This information was necessary for correct application of the optimal solution. Next, test points 1-22 were performed. Prior to execution, the pilot would fly the aircraft straight and level flight at 15,000 ft PA at 310 KGS on a heading that would allow for a direct headwind or tailwind. The first 5 test points were flown to evaluate the performance of the aircraft during direct application of the escape maneuvers. The forward (up) path, left-up path, and right-up path all performed as predicted and held the flight path within ±2°. Of note, it was not possible to maintain 310 KGS with military power for the paths with an upward vector. In these cases, the aircraft maintained the flight path angle with constantly decreasing airspeed. VSS disconnection would typically occur between 140 – 160 kts after completion of the 30 second maneuver. The level paths both trended towards a positive 1.5°-2.0° flight path angle resulting in a 300 ft climb. Though this is within tolerances for the flight path angle, it is slightly more climb than desired. Next, test points 6-22 were performed. These points evaluated the performance of the 3 and 5 path algorithm against various terrain types and bubble sizes. In all but one case, the algorithm performed in accordance with predictions. Test Point 17 was predicted to turn left, and upon initial activation, it went up. The test team re-ran the point and achieved the predicted result. The discrepancy was attributed to poor heading control. The major lesson learned from the first mission was that precise flight path control is required to achieve predicted results and for the aircraft to perform correctly when commanded by the escape maneuvers.

Landing/Post Flight Ground Block: Uneventful

6. RECOMMENDATIONS

R1: Debrief the test team on algorithm sensitivity to flight path prior to maneuver execution before the next sortie.

R2: Update the level escape maneuvers to minimize the climb during path execution.

COMPLETED BY	SIGNATURE	DATE
JOHN V. TROMBETTA, Maj, USAF	//signed/jvt/31August 2015//	20150831

TPS Form 5314 NOV 86

DAILY/INITIAL FLIGHT TEST REPORT

1. AIRCRAFT TYPE	2. SERIAL NUMBER
LJ-25D	N203VS

3. CONDITIONS RELATIVE TO TEST

A. PROJECT / MISSION NO	B. FLIGHT NO / DATA POINT	C. DATE
Have ESCAPE /	Flight #2	1 Sep 2015
D. FRONT COCKPIT *(Left Seat)*	**E. FUEL LOAD**	**F. JON**
Thomas / Allard	5,299	998TMP00
G. REAR COCKPIT *(Right Seat and rest of crew)*	**H. START UP GR WT / CG**	**I. WEATHER**
Wilson / Kemper	15,000	Wind 170/06, SCT 250, 20°C, 29.93"Hg
J. TO TIME / SORTIE TIME	**K. CONFIGURATION / LOADING**	**L. SURFACE CONDITIONS**
0854L / 2.0 hrs	Clean	Dry
M. CHASE ACFT / SERIAL NO	**N. CHASE CREW**	**O. CHASE TO TIME / SORTIE TIME**
N/A	N/A	N/A

4. PURPOSE OF FLIGHT / TEST POINTS

The purpose of this flight was to test the Have ESCAPE 3 and 5 path algorithms IAW the approved test plan. Maneuvers were flown at 15,000' MSL and 310 kts ground speed. The command vectors had been modified since the previous flight, and the game plan was re-fly the entire test matrix using Version 2 of the algorithms. Once airborne, it was decided to revert back to Version 1 of the algorithms and the following test points were successfully flown: 0 to 29, 31, 34, and 37 to 40

5. RESULTS OF TESTS *(Continue on reverse if needed)*

Conditions: The mission was flown in clear skies and no turbulence. Winds aloft averaged 220/12 kts at 15,000 ft PA.

Ground Block: The ESCAPE algorithms interfaced correctly with the VSS and Path 4 was successfully commanded on the ground. It was noticed that the VSS Data Recorder was automatically turning itself On and Off during taxi.

Takeoff: Uneventful.

Mission Results:

The first event was a Pitch Doublet using Version 2 of the algorithms. 2 pitch doublets were flown and data was recorded with the DAS. The next event was to carry out the manual activation of each escape maneuver. Maneuver 1 functioned as planned. Maneuvers 2 and 3 caused a 200-300 ft descent followed by a 500-900 ft climb.

The initial descent was deemed to be unacceptable, and the software version was reverted back to Version 1 of the algorithms. Each maneuver was manually executed and no significant descent was noticed, although maneuvers 2 and 3 did result in climbs of up to 800 ft. Maneuvers 1, 4 and 5 performed within acceptable limits, although the flight path angle did have a tendency to increase throughout the maneuver. Airspeed could not be maintained during climbing maneuvers with max continuous power, and decayed to as low as 150 kts at heavy weight, or 210 kts at light weight.

All 300 ft bubble test points were flown, and the algorithms commanded the expected maneuver in each case. The aircraft bank response was always accurate within 2 degrees, and the climbing maneuvers commanded a flight path angle accurate to within -2 to +5 degrees. The level maneuvers commanded a flight path angle accurate to within 3 degrees, which generally caused a descent of approximately 50 ft, followed by a climb of 150 to 600 ft.

Some of the 100 ft and 200 ft bubble test points were also flown, and the flight test results matched the predictions.

The pitch doublets were re-flown near the end of the flight with a lower fuel load to assess the mass effects on the short period longitudinal response.

Landing/Post Flight Ground Block: Uneventful

6. RECOMMENDATIONS

Continue testing with Version 1 of the algorithms.

COMPLETED BY	SIGNATURE	DATE
Sebastien Allard, Capt, RCAF	//signed//	1 Sep 2015

TPS Form 5314 NOV 86

DAILY/INITIAL FLIGHT TEST REPORT

1. AIRCRAFT TYPE	2. SERIAL NUMBER
LJ-25D	N203VS

3. CONDITIONS RELATIVE TO TEST

A. PROJECT / MISSION NO	B. FLIGHT NO / DATA POINT	C. DATE
Have ESCAPE /	Flight #3	02 Sep 2015
D. FRONT COCKPIT *(Left Seat)*	**E. FUEL LOAD**	**F. JON**
Thomas / Neice	5,500	998TMP00
G. REAR COCKPIT *(Right Seat and rest of crew)*	**H. START UP GR WT / CG**	**I. WEATHER**
Kita / Kemper	15,200	SKC / Winds 230-27/10-20kts @ 15k ft / 23° C
J. TO TIME / SORTIE TIME	**K. CONFIGURATION / LOADING**	**L. SURFACE CONDITIONS**
0900L / 1.9 hrs	Clean	Dry
M. CHASE ACFT / SERIAL NO	**N. CHASE CREW**	**O. CHASE TO TIME / SORTIE TIME**
N/A	N/A	N/A

4. PURPOSE OF FLIGHT / TEST POINTS

The purpose of this flight was to test the Have ESCAPE 3 and 5 path algorithms IAW the approved test plan. Maneuvers were flown at 15,000' MSL and 310 kts ground speed. All Test points were flown (reference Test Point Matrix)

5. RESULTS OF TESTS *(Continue on reverse if needed)*

Conditions: The mission was flown in clear skies and no turbulence. Winds aloft indicated anywhere between 230 and 270/10 to 20 kts at 15,000 ft PA.

Ground Block: NSTR

Takeoff: Uneventful.

Mission Results: The first three maneuvers were manual activation of one of each maneuver type to familiarize the EP with the aircraft response and power addition techniques. Each test point was set up with the aircraft straight and level flight, nominally at 15,000 ft PA at 310 KGS on a heading that would allow for a direct headwind or tailwind. The test team began collecting data with test points 29 through 36. Then the test point matrix was completed, starting at the bottom and working our way towards the top. The aircraft lacked sufficient thrust to maintain airspeed while in any climbing maneuver, and on some "level turns" as the flight path angle was inadequately controlled by the Nz and bank command system (flight path angle went as high as 5° during some level turns). The climb angle did not always capture 15 degrees and did not maintain 15 degrees throughout the maneuver (during climbing maneuvers, the flight path angle varied from 12° to 20°). All maneuver executions were abrupt, but not objectionable. VSS disconnection would typically occur between 140 – 160 kts after completion of the 30 second maneuver. A few test points resulted in an unanticipated ESCAPE maneuver. Those points were subsequently re-flown and produced predicted results.

Landing/Post Flight Ground Block: Uneventful

6. RECOMMENDATIONS

R1: Complete test points 29 – 36, then the rest of the test point matrix.

COMPLETED BY	SIGNATURE	DATE
RUSSELL G. NEICE, Capt, USAF	//signed/rgn/02 September 2015//	20150902

TPS Form 5314 NOV 86

DAILY/INITIAL FLIGHT TEST REPORT

1. AIRCRAFT TYPE	2. SERIAL NUMBER
LJ-25D	N203VS

3. CONDITIONS RELATIVE TO TEST

A. PROJECT / MISSION NO	B. FLIGHT NO / DATA POINT	C. DATE
Have ESCAPE	Flight #4	9 Sep 2015
D. FRONT COCKPIT *(Left Seat)*	**E. FUEL LOAD**	**F. JON**
McCarley / Trombetta	5,299	998TMP00
G. REAR COCKPIT *(Right Seat and rest of crew)*	**H. START UP GR WT / CG**	**I. WEATHER**
Wilson / Cobb	15,000	SCT-BKN 15k ft / Winds 220/06 27° C
J. TO TIME / SORTIE TIME	**K. CONFIGURATION / LOADING**	**L. SURFACE CONDITIONS**
0920L / 1.4 hrs	Clean	Dry
M. CHASE ACFT / SERIAL NO	**N. CHASE CREW**	**O. CHASE TO TIME / SORTIE TIME**
N/A	N/A	N/A

4. PURPOSE OF FLIGHT / TEST POINTS

The purpose of this flight was to test the Have ESCAPE 3 and 5 path algorithms IAW the approved test plan. Maneuvers were flown at 15,000' MSL and 310 kts ground speed. Test points 6-36 were flown (reference Test Point Matrix)

5. RESULTS OF TESTS *(Continue on reverse if needed)*

Conditions: The mission was flown in with light winds and scattered to broken clouds at 15,000 ft PA. Winds aloft were light with no turbulence.

Ground Block: The mission laptop interfaced accurately with the computer.

Takeoff: Uneventful.

Mission Results: The first data point included an analysis of the lateral-directional modes of motion. To do this, a hand flown aileron doublet was executed and the number of overshoots and period were determined. Using this method, zero overshoots were noted. Next, rudder doublets were performed to excite the Dutch Roll mode. The pilot commented that the mode was highly damped, but review of the DAS data showed three overshoots and a damping ratio of 0.71. Next, terrain test points 6-13 were flown. Prior to execution of the maneuver, the pilot would fly the aircraft in straight and level flight at 15,000 ft PA at 310 KGS on a heading that would allow for a direct headwind or tailwind if airspace and weather allowed. After test point 10, the TC realized that the algorithm AOA correction was turned off, rendering the first five test points invalid. The switch was then placed in the 'ON' position for the remainder of the flight, though the points were not re-flown since they were not the priority. Next, the bubble size comparison points in the test matrix were flown. For test efficiency, the VSS would be manually disconnected once the maneuver was executed since the only data required was the path that was chosen and not how the path was actually flown. This benefitted test execution due to the broken cloud deck above the aircraft's flight path limiting climb capability. In all cases, the test points were flown within tolerances and valid data were collected. Ultimately, these points evaluated the performance of the 3 and 5 path algorithm against various terrain types and bubble sizes. In all but one case, the algorithm performed in accordance with predictions. The test team re-ran the point and achieved the predicted result. Additionally, the pilot commented that maneuver execution was abrupt but satisfactory.

Landing/Post Flight Ground Block: Uneventful

6. RECOMMENDATIONS

R1: Add a line in the procedures for test card 3 to turn the AOA correction 'ON' prior to execution.

COMPLETED BY	SIGNATURE	DATE
JOHN V. TROMBETTA, Maj, USAF	//signed/jvt/9 September 2015//	20150909

DAILY/INITIAL FLIGHT TEST REPORT

1. AIRCRAFT TYPE	2. SERIAL NUMBER
LJ-25D	N203VS

3. CONDITIONS RELATIVE TO TEST

A. PROJECT / MISSION NO	B. FLIGHT NO / DATA POINT	C. DATE
Have ESCAPE	Flight #5	9 Sep 2015
D. FRONT COCKPIT *(Left Seat)*	**E. FUEL LOAD**	**F. JON**
McCarley / Allard	5,600	998TMP00
G. REAR COCKPIT *(Right Seat and rest of crew)*	**H. START UP GR WT / CG**	**I. WEATHER**
Kita / Suplisson	15,000	Wind 360/04, SCT 150, 35°C, 29.92"Hg
J. TO TIME / SORTIE TIME	**K. CONFIGURATION / LOADING**	**L. SURFACE CONDITIONS**
1339L / 2.0 hrs	Clean	Dry
M. CHASE ACFT / SERIAL NO	**N. CHASE CREW**	**O. CHASE TO TIME / SORTIE TIME**
N/A	N/A	N/A

4. PURPOSE OF FLIGHT / TEST POINTS

The purpose of this flight was to test the Have ESCAPE 3 and 5 path algorithms IAW the approved test plan. Maneuvers were flown at 15,000' MSL and 310 kts ground speed. The lateral-directional modes of motion from the augmented Learjet equipped with the Have ESCAPE FCS system were characterized by conducting aileron doublets and aileron step inputs to find the frequency and damping in roll. The following test points were successfully flown: 6 to 15, 17, 18, 20, 21, 23, 24, 26, 27, 29, 30, 32, 33, 35, 36, 38 to 41

5. RESULTS OF TESTS *(Continue on reverse if needed)*

Conditions: The mission was flown with broken clouds at 15'000 ft. The test points were successfully flown at 15'000 ft between clouds. The winds aloft shifted rapidly from 020°M to 155°M and from 3 kts to 15 kts.

Ground Block: The ESCAPE algorithms interfaced correctly with the VSS and Path 4 was successfully commanded on the ground.

Takeoff: Uneventful.

Mission Results:

The first event was an Aileron Doublet flown as a square input and then as a sinusoidal input. No oscillations were observed in roll or yaw, and the roll rate gradually decreased without any reversals. Two full deflection aileron steps were flown from 30-to-30 degrees angle of bank. No notable observations were made, but DAS data was collected for analysis.

The remainder of the flight was spent flying test points to evaluate both the 3-path and 5-path algorithms with various bubble sizes. Of note:

1. One maneuver was manually terminated due to airspeed being lower than the safety pilot's comfort level.
2. One maneuver was terminated due to weather and traffic.
3. During the first few test points, the flight path angle continued to increase past 15 degrees. One maneuver was terminated because the flight path angle exceeded 25 degrees, as per the safety plan. Following this event, fuel was pumped forward to move the center of gravity forward, which seemed to help in controlling the flight path angle.
4. Some of the level turn maneuvers caused the VSS to trip off due to a "Software Safety Trip", the cause of which is unknown.

Otherwise, test points were carried out successfully and DAS data was collected as per the test plan for further analysis.

Landing/Post Flight Ground Block: Uneventful

6. RECOMMENDATIONS

Continue with Flight 6 to collect remaining required data.

COMPLETED BY	SIGNATURE	DATE
Sebastien Allard, Capt, RCAF	//signed//	9 Sep 2015

DAILY/INITIAL FLIGHT TEST REPORT

1. AIRCRAFT TYPE	2. SERIAL NUMBER
LJ-25D	N203VS

3. CONDITIONS RELATIVE TO TEST

A. PROJECT / MISSION NO	B. FLIGHT NO / DATA POINT	C. DATE
Have ESCAPE	Flight #6	10 Sep 2015
D. FRONT COCKPIT *(Left Seat)*	**E. FUEL LOAD**	**F. JON**
McCarley / Neice	5,700	998TMP00
G. REAR COCKPIT *(Right Seat and rest of crew)*	**H. START UP GR WT / CG**	**I. WEATHER**
Wilson / Reeder	15,400	SCT 15k / SFC Winds 010/03 21° C 15k Winds 340-300/020
J. TO TIME / SORTIE TIME	**K. CONFIGURATION / LOADING**	**L. SURFACE CONDITIONS**
0900L / 1.6 hrs	Clean	Dry
M. CHASE ACFT / SERIAL NO	**N. CHASE CREW**	**O. CHASE TO TIME / SORTIE TIME**
N/A	N/A	N/A

4. PURPOSE OF FLIGHT / TEST POINTS

The purpose of this flight was to test the Have ESCAPE 3 and 5 path algorithms IAW the approved test plan. Maneuvers were flown at 15,000' MSL and 310 kts ground speed. Test points 6-13, 39-41 were flown (reference Test Point Matrix)

5. RESULTS OF TESTS *(Continue on reverse if needed)*

Conditions: The mission was flown in with light winds and scattered clouds at 15,000 ft PA. Winds aloft were variable between 340 – 300 at 20 knots

Ground Block: The mission laptop interfaced accurately with the computer.

Takeoff: Uneventful.

Mission Results: Each test point was set up with the aircraft straight and level flight, nominally at 15,000 ft PA at 310 KGS on a heading that would allow for a direct headwind or tailwind. The test team began collecting data with test points 39 through 41. The first few data points were conducted with a crosswind due to airspace, but were later repeated as airspace and weather allowed. Additionally, the laptop computer processing speed was limited because it was running in power save mode. The FTE fixed the problem and the test points were re-run. Then test points 6-13 were completed multiple times each. The aircraft lacked sufficient thrust to maintain airspeed while in any climbing maneuver, and on some "level turns" as the flight path angle was inadequately controlled by the Nz and bank command system (flight path angle went as high as 5° during some level turns). The climb angle did not always capture 15 degrees and did not maintain 15 degrees throughout the maneuver (during climbing maneuvers, the flight path angle varied from 12° to 20°). Of note, when the CG was forward (due to fuel transfer), the flight path seemed to be closer to predicted results. All maneuver executions were abrupt, but not objectionable. VSS disconnection would typically occur between 140 – 160 kts after completion of the 30 second maneuver. A few test points resulted in an unanticipated ESCAPE maneuver. Those points were subsequently re-flown and produced predicted results.

Landing/Post Flight Ground Block: Uneventful

6. RECOMMENDATIONS

None

COMPLETED BY	SIGNATURE	DATE
RUSSELL G. NEICE, Capt, USAF	//signed/rgn/10 September 2015//	20150910

TPS Form 5314 NOV 86

Appendix D: Supplementary Plots

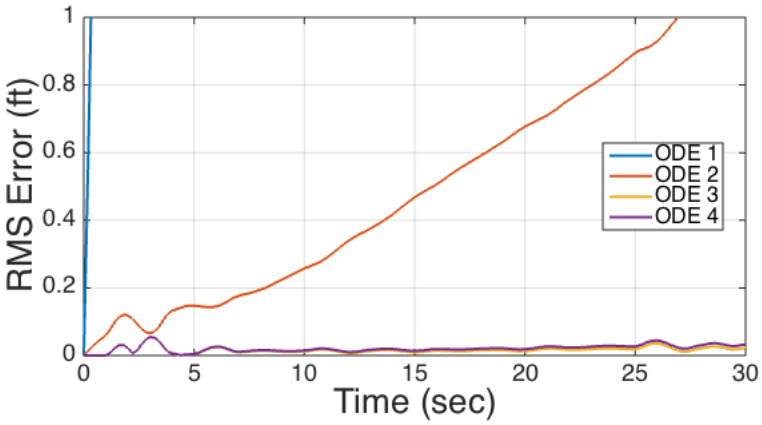

Figure D.1: Forward Path RMSE with 0.2 s Time Step

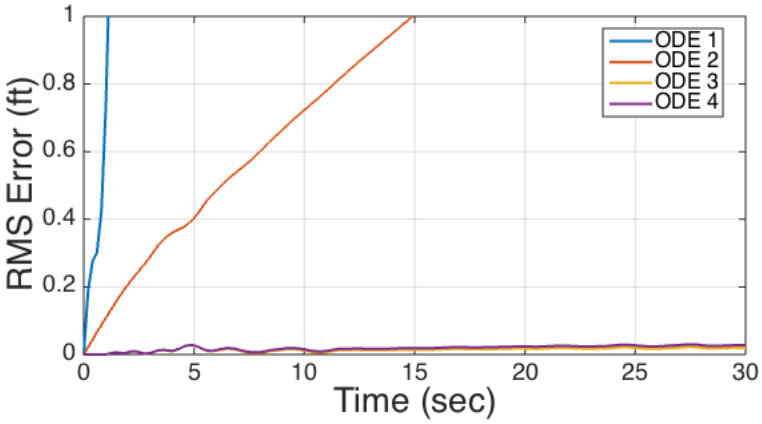

Figure D.2: Lateral Path RMSE with 0.2 s Time Step

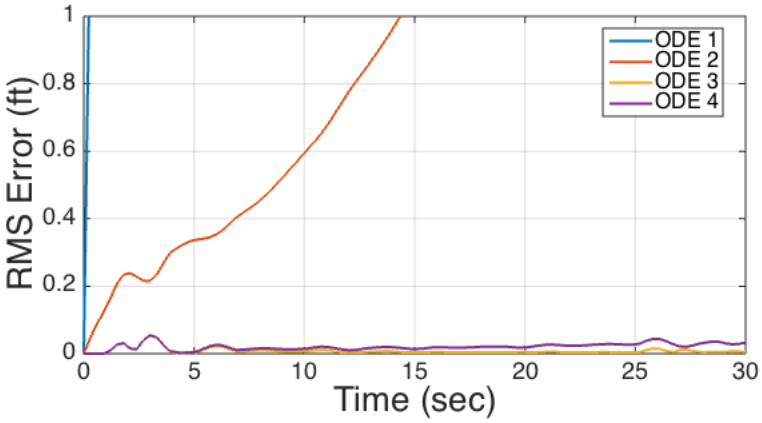

Figure D.3: Forward Path RMSE with 0.3 s Time Step

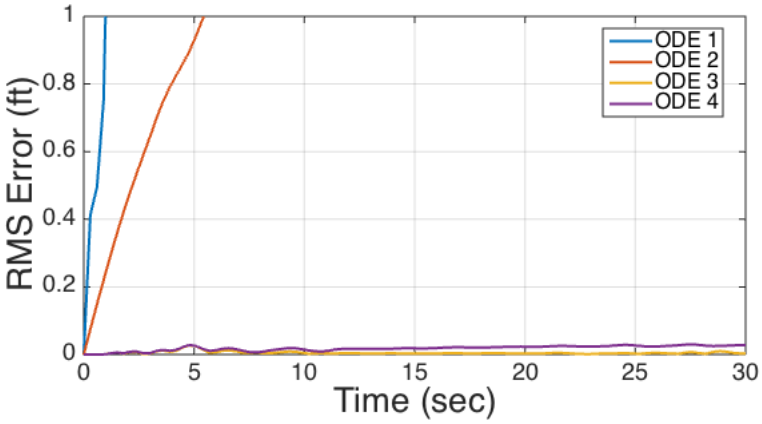

Figure D.4: Lateral Path RMSE with 0.3 s Time Step

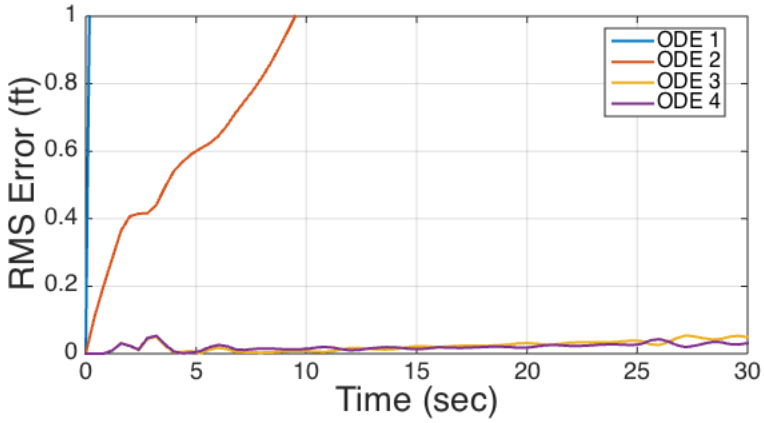

Figure D.5: Forward Path RMSE with 0.4 s Time Step

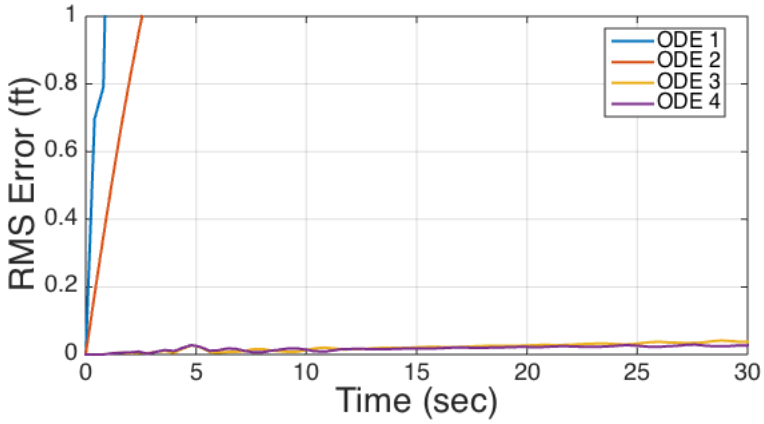

Figure D.6: Lateral Path RMSE with 0.4 s Time Step

The following time history plots illustrate the aircraft response to the control vector. This data supports the discussions and conclusions related to Chapters 4 and 5.

ESCAPE Test Point: 7 (Left Path) Average OAT: -8°C
Test/Virtual Altitude: 15,000/12,000 ft Test Dates: 31 Aug-10 Sep 15
Center of Gravity: 12.5 - 23.8% Test Day Data

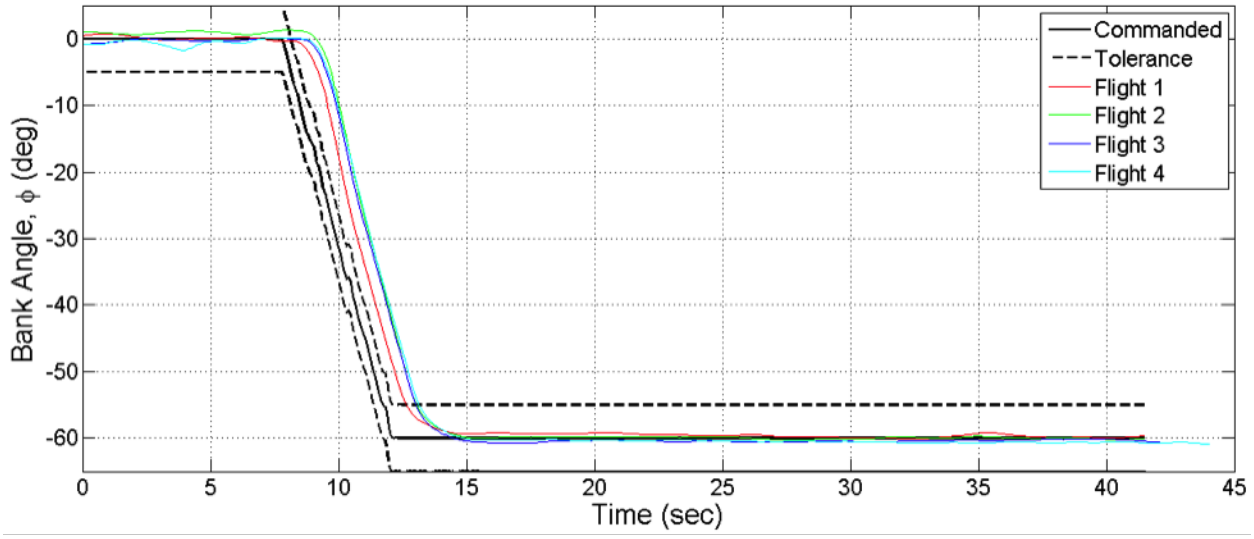

Figure D.7: Bank Angle vs Time for Test Point 7, Left Path

ESCAPE Test Point: 7 (Left Path) Average OAT: -8°C
Test/Virtual Altitude: 15,000/12,000 ft Test Dates: 31 Aug-10 Sep 15
Center of Gravity: 12.5 - 23.8% Test Day Data

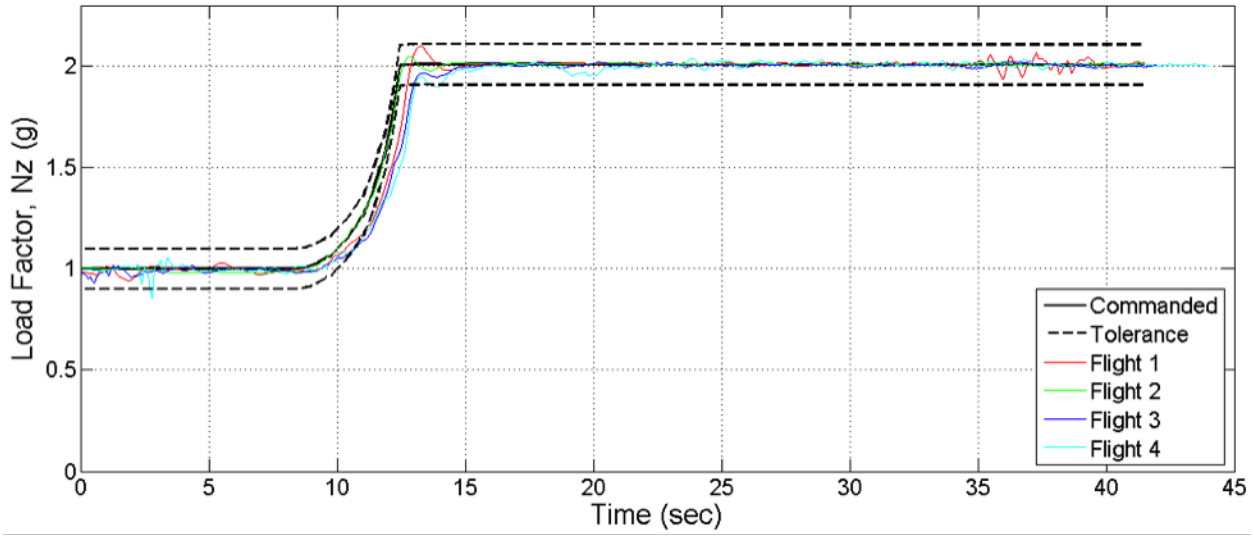

Figure D.8: Load Factor vs Time for Test Point 7, Left Path

ESCAPE Test Point: 7 (Left Path) Average OAT: -8°C
Test/Virtual Altitude: 15,000/12,000 ft Test Dates: 31 Aug-10 Sep 15
Center of Gravity: 12.5 - 23.8% Test Day Data

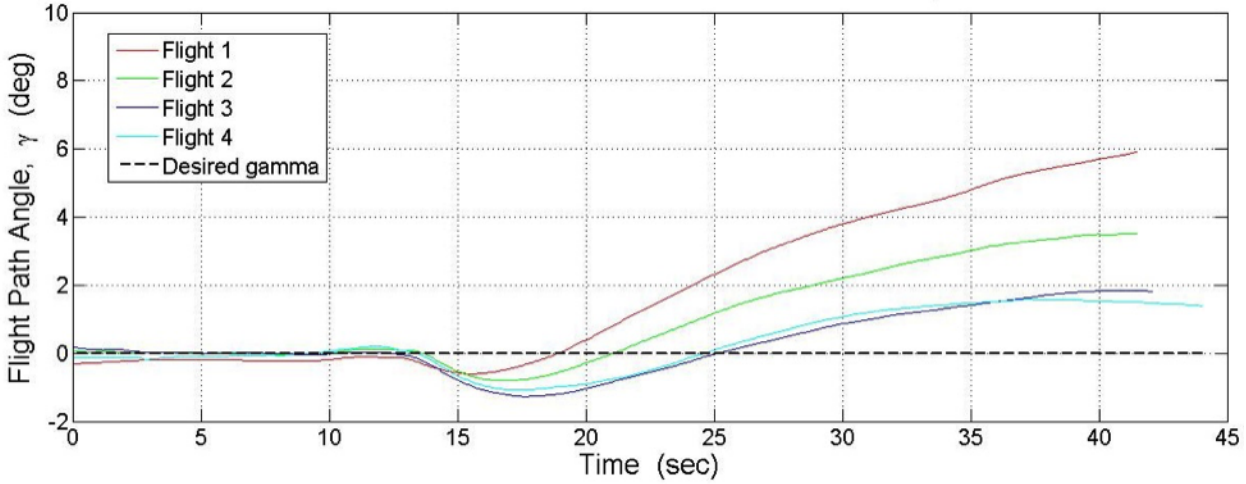

Figure D.9: Flight Path Angle vs Time for Test Point 7, Left Path

ESCAPE Test Point: 8 (Right Path) Average OAT: -8°C
Test/Virtual Altitude: 15,000/12,500 ft Test Dates: 31 Aug-10 Sep 15
Center of Gravity: 12.5 - 23.8% Test Day Data

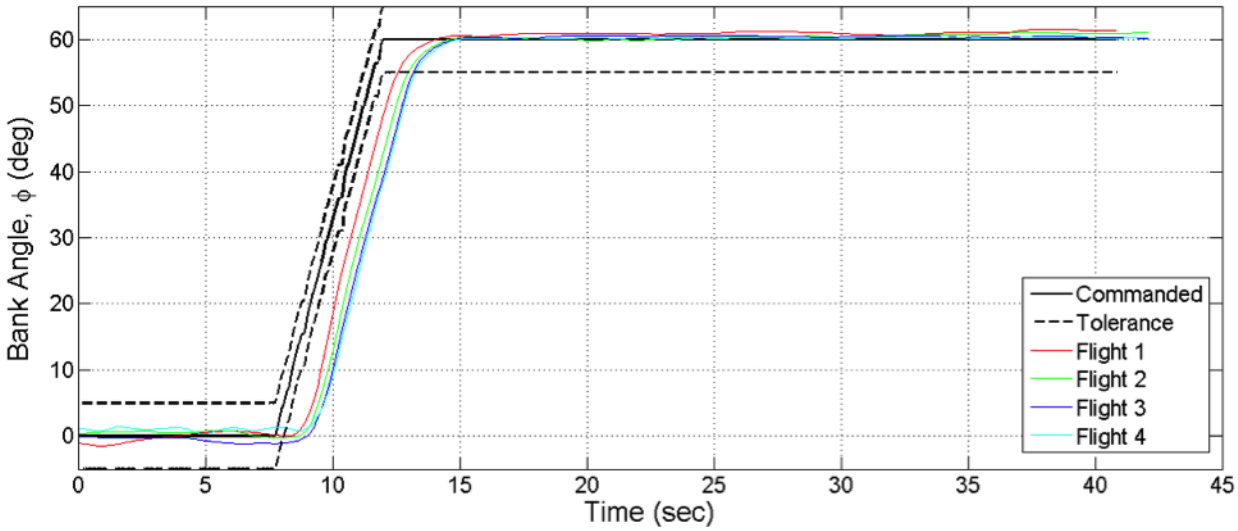

Figure D.10: Bank Angle vs Time for Test Point 8, Right Path

ESCAPE Test Point: 8 (Right Path) Average OAT: -8°C
Test/Virtual Altitude: 15,000/12,500 ft Test Dates: 31 Aug-10 Sep 15
Center of Gravity: 12.5 - 23.8% Test Day Data

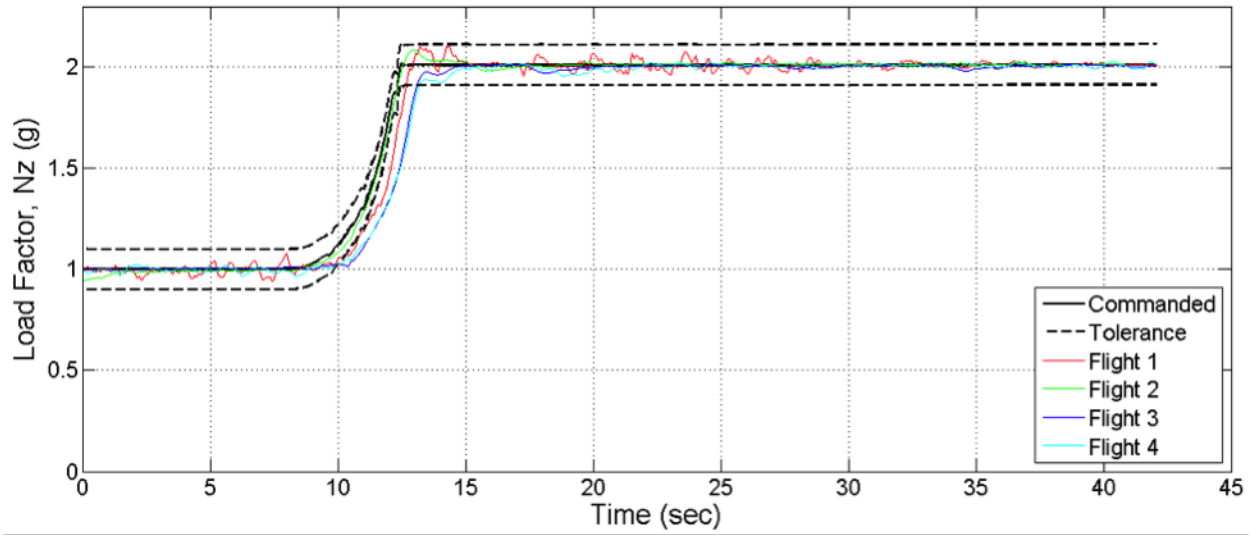

Figure D.11: Load Factor vs Time for Test Point 8, Right Path

ESCAPE Test Point: 8 (Right Path) Average OAT: -8°C
Test/Virtual Altitude: 15,000/12,500 ft Test Dates: 31 Aug-10 Sep 15
Center of Gravity: 12.5 - 23.8% Test Day Data

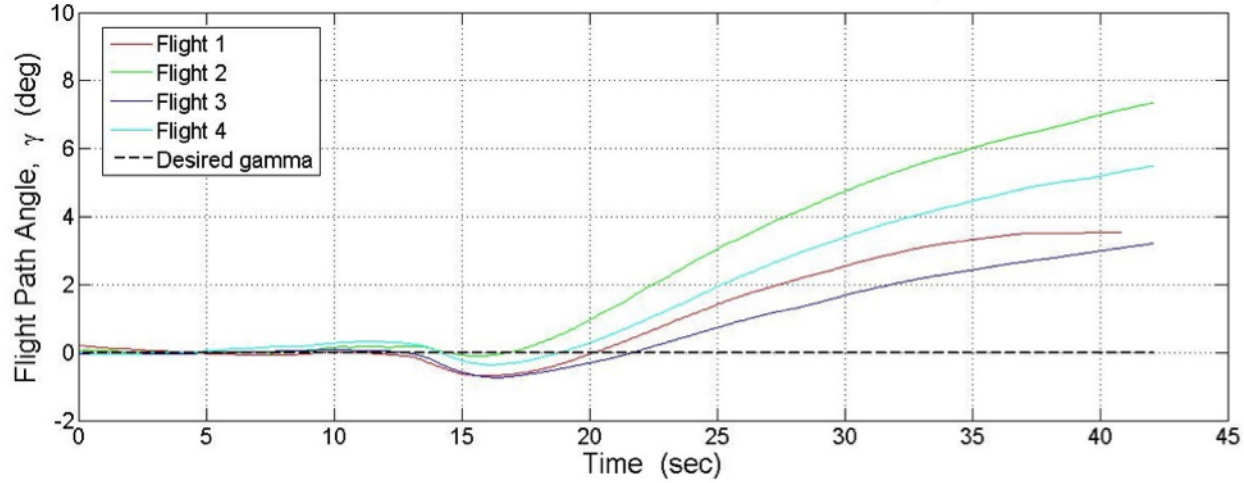

Figure D.12: Flight Path Angle vs Time for Test Point 8, Right Path

ESCAPE Test Point: 7 (Left Path)	Average OAT: -8°C
Test/Virtual Altitude: 15,000/12,000 ft	Test Dates: 31 Aug-10 Sep 15
Center of Gravity: 12.5 - 23.8%	Test Day Data

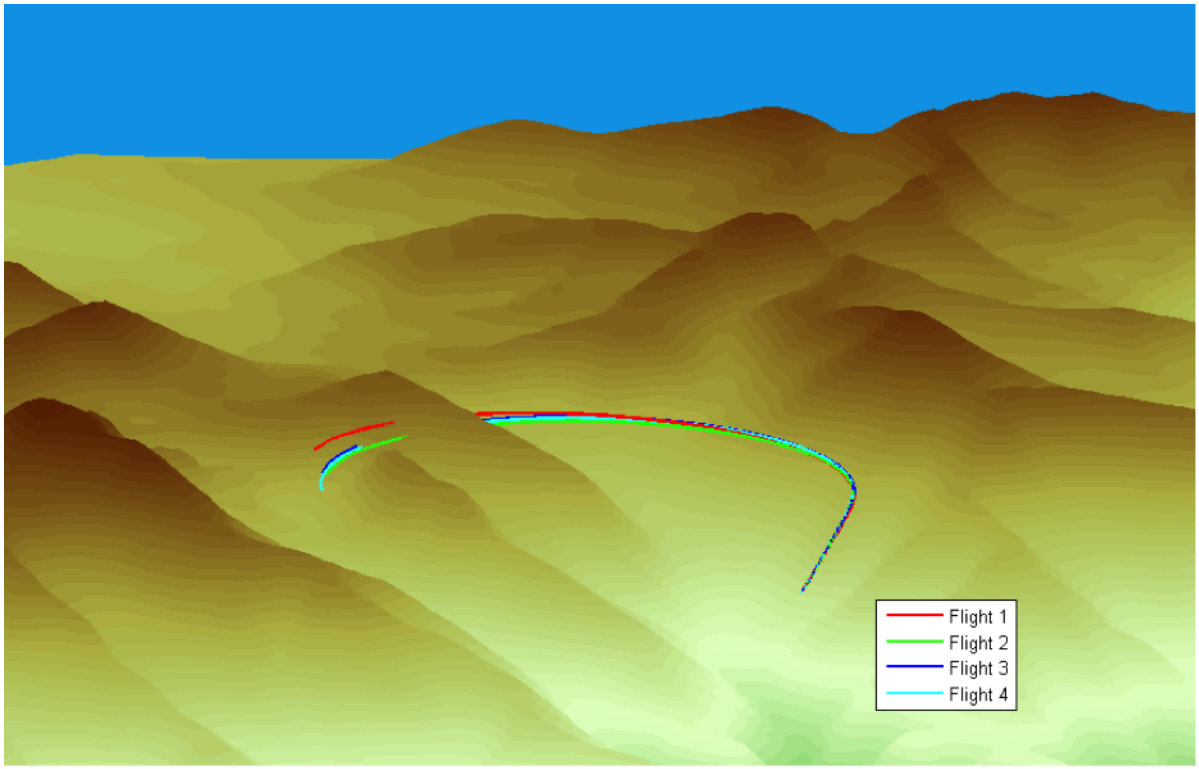

Figure D.13: 3D Presentation of Flight Test Data, Test Point 7, Left Level Path

ESCAPE Test Point: 8 (Right Path) Average OAT: -8°C
Test/Virtual Altitude: 15,0ft Test Dates: 31 Aug-10 Sep 15
Center of Gravity: 12.5 - 23.8% Test Day Data

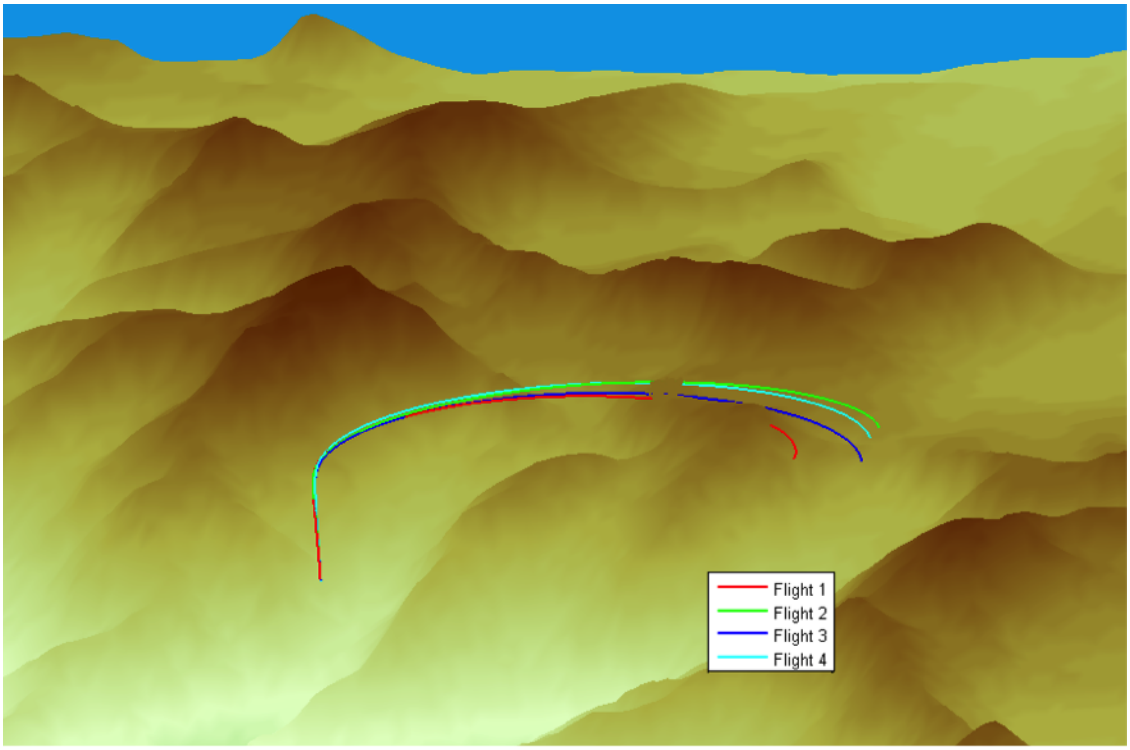

Figure D.14: 3D Presentation of Flight Test Data, Test Point 8, Right Level Path

ESCAPE Test Point: 13 (Right-Up) Average OAT: -8°C
Test/Virtual Altitude: 15,000/12,500 ft Test Dates: 31 Aug-10 Sep 15
Center of Gravity: 12.5 - 23.8% Test Day Data

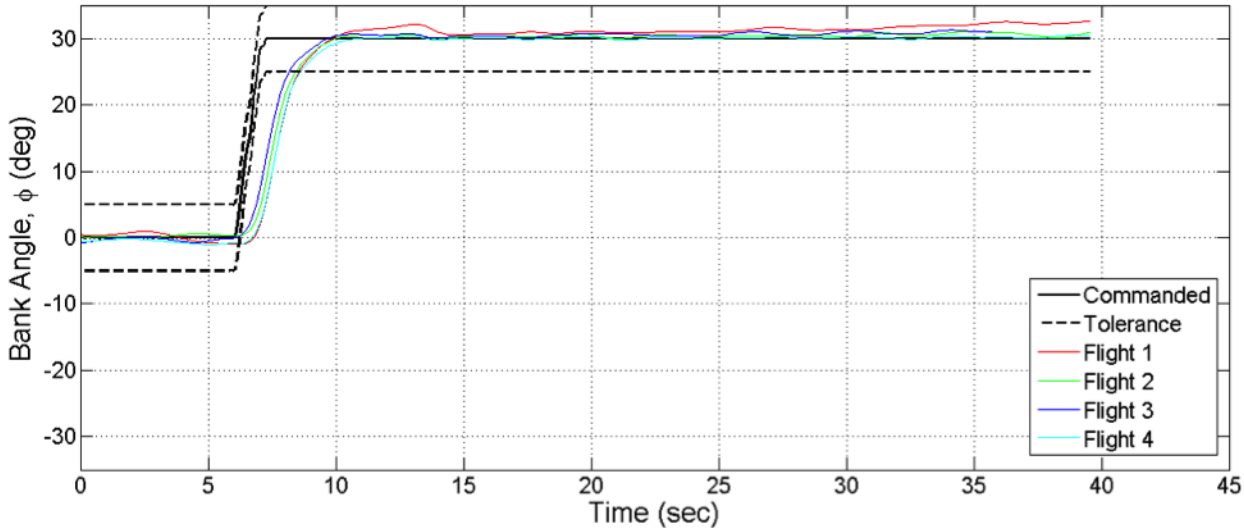

Figure D.15: Bank Angle vs Time for Test Point 13, Right-Up Path

ESCAPE Test Point: 13 (Right-Up) Average OAT: -8°C
Test/Virtual Altitude: 15,000/12,500 ft Test Dates: 31 Aug-10 Sep 15
Center of Gravity: 12.5 - 23.8% Test Day Data

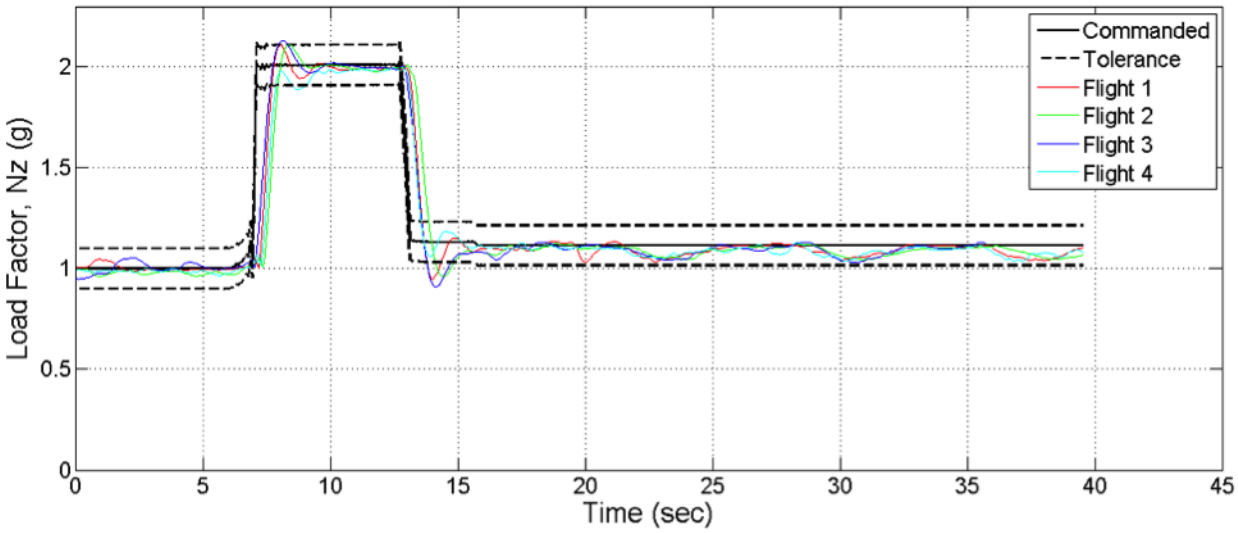

Figure D.16: Load Factor vs Time for Test Point 13, Right-Up Path

ESCAPE Test Point: 13 (Right-Up) Average OAT: -8°C
Test/Virtual Altitude: 15,000/12,500 ft Test Dates: 31 Aug-10 Sep 15
Center of Gravity: 12.5 - 23.8% Test Day Data

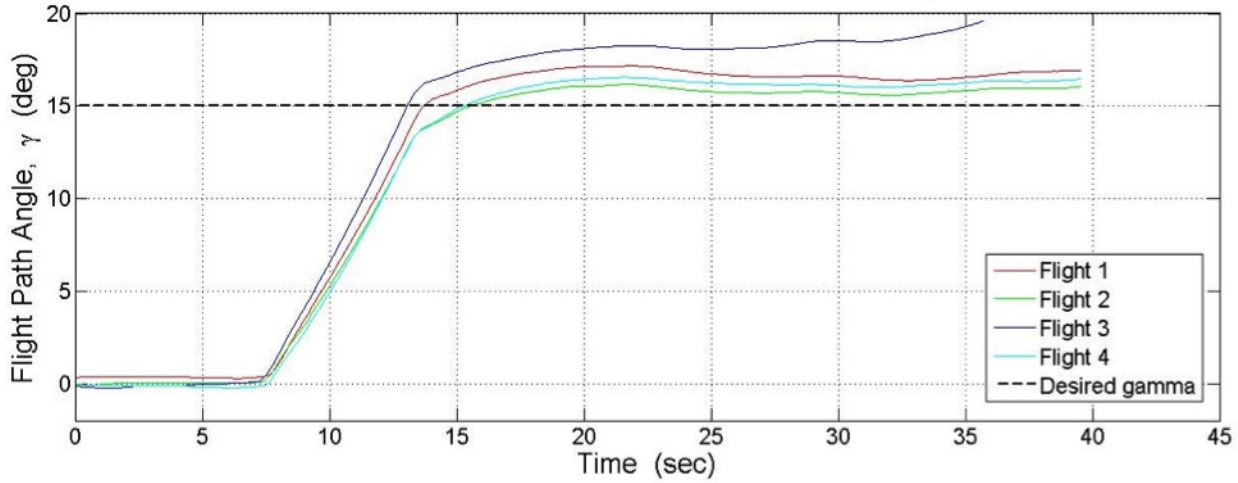

Figure D.17: Flight Path Angle vs Time for Test Point 13, Right-Up Path

ESCAPE Test Point: 13 (Right-Up) Average OAT: -8°C
Test/Virtual Altitude: 15,000/12,500 ft Test Dates: 31 Aug-10 Sep 15
Center of Gravity: 12.5 - 23.8% Test Day Data

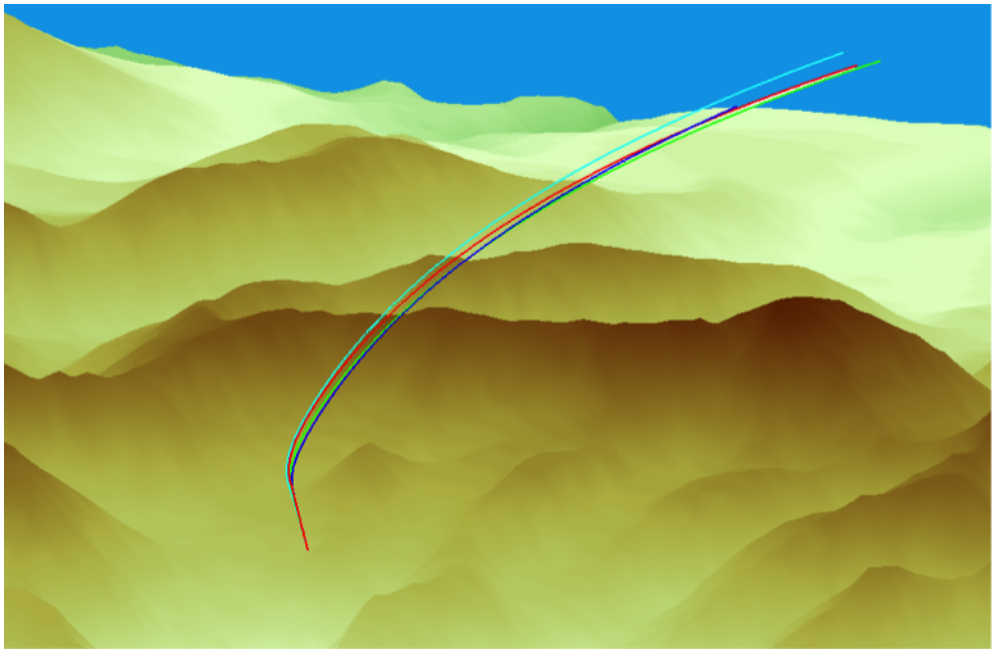

Figure D.18: 3D Presentation of Flight Test Data, Test Point 13, Right-Up Path

ESCAPE Test Point 8 (Left Level) Flight Test Data Flight: 2

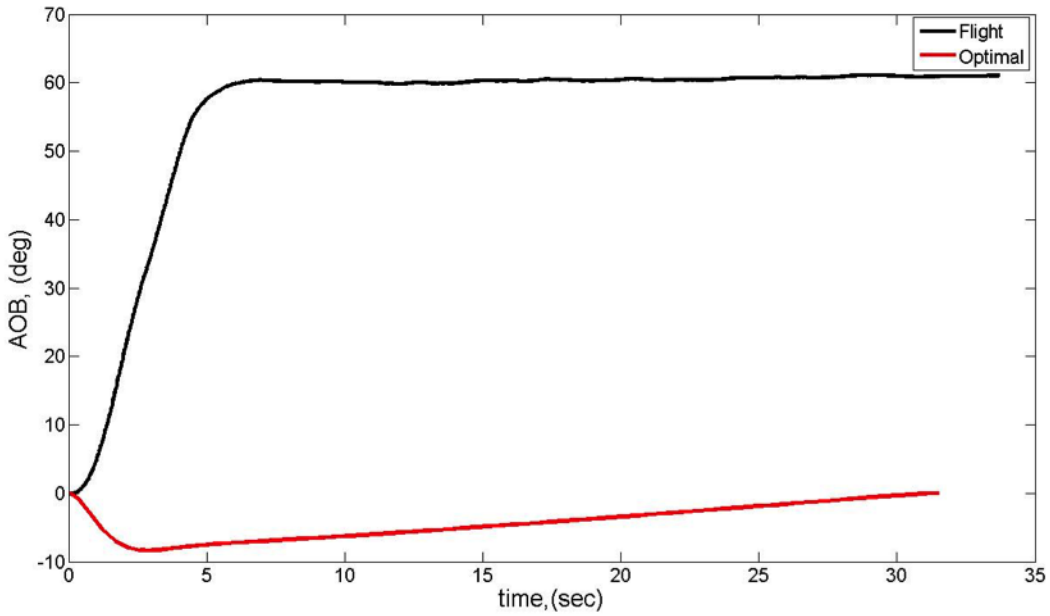

Figure D.19: Flight Test Angle of Bank vs Optimal Angle of Bank

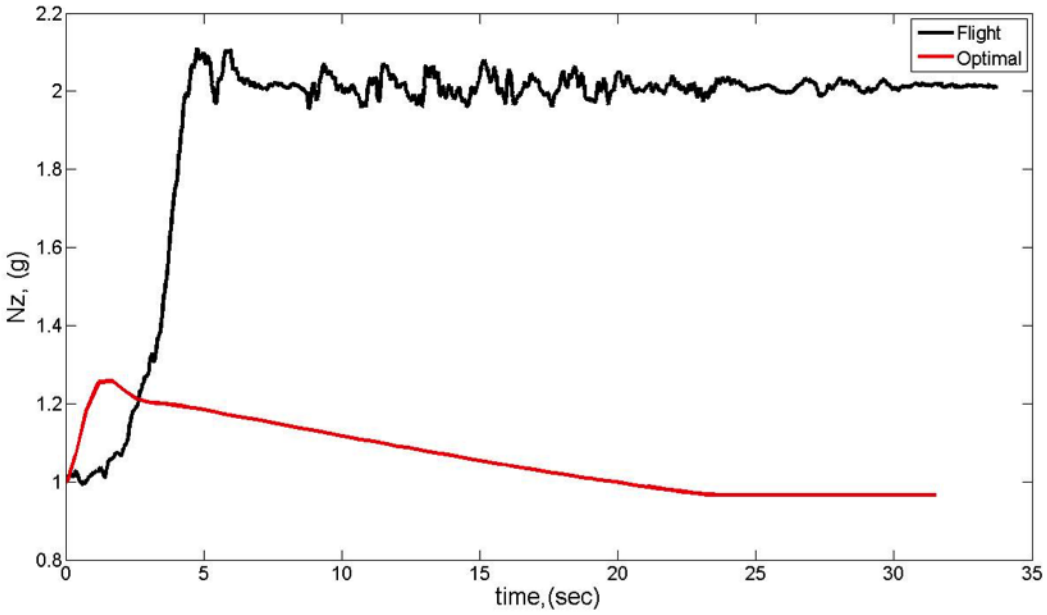

Figure D.20: Flight Test N_z vs Optimal N_z

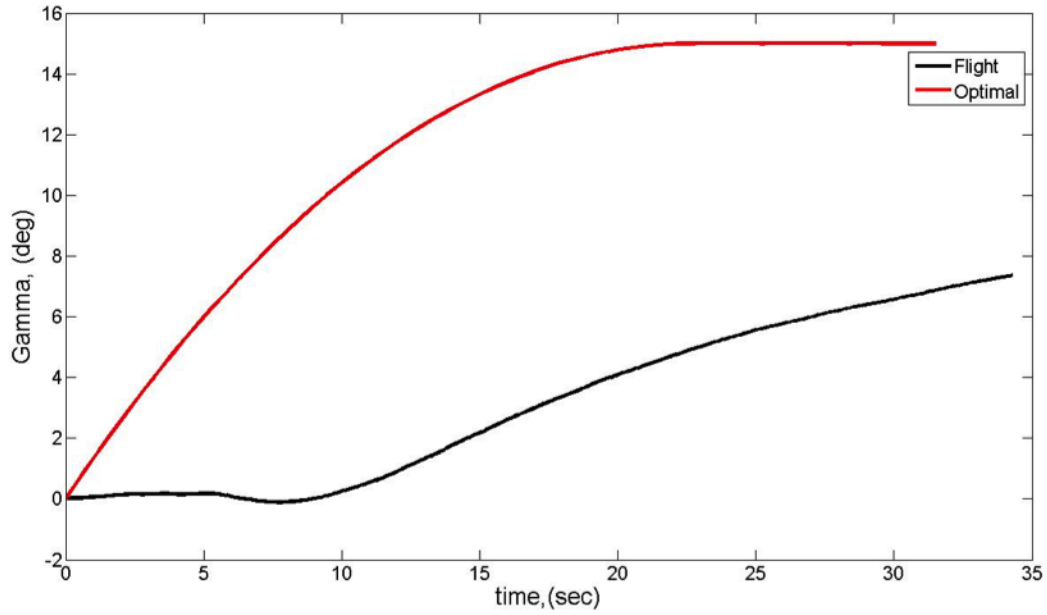

Figure D.21: Flight Test Flight Path Angle vs Optimal Flight Path Angle

ESCAPE Test Point 8 (Left Level) Flight Test Data Flight: 2

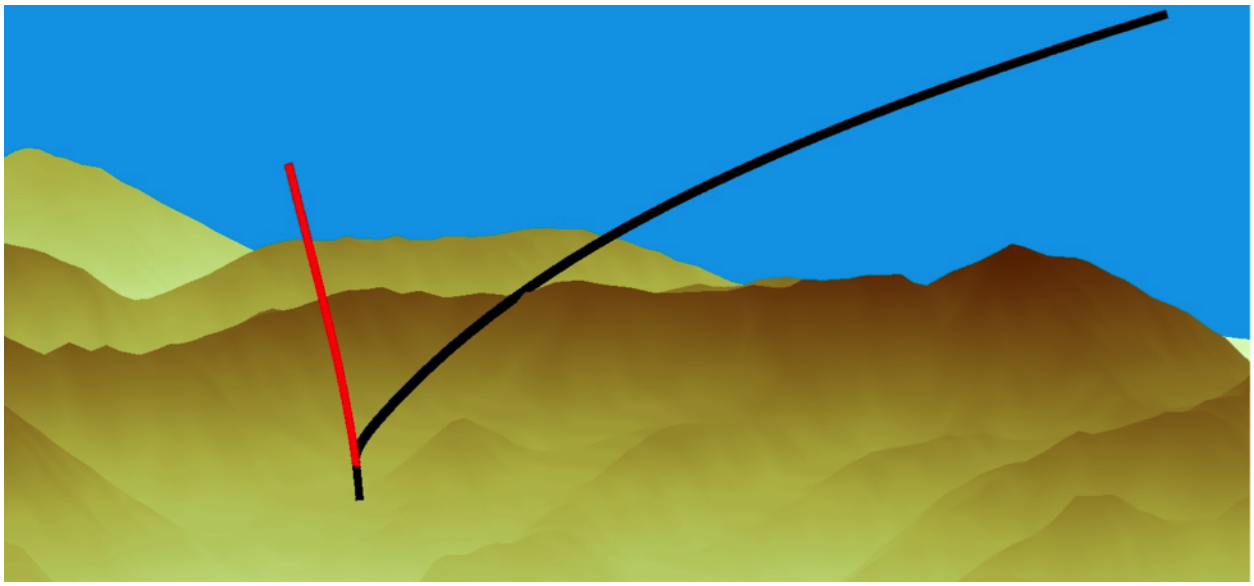

Figure D.22: Test Point 8 3-TPA and Optimal Flight Path

ESCAPE Test Point 9 (Left Up) Flight Test Data Flight: 2

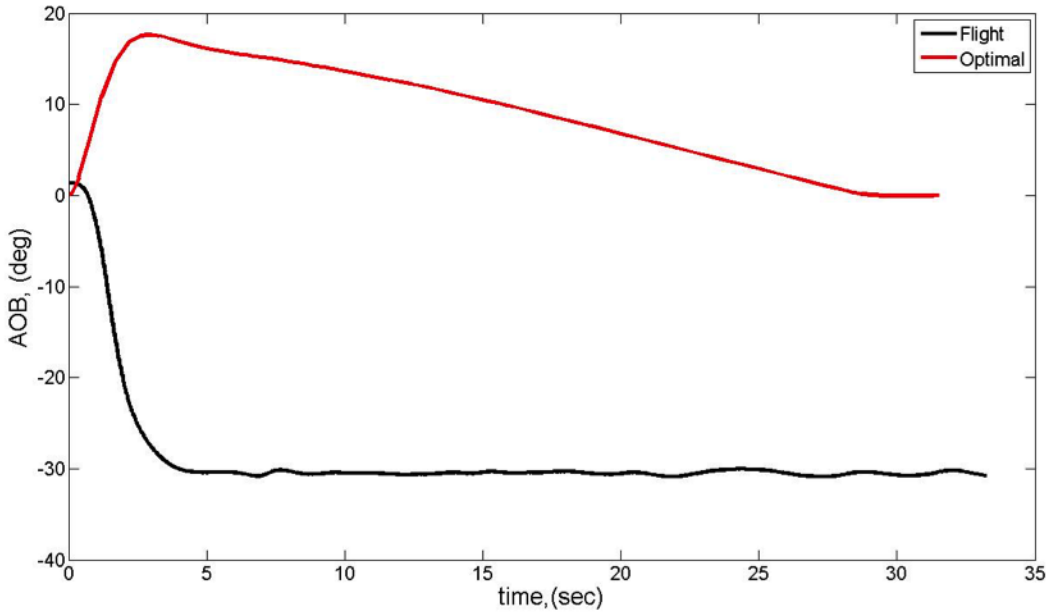

Figure D.23: Flight Test Angle of Bank vs Optimal Angle of Bank

ESCAPE Test Point 9 (Left Up) Flight Test Data Flight: 2

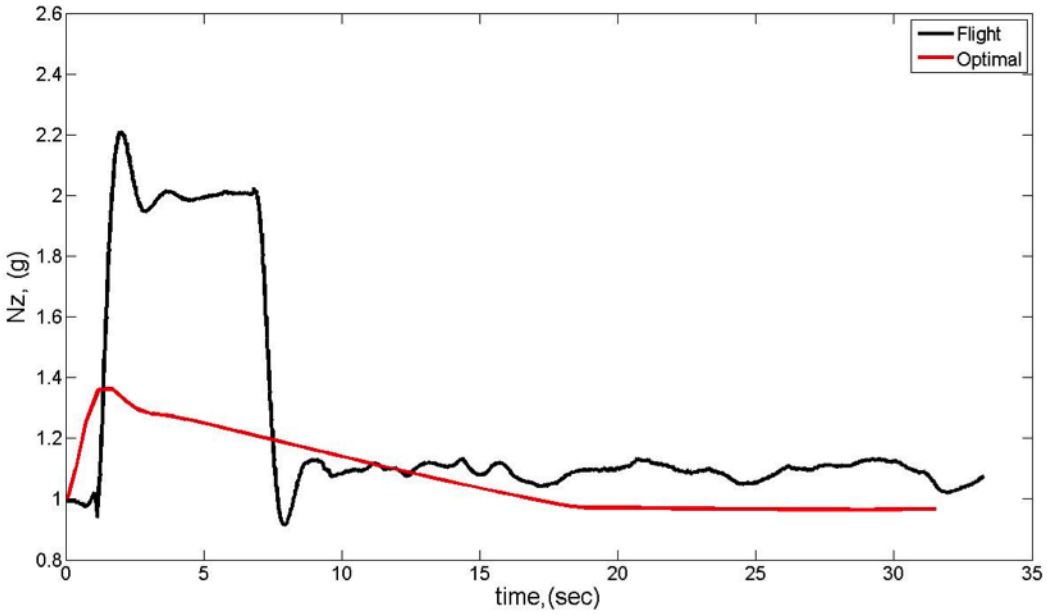

Figure D.24: Flight Test N_z vs Optimal N_z

ESCAPE Test Point 9 (Left Up) Flight Test Data Flight: 2

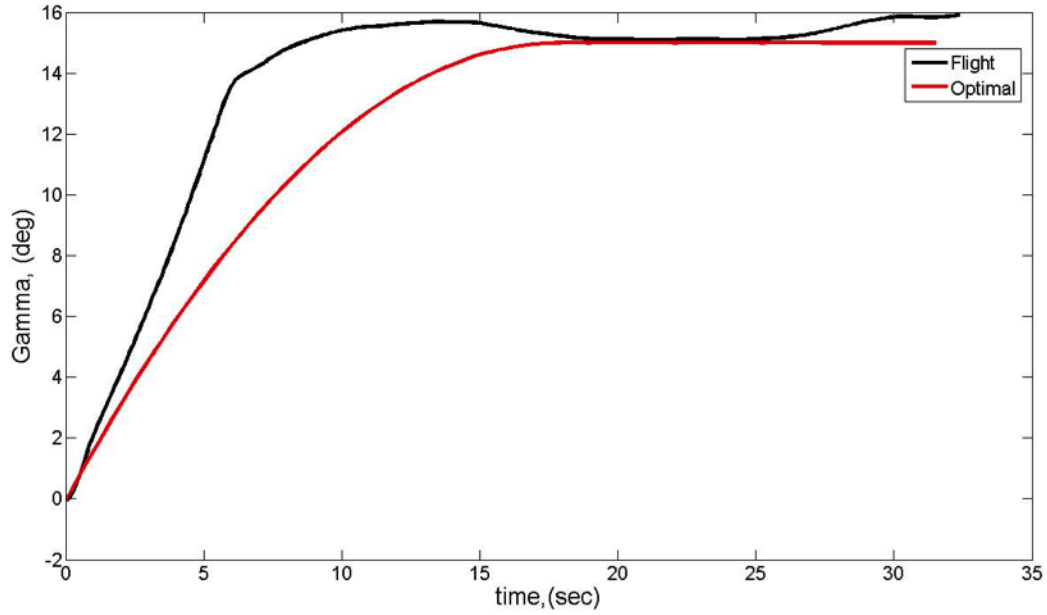

Figure D.25: Flight Test Flight Path Angle vs Optimal Flight Path Angle

ESCAPE Test Point 9 (Left Up) Flight Test Data Flight: 2

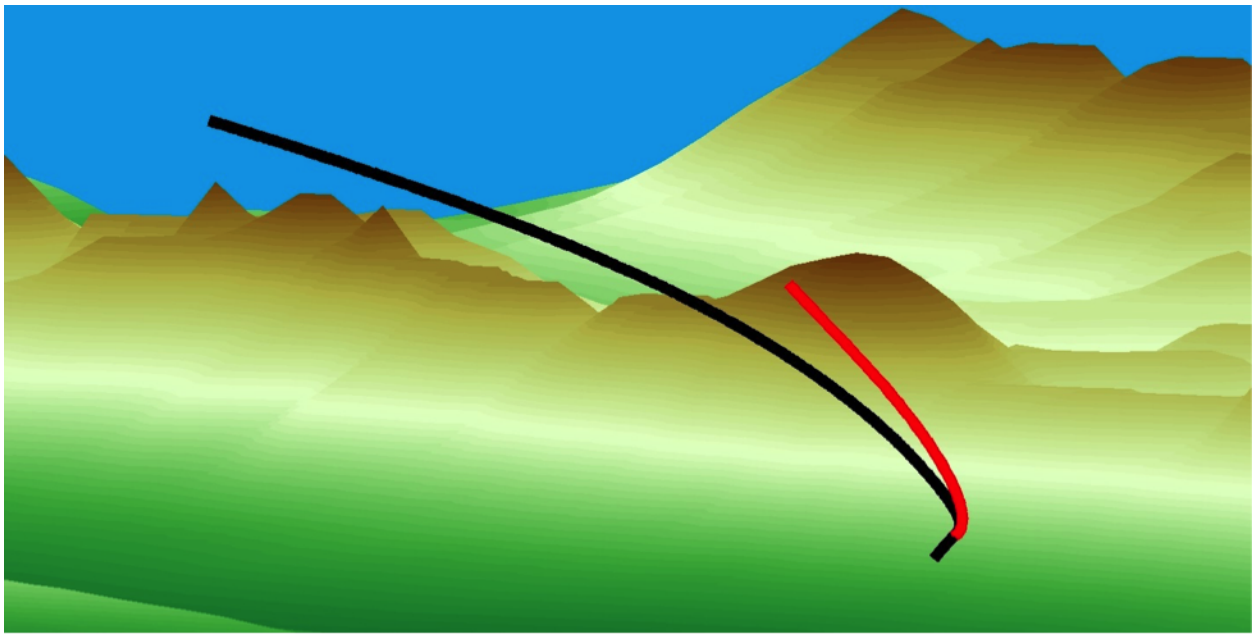

Figure D.26: Test Point 9 5-TPA and Optimal Flight Path

Bibliography

[1] Barfield, A. "AFRL Auto GCAS Chief Engineer". Personal Communication, 2011-2014.

[2] Bicchi, A. and L. Pallottino. "On Optimal Cooperative Conflict Resolution of Air Traffic Management Systems". *IEEE*, 1(4):221–232, 2000.

[3] Bresnik, R. and T. Anderson. "Developmental Flight Testing of the Terrain Awareness Warning System (TAWS) in the F/A-18 Hornet". *Society of Experimental Test Pilots Symposium*, Sep 2001.

[4] Burrough, P.A. *Principles of Geographical Information Systems for Land Resources Assessment*. Clarendon Press, Oxford, 1986.

[5] Calhoun, P. private email correspondence, Cargo, Sept 2014.

[6] Calspan. *Learjet In-Flight Simulators Capabilities*. Technical report, Calspan Flight Research Group, 2014.

[7] Corporation, McDonnell Douglas. *C-17A Flight Manual 1C-17A-1SS-246*, change 6 edition, 1 October 2012.

[8] DoD. *MIL-STD-1797A: Flying Qualities of Piloted Aircraft*. Military standard, Department of Defense, March 1990.

[9] DoD. *MIL-PRF-89020B: Performance Specification Digital Terrain Elevation Data*. Military specification, National Imagery and Mapping Agency, May 2000.

[10] Dragut, L. and T. Blaschke. "Automated Classification of Landform Elements using Object-Based Image Analysis". *Geomorphology*, 81(3):330–344, 2006.

[11] Drake, Samuel Picton. "Converting GPS coordinates [phi, lambda, h] to navigation coordinates (ENU)", 2002.

[12] Durland, Nicolas H. "Defining Mean Sea Level in Military Simulations with DTED". *Northrop Grumman Coporation*, 1–3, 2010.

[13] Easter, J. R. *Learjet Flight Syllabus and Background Material for the US Air Force/US Naval Test Pilot School Variable Stability Programs*. Calspan Corporation, 2011.

[14] FAA. "Federal Aviation Administration Safer Skies General Aviation Controlled Flight into Terrain". *Joint Safety Implementation Team Final Report*, Feb 2000.

[15] FAA. "Code of Federal Regulations, Aeronautics and Space Title 14 Section 95.11-21", annual. Subpart B: Designated Mountainous Areas.

[16] Farr, Tom G, Paul A Rosen, Edward Caro, Robert Crippen, Riley Duren, Scott Hensley, Michael Kobrick, Mimi Paller, Ernesto Rodriguez, Ladislav Roth, et al. "The shuttle radar topography mission". *Reviews of Geophysics*, 45(2), 2007.

[17] Gannett, Henry. *The average elevation of the United States*. Department of the Interior - U.S. Geological Survey, 1894.

[18] Instruction, Air Force. "Instruction 11-202, Vol. 3". *Flying Operations: General Flight Rules*, 2010.

[19] Kaplan, E. D. and C. J. Hegarty. *Understanding GPS: principles and applications*. Artech house, 2005.

[20] Kirvan, Anthony P. *Latitude and Longitude*. National Center for Geographic Information and Analysis: http://www.ncgia.ucsb.edu/education/curricula/giscc/units/u014/tables/table02.html, 1997.

[21] Kuchar, J.K. and L.C. Yang. "Survey of Conflict Detection and Resolution Modeling Methods". *in Proceedings AIAA Guidance Navigation Control Conference*, 1997.

[22] Kuckar, J.K. and L.C. Yang. "A Review of Conflict Detection and Resolution Modeling Methods". *IEEE Transactions on Intelligent Transportation Systems*, 1(4):179–189, 2000.

[23] Marzocca, Pier. "AE 429 Aircraft Performance and Flight Mechanics". Clarkson.edu Class Notes, 2013.

[24] Middleton, M. private email correspondence, Bombers, Sept 2014.

[25] NASA. "Shuttle Radar Topogray Mission homepage". http://www2.jpl.nasa.gov/srtm/. Accessed: Oct 2014.

[26] NAVAIR. "PMA 209 GPWS/TAWS website". http://www.navair.navy.mil/PMA209/Teams/GPWS.aspx. Accessed: Oct 2014.

[27] Patterson, T. private email correspondence, B-1, Nov 2014.

[28] Raghunathan, A.U., V. Gopal, D. Subramanian, L. T. Biegler, and T. Samad. "Dynamic Optimization Strategies for Three-Dimensional Conflict Resolution of Multiple Aircraft". *Journal of Guidance, Control, and Dynamics*, 27(4):586–596, 2004.

[29] Raquet, John. "EENG 533: Navigation Using the GPS Course Notes". Air Force Institute of Technology, 2014.

[30] Rodriguez-Johnson, Dr. Elizabeth. "Defense Safety Oversight Council". *National Defense Intelligence Agency*, 1–15, 2003.

[31] Smith, Col. "PhD Dissertation: Automatic Air Collision Avoidance Systems". *Air Force Institute of Technology, Wright-Patterson AFB*, 61–66, 2013.

[32] Snyder, G. I. *The 3D Elevation Program–Summary of Program Direction: U.S. Geological Survey Fact Sheet 2012-3089*. Technical report, USGS Document http://nationalmap.gov/3DEP, 2012.

[33] Soliton. Lift and Drag Diagram: http://soliton.ae.gatech.edu/, May 2014.

[34] Sorokowski, P., M. Skoog, S. Burrows, and S. Thomas. *Small UAV Automatic Ground Collison Avoidance System Flight Test Results*. Technical report nasa/tm-2014-xxx, NASA Dryden Flight Research Center, Edwards AFB, CA, 2014.

[35] Suplisson, Angela W. "PhD Dissertation: An Optimal Control Approach to Aircraft Automatic Ground Collision Avoidance". *Air Force Institute of Technology, Wright-Patterson AFB*, 2014.

[36] Swihart, D., A. Barfield, E. Griffin, R. Lehmann, S. Whitcome, B. Flynn, M. Skoog, and K. Prosser. "Automatic Ground Collision Avoidance System Design, Integration, and Flight Test". *Aerospace and Electronic Systems Magazine, IEEE*, May:4–15, 2011.

[37] Swihart, D., C. Wiedemann, D. Homan, E. Griffin, M. Skoog, A. Barfield, R. Turner, and E. Smith. "Automatic Collision Avoidance Technology". *Unmanned Vehicle Systems International Conference, Washingtion DC*, 2007.

[38] USGS. "National Elevation Dataset Website". http://ned.usgs.gov. Accessed: Oct 2014.

[39] USGS. "SRTM Topography". *Shuttle Radar Topography Missions*, 1–8, 2014.

[40] Weingarten, N. "History of In-Flight Simulation and Flying Qualities Research at Calspan". *AIAA Journal of Aircraft*, 42(2):1–15, March 2005.

REPORT DOCUMENTATION PAGE

Form Approved
OMB No. 0704-0188

PLEASE DO NOT RETURN YOUR FORM TO THE ABOVE ADDRESS.

1. REPORT DATE *(DD-MM-YYYY)*	2. REPORT TYPE	3. DATES COVERED *(From - To)*
27-03-2016	Master's Thesis	Oct 2013 - Mar 2016

4. TITLE AND SUBTITLE

Multi-Trajectory Automatic Ground Collision Avoidance System with Flight Tests (Project Have ESCAPE)

5a. CONTRACT NUMBER

5b. GRANT NUMBER

5c. PROGRAM ELEMENT NUMBER

6. AUTHOR(S)

Trombetta, John V., Major, USAF

5d. PROJECT NUMBER

14Y232, 15Y192

5e. TASK NUMBER

5f. WORK UNIT NUMBER

7. PERFORMING ORGANIZATION NAME(S) AND ADDRESS(ES)

Air Force Institute of Technology
Graduate School of Engineering and Management (AFIT/EN)
2950 Hobson Way
Wright-Patterson AFB OH 45433-7765

8. PERFORMING ORGANIZATION REPORT NUMBER

AFIT-ENY-MS-16-M-244

9. SPONSORING/MONITORING AGENCY NAME(S) AND ADDRESS(ES)

Major Sean Musil
United States Air Force Test Pilot School
220 Wolfe Ave.
Edwards, CA 93524
sean.musil@us.af.mil

10. SPONSOR/MONITOR'S ACRONYM(S)

USAF TPS

11. SPONSOR/MONITOR'S REPORT NUMBER(S)

12. DISTRIBUTION/AVAILABILITY STATEMENT

DISTRIBUTION STATEMENT A:
APPROVED FOR PUBLIC RELEASE; DISTRIBUTION UNLIMITED

13. SUPPLEMENTARY NOTES

This work is a declared work of the U.S. Government and is not subject to copyright protection in the United States.

14. ABSTRACT

Multi-trajectory automatic collision avoidance techniques for heavy-type aircraft are explored to increase aviation safety. This research includes flight test results from the United States Test Pilot School's Test Management Project (TMP) titled Have Emergency Safe Calculated Autonomous Preplanned Exit (ESCAPE). The tested algorithm includes both a 3-path and a 5-path terrain avoidance technique that is compared to an optimal solution. The research utilizes Level 1 Digital Terrain Elevation Data (DTED) to analyze the terrain and a 3-Degrees of Freedom (DOF) Equations of Motion (EOM) model to predict potential terrain avoidance paths for the aircraft. The algorithm was flight tested against DTED using the Calspan Learjet to determine actual 3 and 5-path performance, parameter specification, and comparison to the optimal solution. The important recommendations include a need for flexible entry parameters based on current aircraft state, continued evaluation of the terrain during avoidance maneuver execution, and more precise control of the aircraft flight path angle. It is concluded that an acceptable avoidance solution is possible using only a 3-path solution given that all three paths include a climbing maneuver.

15. SUBJECT TERMS

GCAS, TPA, Optimization, Collision Avoidance, Have ESCAPE

16. SECURITY CLASSIFICATION OF:			17. LIMITATION OF ABSTRACT	18. NUMBER OF PAGES	19a. NAME OF RESPONSIBLE PERSON
a. REPORT	b. ABSTRACT	c. THIS PAGE			Dr. Richard G. Cobb, AFIT/ENY
U	U	U	UU	208	19b. TELEPHONE NUMBER *(Include area code)* (937) 255-3636 x4559 richard.cobb@afit.edu

Reset